**Charles University**

**First Faculty of Medicine**

UNIVERZITA KARLOVA
1. lékařská fakulta

**Mgr. Ingrida Šmeringaiová**

# Použití endotelu rohovky a amniové membrány k transplantačním účelům

# Use of corneal endothelium and amniotic membrane for transplantation purposes

Doctoral thesis

Supervisor: doc. Mgr. Kateřina Jirsová, Ph.D.

Prague, 2020

**Declaration**

I, Ingrida Šmeringaiová, declare that I have prepared the final work independently and that I have duly stated and quoted all the sources and literature used. At the same time, I declare that the work was not used to obtain another or the same university degree. On the other hand, I would like to emphasize, that I am a co-author of one herein mentioned paper, which was used by Mgr. Peter Trošan, Ph.D., my ex-collegue and Ph.D. student from The Laboratory of the Eye Biology and Pathology, in his doctoral thesis, which he succesfully defended in year 2019.

I agree with the permanent storage of the electronic version of this thesis in the database system of the inter-university project Theses.cz in order to continuously check the similarity of theses.

In Prague, on July 10, 2020

Mgr. Ingrida Šmeringaiová

**Identification record**

SMERINGAIOVA, Ingrida. Použití endotelu rohovky a amniové membrány k transplantačním účelům. *[The use of corneal endothelium and amniotic membrane for transplantation purposes].* Prague, 2020. 98 pages, 5 appendices. Doctoral thesis (Ph.D.). Charles University, First Faculty of Medicine, Institute of Biology and Medical Genetics. Supervisor: JIRSOVÁ, Kateřina.

**Acknowledgements**

Special thank goes to my supervisor doc. Mgr. Kateřina Jirsová, Ph.D. for her scientific and critical guidance during my postgraduate studies.

I would also like to give many thanks to all current and former colleagues from the Laboratory of Cell Biology and Pathology for all their help, advice and support that they ever gave me during my doctoral studies. I also thank colleagues from other institutions who I ever cooperated with for their kind help.

I would also like to thank to the National Cell and Tissue Centre (Brno, Czech Republic), Eye Bank Prague (Prague, Czech Republic), University Hospital Kralovske Vinohrady (Prague, Czech Republic), The Bank of Biological Material of the 1st Faculty of Medicine, Charles University (Prague, Czech Republic) and General University Hospital in Prague (Prague, Czech Republic) for providing the corneal tissue for this research and also to the Motol University Hospital for providing the clean room facility for preparation of amnion allografts.

And finally, I would like to thank to my partner, my family and friends for their support.

**Financial support**

This work was supported by the Norwegian Financial Mechanism 2009-2014 and the Ministry of Education, Youth and Sports under Project Contract no. MSMT-28477/2014, project 7F14156, the Progres Q25/LF1, European Regional Development Fund, project EF16_013/0001674, BBMRI_CZ LM2015089, and SVV, project 260256/2016, 260367/2017 and AZV ČR_NV18-08-00106.

## Abstrakt

Část I: Endotelové buňky tvoří zadní vrstvu rohovky a jsou důležité pro udržení její průhlednosti. Dysfunkční endotel lze obnovit pouze transplantací. Globální nedostatek rohovek dárců vyžaduje hledání alternativních způsobů léčby. Přípravu štěpu metodami tkáňového inženýrství komplikuje nízká proliferační kapacita endotelu. Dosud nebyl definován marker, jenž by byl exprimován pouze endotelem a nebyla potvrzena existence kmenových buněk pro endotel.

Připravili a zavedli jsme protokol pro kultivaci endotelových buněk z tkáně určené k výzkumu, tj. korneosklerálních rimů získaných po transplantaci nebo rohovek vyřazených z transplantačního procesu. Sledovali jsme lokalizaci vybraných proteinů, včetně markerů kmenových buněk, v nativní tkáni a v primárních buněčných kulturách. Z jedné hypotermicky uskladněné tkáně jsme připravili až 6,4 $cm^2$ buněk endotelu, které měli buněčné rysy srovnatelné s nativním endotelem. Tímto přístupem lze zvýšit množství endotelu pro výzkumné či transplantační účely. Pomocí nepřímé imunohistochemie jsme prokázali, že žádný z dříve navrhovaných molekulárních markerů endotelu není pro tyto buňky specifický a detekovali jsme expresi markerů kmenových buněk v celé vrstvě endotelu. Na modelu prasečí rohovky jsme po navození cenrálního poškození endotelu sledovali jeho reparační kapacitu. Zjistili jsme, že reparaci neovlivňuje přítomnost periferního endotelu, ale především délka kultivace a vyšší množství séra v médiu.

Část II: Lidská amniová membrána (amnion) je membrána placenty, která má velký potenciál při léčbě dlouhodobě nehojících se ran různých etiologií. Mechanismem je akcelerace a urychlení granulace a epitelizace defektu. V České republice byla dosud terapie pomocí amnionu standardizována pouze pro rekonstrukci očního povrchu. Důležitou součástí přípravy amnionu je účinná, ale netoxická dekontaminace. V klinické praxi se k transplantaci používá především intaktní amnion, deepitelizovaný amnion se preklinicky využívá jako nosič pro kultivaci buněk k transplantačním účelům.

Připravili jsme laboratorní dekontaminační roztok s vlastnostmi (vysoká mikrobiologická účinnost, nízká toxicita) obdobnými komerčnímu roztoku. Vyvinuli jsme protokol pro deepitelizaci amnionu, pomocí kterého jsme získali jednak amnion s intaktní bazální membránou, ale také vitální epitelové buňky, které lze dále využít metodami tkáňového inženýrství. Na základě předběžných výsledků ukazujeme pozitivní účinek amnionu na hojení nehojících se ran u pacientů zařazených do multicentrické studie.


**Klíčová slova:** rohovka, endotel, amniová membrána, kmenové buňky, kultivace, imunohistochemie, transplantace

## Abstract

Part I: Endothelial cells form the posterior layer of the cornea and are important for maintaining its transparency. Dysfunctional endothelium can only be restored by transplantation. The global shortage of donor corneas requires the search for alternative treatments. The preparation of the graft by tissue engineering methods is complicated by low proliferative capacity of endothelium. To date, no endothelium-specific marker has been defined and the existence of endothelial stem cells has not been confirmed yet.

We have prepared a protocol for culturing endothelial cells from research-grade tissue - corneoscleral rims obtained after transplantation or corneas excluded from the transplant process. We monitored localization of selected proteins, including stem cell markers, in native tissue and in primary cell cultures. We prepared up to 6.4 $cm^2$ of endothelium from one cornea/rim, which had cellular features comparable to the native endothelium. This approach can increase the amount of endothelium for research or transplantation purposes. Using indirect immunohistochemistry, we showed that none of the previously proposed endothelial molecular markers is specific for these cells. We detected the expression of stem cell markers throughout the endothelial layer. In the porcine cornea model, we monitored its repair capacity after inducing central damage to the endothelium. We found that the repair is not affected by the presence of peripheral endothelium, but mainly by the length of organ culture and higher amounts of serum in the medium.

Part II: The human amniotic membrane (amnion) is a placental membrane that has a great potential in the treatment of non-healing wounds of various etiologies. The mechanism is acceleration of granulation and epithelialization of the defect. In the Czech Republic, amnion therapy has been standardized so far only for the reconstruction of the ocular surface. An important part of amnion preparation is effective but non-toxic decontamination. In clinical practice, intact amnion is mainly used for transplantation, but de-epithelialized amnion is used preclinically as a carrier for culturing cells for transplantation purposes.

We prepared our laboratory decontamination solution with properties (high microbiological efficiency, low toxicity) similar to a commercial solution and developed a protocol for amnion de-epithelialization, with which we obtained both amnion with an intact basement membrane, but also vital epithelial cells, which can be further used by tissue engineering methods. Based on preliminary results, we show a positive effect of amnion on healing of non-healing skin wounds in patients enrolled in a multicenter study.


**Key words:** cornea, endothelium, amniotic membrane, stem cells, cultivation, immunohistochemistry, transplantation

# Table of contents

# Abbreviations

| | |
|---|---|
| **5HT1D/HTR1D** | 5-Hydroxytryptamine Receptor 1D |
| **AECs** | amniotic epithelial cells |
| **AESCs** | amniotic epithelial stem cells |
| **AM** | human amniotic membrane |
| **AMCs** | amniotic mesenchymal cells/stromal keratocytes |
| **AMSCs** | amniotic mesenchymal stem cells |
| **BL** | Bowman's layer |
| **BM** | basement membrane |
| **CD166/ALCAM** | Activated Leukocyte Cell Adhesion Molecule |
| **CE** | corneal endothelium |
| **CECs** | corneal endothelial cell(s) |
| **CK** | cytokine |
| **CM** | chorionic membrane/chorion |
| **COL8A2** | collagen Type VIII Alpha 2 Chain |
| **DM** | Descemet membrane |
| **DMEM** | Dulbecco's Modified Eagle Medium |
| **ECM** | extracellular matrix |
| **EDTA** | ethylenediaminetetraacetic acid |
| **EGF** | epidermal growth factor |
| **EnMT** | endothelial-to-mesenchymal transition/transformation |
| **EP** | corneal epithelium |
| **EPC** | corneal epithelial cells |
| **FBS** | fetal bovine serum |
| **FECD** | Fuchs endothelial corneal dystrophy |
| **FGF-2/b-FGF** | basic-fibroblast growth factor |
| **FNC** | a mixture of fibronectin, collagen I and bovine serum albumin |
| **GF** | growth factor |
| **GPC4** | glypican 4 |
| **GRHL2** | Grainyhead Like Transcription Factor 2 |
| **HGF** | hepatocyte growth factor |
| **h-SFM** | human-endothelial serum free medium |

| | |
|---|---|
| **HT** | hypothermia/hypothermic |
| **KC** | keratocytes |
| **LGR5** | Leucine Rich Repeat Containing G Protein-Coupled Receptor 5 |
| **M199** | medium 199 |
| **MRGX3/MRGPRX3** | Mas-Related G-Protein Coupled Receptor Member X3 |
| **NGF** | nerve growth factor |
| **OC** | organ culture(-ed) |
| **OCT4/POU5F1** | octamer-Binding Protein 4/POU Class 5 Homeobox 1 |
| **OVOL2** | Ovo Like Zinc Finger 2 |
| **PCR** | polymerase chain reaction |
| **PPCD** | posterior polymorphous corneal dystrophy |
| **PRDX6/Prdx6** | peroxiredoxin 6 |
| **ROCK** | rho-associated protein kinase inhibitor |
| **SLC4A11** | Sodium Bicarbonate Transporter-Like, Member 11 |
| **SOC** | standard-of-care |
| **SOX2** | SRY (Sex Determining Region Y)-Box 2 |
| **ST** | stroma |
| **TF** | transcription factor |
| **TFC4** | transcription Factor 4 |
| **TGF-β** | transforming growth factor -ß |
| **TM** | Trabecular meshwork |
| **Tx** | transplantation |
| **TZ** | transition zone |
| **ZEB1** | Zinc Finger E-Box Binding Homeobox 1 |
| **ZO1/TJP1** | Zona Occludens Protein 1 |
| **ZP4** | Zona Pellucida Glycoprotein 4 |
| **α-SMA** | alpha smooth muscle actin |

# Introduction

The human cornea is an exceptional tissue that, despite the content of millions of cells, remains transparent, allowing light to enter the human eye. Its inner surface is covered by a monolayer of corneal endothelium (CE), which play a key role in maintaining corneal transparency. Despite their important function, human corneal endothelial cells (CECs) have not been endowed with the proper ability to regenerate. Small CEC losses (small lesions) can be replaced by migration and enlargement of healthy CECs adjacent to the lesion, but larger defects, arising consequently to damage or disease, lead to corneal opacity and loss of vision. At present, the only possible solution to CE dysfunction is treatment with CE grafts obtained from cadaveric donors. It is well known that the number of patients waiting for a transplant exceeds the number of available donor corneas. Therefore, alternative ways are being sought to increase the supply of available CE grafts, e.g. by tissue-engineering.

Although the cornea is a tissue that is relatively easy to mimic by tissue engineering due to its properties (relatively simple structure, avascularity, immune-privileges), the development of such graft is complicated by several factors, mainly related to CEC properties and their different *in vivo* and *in vitro* behavior. Although there is growing evidence for existence of CE stem cells in the peripheral region of the cornea, these cells have not been precisely localized and characterized, delaying their possible use for graft preparation or induction of *in vivo* regeneration in patients. Despite the great efforts of many researchers around the World, it has not been possible yet to develop an effective protocol for culturing CE with a preserved phenotype similar to *in vivo* CE.

In order to expand the possibilities of preparing endothelial tissue for research or transplantation (Tx) purposes, we investigated the possibility of preparing CEC cultures from corneas containing residual (peripheral) CE after Tx, i.e. corneoscleral rims, or whole corneas excluded from the Tx process. Mainly the dual-media system developed for expansion of CECs obtained from high-quality corneas with good endothelial parameters was used. We also focused on investigating the localization of some molecular markers, e.g. CD166, Prdx6, GPC4, ZP4, etc., which expression exclusively by the CE was described in some studies, but their specificity was not confirmed by other studies. We also examined the presence and localization of other (bio)markers, such as CD44, K7, K19, α-SMA to investigate their possible presence in the native CE and *in vitro* prepared CE. Finally, we examined stem cell markers (Sox2, Oct4, Nanog) and proliferation marker (Ki-67) in the peripheral CE, where endothelial stem cells should be located.

The human amniotic membrane (AM, amnion), obtained from the placenta as waste after delivery by caesarean section, has long been known as an exceptional tissue with a wide range of uses. Amnion is used as an adjunct in the treatment of various types of wounds, especially when standard healing methods fail, and is also a relatively available source of stem cells that can be differentiated into desired tissue, such as liver, skin or nerve tissue via tissue engineering methods. In a multicenter study, we investigated a possibility of treating chronic, long-term non-healing wounds of common etiology (venous leg ulcers, diabetic foot ulcers, arterial or pressure ulcers, etc.) in which standard treatment methods failed, using AM allografts prepared in clean rooms under strictly sterile conditions. Given the importance of sterility of AM grafts, we explored the possibility of preparing a decontamination solution that would have properties similar to a certified commercial solution, which could be used as a replacement in the event of a supply outage or for financial reasons.

Due to the existence of differences between intact and de-epithelialized (denuded) AM, it is necessary to properly examine the areas of application of intact and denuded tissue. Previously published protocols have discussed the possibility of obtaining either de-epithelialized tissue or intact vital epithelial cells for further use. We explored the possibility of obtaining both in one step, by comparing different enzymatic technics.

Finally, we used cryopreserved or air-dried amnion allografts in a multicenter preclinical study in human patients, with non-healing skin wounds, to study the benefits of amnion application in wound healing. We hypothesized that AM allografts would cause wound healing, shorten wound closure time, and reduce pain more than standard-of-care method. We also hypothesized that the cryopreserved AM will be more efficient in wound healing than dry AM, due to the higher concentration of biologically active substances.

# Part I: Cornea and corneal endothelium

## Cornea – structure and function

The human cornea is the outermost transparent part of the eye, which allows light to enter the eye. This tissue is the strongest lens of the eye, having about +43 diopters. It consists of the following layers, from anterior to posterior: the corneal epithelium with its basement membrane, the acellular Bowman's layer, corneal stroma, the Descemet's membrane and corneal endothelium, Figure 1**.** The cornea is devoid of blood and lymphatic vessels, except its limbal zone, which is a border between corneal and conjunctival epithelium, and is an immunologically privileged tissue, due to the presence of very few immune cells, e.g. the antigen-presenting cells (Hamrah and Dana, 2007; Keino et al., 2018).

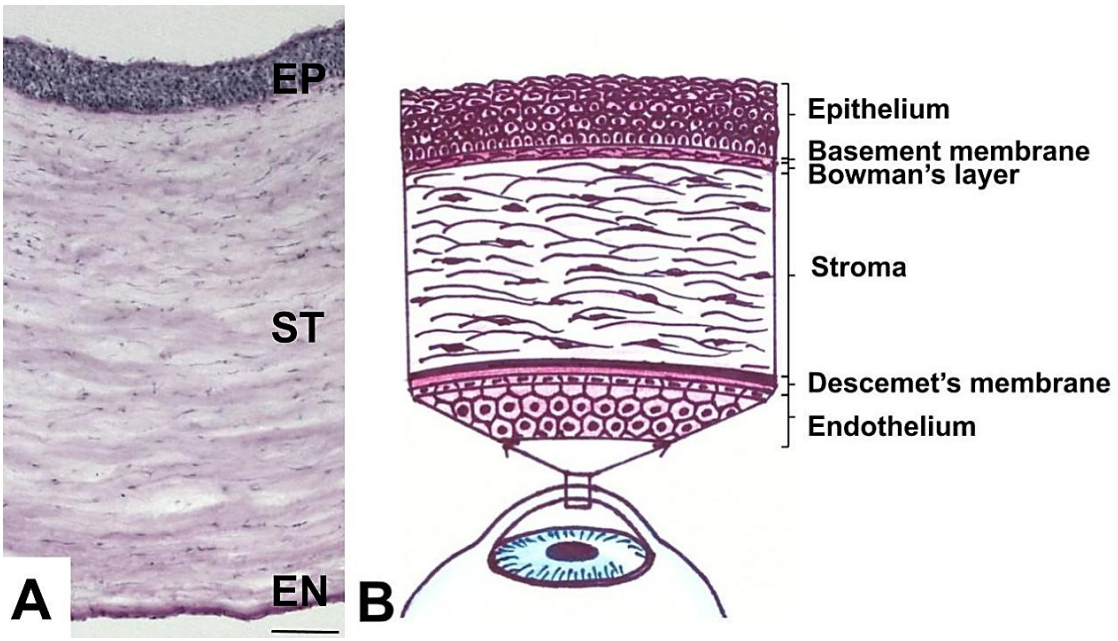


**Figure. 1** Cross-section of the human cornea. (A) A histological view; hematoxylin and eosin stained; EP = epithelium, ST = stroma, EN = endothelium; (B) A schematic view, showing the endothelial mosaic, *en face* view. Scale bar: 100 μm. Source: author's archive.

The corneal epithelium (EP) forms the 50 μm thick uppermost layer of the cornea. It maintains the smooth surface of the cornea and together with the tear film protects the cornea from external insults. The EP is formed from five to six layers of superficial, wing and basal cells (Pfister, 1973) and renewed approximately every seven days - sloughed off superficial cells are replaced by underlying cells, derived from mitotically active cells, i.e. basal cells, transient amplifying cells and the limbal stem cells (LSC) (Hanna et al., 1961) that reside within an undulated structure called the Palisades of Vogt (Goldberg and Bron, 1982). LSC

are normally slowly cycling cells, producing transient amplifying cells and basal cells which migrate towards the corneal center, where they differentiate to post-mitotic suprabasal wing cells and then terminally differentiated superficial squamous cells (Tseng, 1989). The LSC proliferation is increased in case of injury (Lehrer et al., 1998).

The corneal epithelial cells (EPC) produce about 40–60 nm thick basement membrane (BM) to which basal cells are strongly attached. The BM is rich in collagens (IV, VII, XII, XV, XVII, XVIII), fibronectin, fibrin, nidogen and is important for adhesion, cell polarity, migration, differentiation, signal transduction, cytokines (CK) and growth factor (GF) regulation and modulation of wound healing in case of injury (Toricelli et al., 2013).

Below the BM, the 8–14 μm thick Bowman's (BL) lies, which is produced by stromal cells. It consists of collagens (I, III, V, VII) and proteoglycans giving it its rigidity. The exact role of this layers is unknown, but it is supposed to maintain the corneal shape or strength (Wilson and Hong, 2000) and it may play a role in modulating the epithelial–stromal wound-healing process (Tong et al., 2019).

About 90% of human cornea is made up by corneal stroma (ST), 465 to 500 μm thick, which is crucial for normal visual function. The bulk of the ST is made of predominantly orthogonally arranged lamellae of type I, III, V, VI collagens (Komai and Ushiki, 1991). Stromal proteoglycans (lumican, keratocan, mimecan, decorin, biglycan) regulate spacing and orientation of the collagen fibrils, due to their hydrophilic nature (Muller et al., 2004). The stroma contains keratocytes (KCs), and low numbers of macrophages, dendritic cells and transient bone marrow derived cells (Hassel and Birk, 2010). KCs communicate with each other via their 3D network of lamellipodia and cooperate with EP (Wilson et al., 2014). The KCs produce components of extracellular matrix (ECM) and their cell turnover is usually 2-3 years (Ha et al., 2004). After corneal injury or during *in vitro* expansion KCs inevitably differentiate into corneal fibroblasts and lose the unique phenotype, characterized by CD34 transmembrane sialomucin, L-selectin and 3G5 ganglioside expression (Joseph et al., 2003; Stramer et al., 2004). Upon injury, regular organization of stromal fibrils is lost at the site of injury and KCs near the pathology can transform to myofibroblasts (characterized by expression of α-smooth muscle actin, α-SMA) and activated fibroblasts, producing disorganized matrix.

The Descemet's membrane (DM) is produced by corneal endothelial cells (CECs) during fetal development, and its production continues throughout the life, reflected as

thickening of DM. The DM is composed of collagens (IV, V, VI, VIII, XVIII), fibronectin, laminin, thrombospondin (Kabosova et al., 2007). Under physiological conditions, the DM helps maintaining the phenotype and function of CECs. After injury of CE, the DM supports its regeneration (Bhogal et al., 2017). DM is also an important regulator of fibrotic response after trauma, infection or disease (Toricelli et al., 2016). The DM cannot regenerate itself, but the CECs can cover the bare stroma and lay down new DM (Loh et al., 2018).

**Corneal endothelium and its function**

The corneal endothelium (CE) is the innermost layer of cornea, bathed with aqueous humor (AqH). It is a 4-6 μm thick monolayer, Figure 1, which preserves corneal transparency (Bonnano, 2012).

The term "endothelium", derived from its similarity to the vascular endothelium, is a misnomer (Shamsuddin et al., 1986). The CECs are derived from the neural crest (Bahn et al., 1986) and mesoderm (Gage et al., 2005) during fetal development, under action of a wide range of transcription factors, mainly Pitx2 and Foxc1 genes (Cvekl and Tamm, 2004; Bohnsack et al., 2012). The adult CECs have a mixed gene expression profile, as they express markers of neuronal origin, i.e. neuron-specific enolase or neural cell adhesion molecule (NCAM) (Chen et al., 2013; He et al., 2016), epithelial origin, i.e. keratins (K) K8, K18 (Merjava et al., 2009), K7, K19 (Foets et al., 1990) or produce proteins typical of mesothelial cells, i.e. mesothelin or calbindin-2 (Jirsova et al., 2010).

The CECs are polarized and have polygonal (mostly hexagonal) shape, Figure 2. Their apical surface covered by microvilli is highly interdigitated (He et al., 2016), containing various junctional complexes, such as focal tight junctions (macula occludens), gap junctions, characterized by protein zonula occludens (ZO-1) and adherens junctions (AJs), composed by type I cadherins (N-, E-, VE-cadherin) and associated proteins, i.e. α/ß-catenin, p120-catenin, etc., forming adhesion to actin cytoskeleton (Ickes et al., 2002; Zhu et al., 2008). Physiologically, the N-cadherin and VE-cadherin are at cell membranes, while E-cadherin is localized in the cell cytoplasm (Zhu et al., 2008; Wu et al., 2017). The N-cadherin seems to be specific for CECs, as it was not found in stromal KCs or EPC (Reneker et al., 2000, He et al., 2016). The N-cadherin maintains the functional cell-cell junctions and it serves as signal transducer influencing CECs differentiation and survival (Koh, 2012).

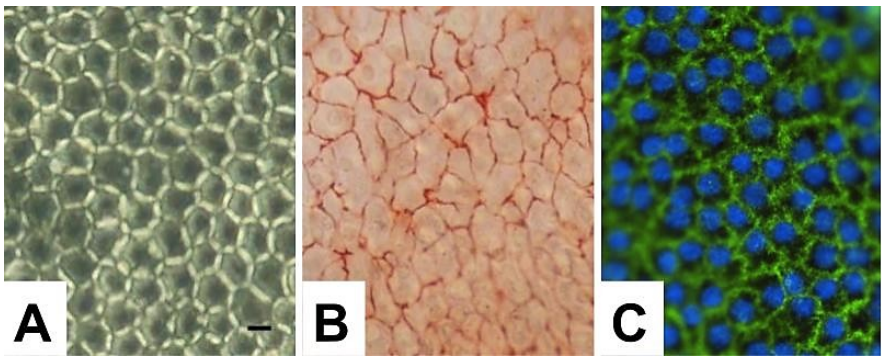


**Figure 2.** CECs mosaic: (A) light microscopic (phase contrast) view after swelling cell gaps with 1.8% (v/v) saccharose; (B) endothelium after staining with alizarin red S; c) immunofluorescent staining of the CECs membrane – Na+/K+-ATPase pump (green), DAPI (blue). Scale bar: 10 μm. Source: laboratory (A) and author's archive (B, C).

The CECs maintain the stable stromal hydration by "pump-leak" mechanism, where the CE pump rate equals the inward passive leak (Bonnano, 2012). The CECs actively pump excessive water and electrolytes, leaked through focal junctions, out from the hydrophilic stroma (Scott and Bosworth, 1990) using transport proteins, located at their basal-lateral membranes, such as Na+/K+-ATPase pump, carbonic anhydrase, solute carrier family 4 member 11/sodium borate cotransporter (SLC4A11) and many others (He et al., 2016).

Among all ocular cells, the CECs have the second highest aerobic metabolic rate, following retinal photoreceptors (Okumura et al., 2017). The native cells have up-regulated expression of metabolism genes, such as ENO1, GAPDH, CA3, LDHA, ALDOA, ATP5B, ATP5A1 (Chen et al., 2013; Chng et al., 2013). Other up-regulated genes in CECs are membrane transporters genes (SLC2A1, ATP5B, ATP1A1, ATP5A1), and genes of cytokine receptors and transcription factors (TFs) involved in transforming growth factor (TGF)-ß and Wnt signalling pathways, which are important in the development of the anterior cornea (Chng et al., 2013). Interestingly, out of 20 essential amino acids, only a cysteine seems to be indispensable for CE metabolism, cell growth and survival (Okumura et al., 2017).

The endothelial cell density (ECD) is about 6000 cells/mm$^2$ at birth but declines every year by about 0.3-0.6% to about 2300 cells/mm$^2$ by age 85 (Bahn et al., 1986). This marked decline in ECD is related to growth of cornea to its final size, approx. 11.75 mm in diameter (Murphy et al., 1984). After cell loss, the CECs enlarge and migrate to maintain overall CE pump function. The ECD below 500 cells/mm$^2$ leads to corneal opacification (Lass et al., 2010), due to CE thinning and loss of proteins participating on CE barrier integrity (Singh et al., 2013). The cell shape and size influence the functionality of CE monolayer. The size

of individual cells (polymegethism) and polygonality of cells (pleomorphism) reflect the quality of CE and are analyzed prior CE grafts are released for transplantation (Tx). They usually go hand in hand and affect the same cells. Shapes other than hexagonal are more frequently found in corneas suffering from trauma, pathological processes or older corneas (Laing et al., 1976).

## Corneal endothelium – repair and regeneration

### Regeneration of corneal endothelium

Anatomically, the peripheral CE is bordered by a smooth zone of CECs, called the transition zone (TZ), which merge into the trabecular meshwork (TM) area, Figure 3.

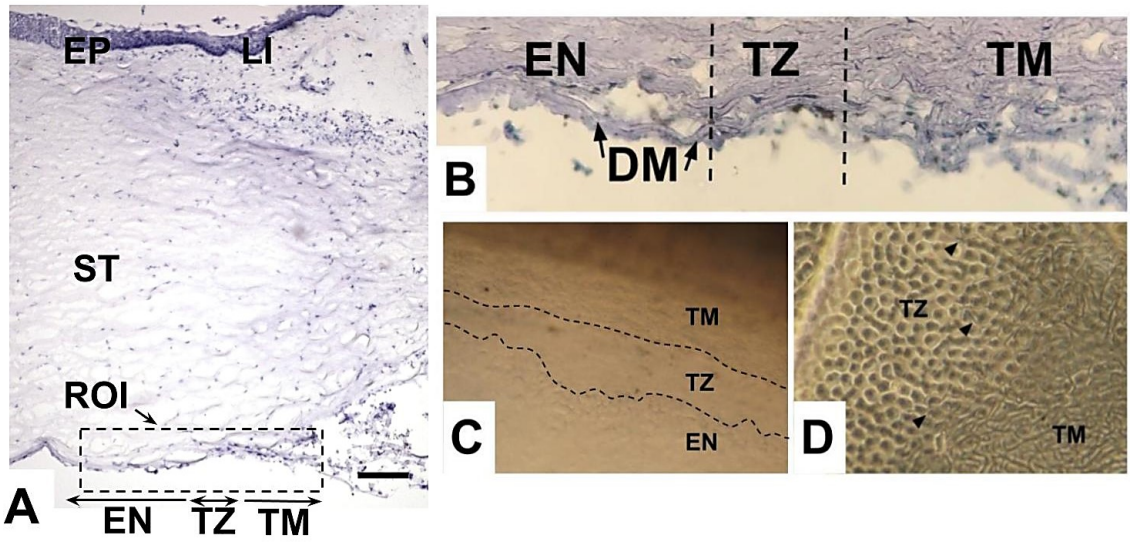


**Figure 3.** Periphery of the cornea. (A) A histological cross section; (B) A detail of periphery (hematoxylin dye). EP = epithelium, LI = limbus, ST = stroma, EN = endothelium, DM = Descemet's membrane, TZ = transition zone, TM = trabecular meshwork, ROI = region of interest; (C, D) *En face* view (phase contrast) of the corneal periphery from posterior side; (D) arrows in a TZ detail indicate TM fibers extending into the TZ. Scale bar: 100 μm. Source: author's archive.

Adult human CECs do not undergo cell division, as they are arrested in G1-phase of the cell cycle (Joyce, 2012a). Unlike in human, primates, pig or cat, the regenerative capacity of CEC was reported to be conserved in rodents and rabbits (Chen et al., 2017; Barnett and Jun, 2019). The CECs do not divide for several reasons: 1) suppression of S-phase entry by CK TGF-β, 2) an increased cellular level of cyclin-dependent kinase inhibitor (CKI) p27Kip1 due to formation of mature cell-cell contacts between CECs, 3) an increased level of CKI p21Cip1, induced by a transcription factor p53, due to DNA damage or lack of effective stimulation by GFs, despite their presence in the AqH (Joyce, 2012a).

It is believed that CE contains stem/progenitor cells in the CE periphery, including the TZ and TM, Figure 3. This is because in these regions an active DNA synthesis, telomerase activity, the expression of stem/pluripotency markers Sox-2, Oct-3/4, nanog, nestin or alkaline phosphatase have been found (Bednarz et al., 1998; McGowan et al., 2007; Joyce, 2012a; Yam et al., 2019). Moreover, in the peripheral CE, the expression of the leucine-rich repeat G protein-coupled receptor 5 (Lgr5), a target of Hedgehog and Wnt signaling that maintains proliferative potential of cells, was found (Hirata-Tominaga et al., 2013). The peripheral CECs also express low levels of proteins p53 and p63 that are known to be involved in the negative regulation of cell division (Paull and Whikehart, 2005).

In case of CECs death, either via necrosis (Corwin et al., 2013) or apoptosis (Fuchsluger et al., 2011), the CECs detach from the underlying DM and residual healthy CECs migrate over the denuded DM to close the wound. Thus, the CE is repaired by cell spreading/flattening and migration. It is associated to reorganization of actomyosin and microtubule networks (Gordon and Stanley, 1990) and reassembly of cell-cell junctions (Srinivas, 2010). The wound can be fully repaired within days or weeks, depending on a size and character of a defect, as well as a quality of the residual tissue (Mimura et al., 2013).

Even though the CE can migrate on a bare corneal stroma (Choi et al., 2010) the migration is slower than over bare DM, accompanied by gradual deposition of new DM by CECs (Soh et al., 2016). Various extracellular factors, such as ECM proteins, CKs, GFs, hormones, etc., can modulate the migration and spreading of CECs during wound healing and influence the integrity of the CE barrier (Ljubimov and Saghizadeh, 2015). Studies on various *ex vivo* wound models showed activation of mitosis in human CECs after injury, as a response to stimulation by growth promoting agents, such as animal serum, epidermal growth factor (EGF) or a combination of the two, with different cell cycle kinetics between old and young CECs (Zhu and Joyce, 2004).

**The influence of age on corneal endothelium repair**

The age has an impact on quality and repair/regenerative capacity of CE. In older corneas, telomere length decreases and DNA damage increases, leading to more senescent CECs than in younger corneas (Joyce, 2012a; Walshe and Harkin, 2014). This can be caused by oxidative stress from a constantly high mitochondrial activity of CECs (Drigeard Desgarnier et al., 2016) but also by a chronic exposure to UV irradiation (Gendron and Rochette, 2015). It seems that central CECs are more prone to oxidative damage by UV irradiation than the peripheral CECs, which are better protected against light (Doutch et al.,

2012). In older tissue the CECs have also an increased protein expression of CKIs, the p16INK4a and p21Cip1 (Enomoto et al., 2006). Moreover, the hyper-phosphorylation reaction of the Rb tumor suppressor, which is necessary for the S-phase entry of cells, is slower in older than in younger CECs, which partially explains the worsened response of older CECs to mitogenic stimulation (Joyce, 2012a). The expressions of proteins important for cell metabolism or protein degradation is altered in older CE (Zhu et al., 2008).

The CE possess the anti-oxidant systems, such as the membranous protein peroxiredoxin 6 (Prdx6), which reduces pre-oxidized membrane phospholipids (Lovatt et al., 2018) or the enzyme glutathione peroxidase 4 (Gpx4), which decreases lipid-peroxidation and thus protects CECs from oxidative stress, as shown on cultured immortalized CECs (Uchida et al., 2017). Antioxidants are present in AqH as well (Chowdhury et al., 2010).

The CECs from old donors can be expanded *in vitro*, but when propagated, the cells become larger and more variable in shapes than cells from young donors, expanded under same conditions (Zhu et al., 2008). Younger CECs reach confluence in shorter time than older CECs, and can be passaged more times, without occurrence of alternated morphology (Peh et al., 2011; Bartakova et al., 2018). The CECs from older corneas show weaker attachment to substrate after seeding than younger CECs. The older corneas seem to be better for Tx, as they have thicker DM, which allows easier unfolding of transplanted graft and its attachment to the recipient's stroma within a shorter time (Bennett et al., 2015).

**The endothelial-to-mesenchymal transformation**

The wound healing (Miyamoto et al., 2010) or *ex vivo* propagation (Wu et al., 2017) of the CECs may lead to unwanted phenotypic switch towards fibroblastic appearance, called the endothelial-to-mesenchymal transition (EnMT) (reviewed by Roy et al., 2015), which may affect the function of CE. If the switch lead to irreversible change of CE phenotype, i.e. loss of cell polarity and migratory fibroblastic phenotype, it can lead to corneal edema and haziness. During EnMT a massive reorganization of the actin cytoskeleton and activation of the RhoA GTPase occurs (Wheelock et al., 2008). The CECs transformed by EnMT start expressing the mesenchymal makers such as α-SMA and producing abnormal ECM components, such as type I collagen (Okumura et al., 2015a), which contrasts with physiological secretion of type IV and type VIII collagens. Corneal epithelium can undergo similar process, the epithelial-to-mesenchymal transition (EP-MT) (Loh et al., 2019).

The mechanisms underlying the EnMT in CE is still unknown. It seems that EnMT/EP-MT are complex processes, including various triggering factors, such as TGF-β, EGF, fibroblast growth factor (FGF), hepatocyte growth factor (HGF), interleukin-6, and a crosstalk between multiple signaling pathways (Loh et al., 2019): 1) canonical Wnt/β-catenin signaling, which is activated after disruption of cell junctions (Zhu et al., 2012), 2) the TGF-β/Smad and TGF-β/non-Smad signaling (Okumura et al., 2013), or 3) the FGF-2/SNAI1 (snail family transcriptional repressor 1) pathway (Lee et al., 2018), or 4) the Notch signaling (Li et al., 2013).

During EnMT, the overall gene expression is altered. The hallmark of EnMT is the upregulation of N-cadherin followed by the downregulation of E-cadherin, the phenomenon called cadherin switch (Wu et al., 2017). In CECs, the N-cadherin translocates from cell membranes into a cytoplasm of transformed cells (Zhu et al., 2012; Wu et al., 2017). Downregulation of E-cadherin is often found in malignant epithelial cancers. In case of EP-MT, the loss of E-cadherin expression alone is insufficient to drive cell transformation, but it is associated with more aggressive and less differentiated malignant cells and activation of several signaling pathways (Wnt/β-catenin, PI3K/AKT, TCF/LEF, RhoA), leading to a motile cell state. The E-cadherin downregulation is mediated through transcriptional inhibition by zinc finger protein SNAI and ZEB (zinc finger e-box binding homeobox) families of TFs, which upregulate an expression of fibronectin, vimentin and α1/α2 chains of type I collagen (Lee et al., 2018a; 2019). In certain tumors, a soluble form of E-cadherin expression is increased and seems to promote metastasis (Loh et al., 2019).

The β-catenin released after cleavage of E-cadherin, is translocated into a nucleus, where it can activate the expression of genes associated with a mesenchymal phenotype (α-SMA, vimentin) and work as a transcriptional activator for cell proliferation. The β-catenin activates the ras homolog gene family member A (RhoA), which is a GTPase, playing an important role in EP-MT and EnMT, together with the Ras-related C3 botulinum toxin substrate (Rac). RhoA induces the formation of actin stress fibers and the stabilization of N-cadherin mediated AJs, while Rac1 induces cytoskeletal reorganization and migration (Heuberger and Birchmeier, 2010; Niehrs, 2012). It seems that there exists a threshold in the level of nuclear β-catenin, which overrun leads to EnMT (Roy et al., 2015).

The EnMT manifests as pathological fibrosis in disease such as Fuchs endothelial corneal dystrophy (FECD) or formation of retrocorneal fibrous membrane (RCFM) between CE and DM after graft failure following penetrating keratoplasty or Descemet's membrane

endothelial keratoplasty (Kremer et al., 1993; Bayyoud et al., 2019). Besides RCFM formation *in vivo*, the EnMT negatively influences the *in vitro* expansion of CECs and thus, strategies to antagonize EnMT are being examined by various researchers. To revert EnMT, some TGF-β-signaling pathway inhibitors, such as SB431542 (Okumura et al. 2013; Beaulieu Leclerc et al., 2018) or the LY2109761 (Zhang et al., 2018a) can be possibly used.

Besides mesenchymal phenotype, the CECs can acquire abnormal epithelial-like morphology, called endothelial-to-epithelial transition (EnET). It occurs in diseases such as posterior polymorphous corneal dystrophy (PPCD) (Jirsova et al., 2007; Dudakova et al., 2019). In PPCD, the epithelial-like features occur within CECs, such as stratification of the normal CE monolayer, the expression of epithelial cell-associated keratins, such as K7 and K19 (Jirsova et al., 2007), and up-or down-regulation of endothelial-specific genes (Frausto et al., 2019). The altered morphology of CEC is most likely congenital and may progress throughout the life. The ZEB1 transcription factor is a master regulator of the EP-MT, its reverse reaction, and seems to also regulate EnET as well (Frausto et al., 2019).

**Preparation of a tissue-engineered corneal endothelial graft**

Cultivation of human CECs in a satisfactory quantity and quality for clinical use has proven surprisingly difficult. The main reason is naturally low proliferative capacity of adult CECs and changes of their phenotype during *ex vivo* expansion (Ueno et al., 2016), followed by EnMT and senescence (Okumura and Koizumi, 2020). The cultured CECs' transcriptome and proteome can vary according to donor, culture conditions and number of cell passage (Miayi et al., 2008; Hamuro et al., 2016; Frausto et al., 2016). Current culture protocols and techniques vary and a comparison of the results of such studies is difficult. No protocol specifically designed for clinical application has been established yet.

**Sources of corneal endothelial cells**

A replacement CE graft can be prepared by growing cells from several possible sources. The best candidates for the preparation of transplantable CE grafts seem to be the cells obtained from cadaveric corneas, which share about 88 % of genes with native CEC after *in vitro* culture (Thi et al., 2014; Frausto et al., 2016; Parekh et al., 2017). Due to complicated expansion of these cells, the alternative sources of CECs have been examined, either for experimental or clinical use, such as immortalized CEC (imCECs) (Frausto et al., 2016), induced pluripotent stem cells (iPSC) (Wagoner et al., 2018), embryonic stem cells (ESC) (Chen et al., 2018), corneal stromal stem cells (Hatou et al., 2013), multipotent progenitor cells isolated from trabecular meshwork (Zhang et al., 2018b), bone marrow cells

(Shao et al., 2011), umbilical cord blood cells (Joyce et al., 2012b), adipose tissue cells (Dai et al., 2014) or skin cells (Shen et al., 2017). Known disadvantages of ESC are the risk of tumorigenicity and immune rejection, iPSC can retain the epigenetic memory of its tissue of origin and cause oncogenesis, and imCEC can increase the risk of tumor development, aneuploidy and structural rearrangement of the cornea (Bartakova et al., 2014; Navaratnam et al., 2015). The *in vitro* propagated imCEC have a completely different gene transcription profile than the cells from cadaveric donors (Thi et al., 2014; Frausto et al., 2016).

**Storage of donor corneas**

Storage of donor tissue prior use may affect donor CE, and thus a quality of *in vitro* culture (Grabska-Liberek et al., 2003; Parekh et al., 2019a). The donor corneas for Tx are usually stored either in hypothermia at 4-8 °C (HT) or in organ cultures (OC) at 30-37 °C. Each of the two methods have its pros and cons. HT can induce apoptosis or necrosis (Corwin et al., 2013; Fuchsluger et al., 2011) thus should not exceed 14 days. Usually corneas stored for less than seven days in HT are used for Tx, as longer storage increases risk of primary graft failure, especially in patients with impaired ocular surface (Wagoner and Gonnah, 2005). Unlike HT, the OC corneas are nourished by a higher amount of regularly changed medium, which may promote repair of CE (Nejepinska et al., 2010), even in corneas of older (>50 years) donors (Slettedal et al., 2008). Survival of CECs during storage can be prolonged by addition of specific caspase inhibitors increasing CEC tolerance to cold stress (Corwin et al., 2013), gene therapy (Fuchsluger et al., 2011), or using specialized bioreactors to mimic eye environment (Garcin et al., 2019). Either the whole cornea or parts of the cornea, e.g. corneoscleral rims, remaining after Tx, can be used for CEC culture (Parekh et al., 2019b).

**Peel-and-digest method**

Current culture protocols standardly include a two-step procedure, called peel-and-digest method, which includes manual peeling of CE on DM lamella from cornea and the second step is an enzymatic digestion of DM (Choi et al., 2014; Parekh et al., 2017). The disadvantage of this method is that peeling is associated with CE death due to mechanical stress and possible co-isolation of stromal cells (Peh et al., 2012), which can rapidly outgrow CE in culture. Contaminating cells can be removed from the CE culture by, for example, centrifuging of the cell suspension in a density gradient (Okumura et al., 2015b) or separating the cells using magnetic particles (Peh et al., 2012). Another way is to distinguish CECs from other cell types in culture staining them for specific cell marker(s) and separating them

by flow cytometry (Okumura et al., 2014). Digestion is done with various reagents, such as EDTA (Bartakova et al., 2018), trypsin-EDTA mixture (Senoo and Joyce, 2000), collagenase (Engelmann et al., 1988), dispase (Ishino et al., 2004), or Accutase® (Hara et al., 2019). However, EDTA or trypsin-EDTA digestion can induce EnMT. Dispase II digestion is not as effective as collagenase A digestion (Li et al., 2007). Thus, collagenase is standardly used in current culture protocols, as it digests only DM and is gentle to cells.

**Seeding density**

The initial seeding density affects the proliferation rate and morphology of cultured CECs. When CECs, even that from young donors (19-35 years), are seeded at low density (25 cells/mm$^2$), their proliferation rate is high, but the cells usually undergo senescence and EnMT rapidly. Seeding density above 100 cells/mm$^2$ seems to be optimal (Peh et al., 2013), especially for seeding CECs from older donors, as a higher seeding density leads to a faster formation of confluent CEC monolayer (Parekh et al., 2017).

**Substrates for *in vitro* expansion of endothelium**

Proper cell substrate or coating of the culture plate is important, as they may influence survival, division and proper function of cultured CECs (Choi et al., 2014). Various substrates (biological, biosynthetic, synthetic), mimicking DM, have been tested for expansion of CECs (Teichmann et al., 2013; Navaratnam et al., 2015), for example, natural polymers, such as collagen, laminin, fibronectin, gelatin or FNC Coating Mix® (FNC), a mixture of fibronectin, collagen I and bovine serum albumin (Navaratnam et al., 2015). The best adhesion was observed when collagen IV, laminin or FNC were used (Engelmann et al., 1988; Yamaguchi et al., 2011; Peh et al., 2017).

Biological substrates, such as a decellularized human corneal stroma (Choi et al., 2010), human amniotic membrane (Ishino et al., 2004) or human crystalline lens capsule (Van den Bogerd et al., 2018a) were also tested.

The ideal substrate should mimic the thickness, transparency, porosity, elasticity of DM, which can be achieved by synthetic substrates. For example, the poly-ε-lysine crosslinked with octanedioic-acid (Kennedy et al., 2019), the collagen IV + laminin-coated collagen I film (Palchesko et al., 2016), or the poly(D,L-lactide), a highly transparent, biodegradable and non-toxic material, approved by FDA for use in the human body (Van den Bogerd, 2020) can be used.

**Culture medium, dual-media approach**

Culture medium and its supplements have a significant effect on the phenotype and differentiation capacity of the cells (Peh et al., 2011). Several culture media have been used for the expansion of CEC, such as the Dulbecco's Modified Eagle Medium (DMEM) (Ishino et al., 2004), DMEM/F12 (Noh et al., 2015), minimal essential medium (MEM) (Zhu and Joyce, 2004), M199 (Pistsov et al., 1988), F99 (Ham's F12/M199 in a ratio 1:1) medium (Engelmann and Friedl, 1995), endothelial growth medium 2 (Choi et al., 2014), endothelial serum free medium (Jackel et al., 2011), supplemented hormonal epithelial medium, which is the DMEM/F12 (1:1) + fetal bovine serum (FBS), EGF, dimethyl sulfoxide, cholera toxin, etc. (Li et al., 2007), and finally, an improved MEM, the Opti-MEM-I® (Zhu and Joyce, 2004; Bartakova et al., 2018) that contains insulin, transferrin, hypoxanthine, thymidine, and trace elements and thus allows one to keep cells in reduced serum conditions.

In current expansion protocols, F99 or Opti-MEM-I media are used the most (Peh et al., 2015, Frausto et al., 2016; Bartakova et al., 2018; Okumura and Koizumi, 2020). In fact, the most used method nowadays is the dual-media method (Peh et al. 2015), including two different culture media, the proliferation medium (PM), supporting proliferation of CECs, and stabilization medium (SM), allowing maintenance of CECs and preserving CEC phenotype before next passage.

Standardly, culture media are supplemented with FBS (5%-F99, 8%-Opti-MEM I), ascorbic acid, calcium chloride, chondroitin sulfate, antibiotics (AA) and GFs, such as EGF, basic FGF, or nerve growth factor (NGF) (Zhu and Joyce, 2004; Bartakova et al., 2018). Newer supplements include substances that were shown to inhibit apoptosis, significantly enhance adhesion, wound healing, and possibly also a proliferation of CECs, such as Rho associated coiled-coil containing protein kinase (ROCK) inhibitors Y27632, Y-30141, Y-39983 or thiazovivin (2,4-disubstituted thiazole) (Wu et al., 2017).

# Part II: Amniotic membrane

## Placenta and placental membranes – structure and features

The human placenta is a unique organ that, together with amniotic fluid, provides nutrition of fetus during pregnancy. Anatomically its structure does not resemble placenta of any common laboratory animal (Schmidt et al., 2015). A full-term human placenta is composed of the placental disc/chorionic plate, placental membranes and the umbilical cord (UC). The placental membranes include the amniotic membrane (AM) and the chorionic membrane (CM), Figure 4 (Bourne 1962; Huppertz, 2008).

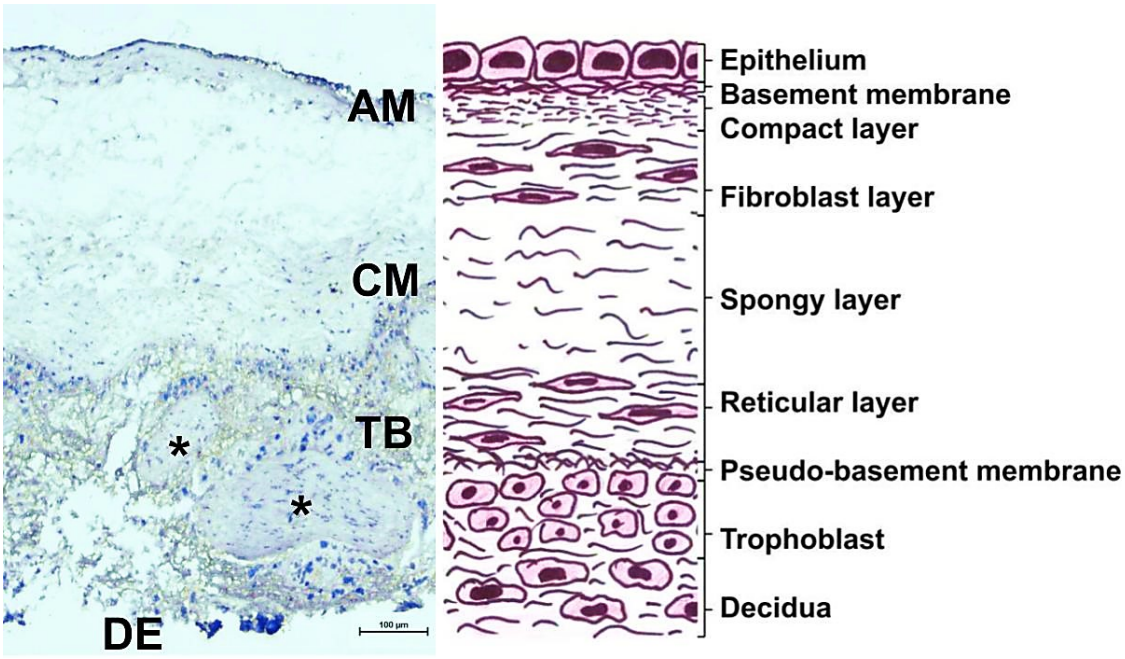


**Figure 4** Histological cross-section of human placenta; stained with hematoxylin (A) and the schematic view of placental layers from amnion to decidua (B). AM = amnion, CM = chorion, TB = trophoblast, DE = decidua, * = ghost villi (remnants of chorionic villi after atrophy during pregnancy). Scale bar (A): 100 µm. Sources: author's archive.

### Structure of amnion

AM is a 35–60 µm thin innermost layer of the placenta that surrounds the embryo/fetus and encloses the fluid-filled amniotic cavity (Benirschke et al., 2012). AM is derived from a layer of extraembryonic ectoderm; it does not contain blood or lymph vessels and is nourished by diffusion of nutrients from amniotic fluid and fetal surface vessels. The main function of AM is to protect the fetus from unwanted materials during intrauterine development (Toda et al., 2007; Benirschke et al., 2012).

AM can be separated from underlying CM by blunt dissection in an area of spongy layer, Figure 5, which is the result of incomplete fusion of the AM and CM mesoderm. Because the spongy layer of AM continues without sharp demarcation into the CM mesoderm, the dissected AM can be variable in its thickness (Niknejad et al., 2008).

AM is composed of five layers: the innermost layer of epithelial cells, basement membrane, compact layer, fibroblast layer and spongy layer, Figure 6 (A). The inner layer of AM is covered by a monolayer of metabolically active cuboidal epithelial cells (AECs), Figure 6 (B). The AECs are derived from the embryonic ectoderm. The AECs have many microvilli at their apical surface, large irregular nucleus with a large nucleolus and many pinocytic vesicles, as the cells are very metabolically active (Enders and King, 1988).

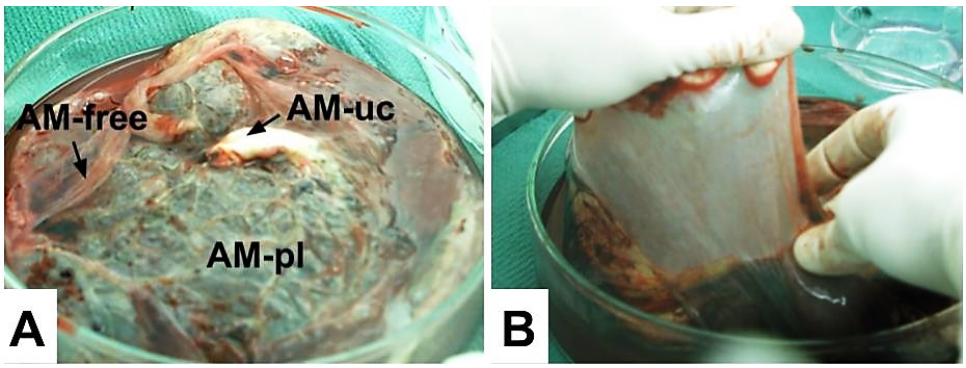


**Figure 5.** Placenta with anatomical regions of amnion (A) placental amnion (AM-pl), reflected amnion (AM-free) and umbilical cord amnion (AM-uc). (B) The AM can be separated from underlying chorion by blunt dissection. Source: laboratory archive.

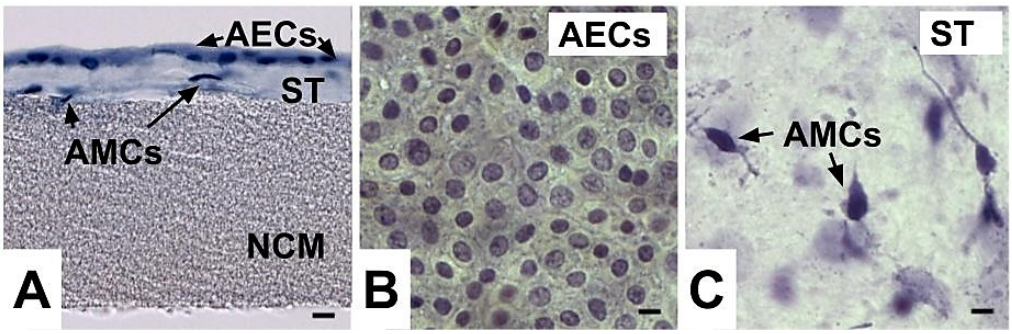


**Figure 6.** Amniotic membrane (AM) structure. (A) A histological cross-section of AM on nitroacetate-cellulose membrane (NCM) with a monolayer of epithelial cells (AECs) and stroma (ST) with mesenchymal cells (AMCs); (B) AECs; (C) stroma with AMCs. Tissue stain: hematoxylin, DAPI. Scale bar: 10 μm. Source: Jirsova and Jones (2017).

AECs contain populations of stem/pluripotency-like cells (AESCs). These cells express molecular markers such as stage specific embryonic antigen (SSEA)-4, tumor rejection antigen (TRA) 1-60 and TRA1-81, octamer-binding protein (Oct)-4, nanog, sex

determining region Y-box 2 (Sox2) or Kruppel-like factor 4 (Klf-4) (García-López et al., 2019) and do not express human leukocyte antigen (HLA) class II (Koike et al., 2014). These AECSs have a great clinical potential, as they can be differentiated towards multiple cell lineages, such as neuroectodermal, osteogenic, chondrogenic, etc. (Miki, 2018).

AECs are strongly attached to their basement membrane (BM), which is mainly composed of collagens (IV, V, VII), laminin and large amounts of proteoglycans, mostly heparan sulfate. It also contains actin, α-actinin, spectrin, ezrin, keratins, vimentin, desmoplakin that have a role in the structural integrity, modulation of cell shape and junctional permeability, influencing amniotic fluid transfer (Benirschke et al., 2012). AECs most probably produce also components of the compact layer, lying below the BM. This condensed acellular layer is composed of collagens (I, III, V, VI) and fibronectin and gives mechanical strength to AM (Farazdaghi et al., 2001).

The compact layer of AM sits on a fibroblast(ic) and spongy layer. The spongy layer is composed of wavy bundles of reticulum bathed in mucin and allows separation of AM from CM, Figure 5 (B). The spongy layer continues without sharp demarcation into the chorion leave. Both layers contain the scattered amniotic mesenchymal cells (AMCs) (Bulmer and Johnson, 1984; Whittle et al., 2000; Benirschke et al., 2012).

The amniotic stroma contains stem/pluripotent cells, the amniotic mesenchymal stem cells (AMSCs). The AMSCs express stem cell/pluripotency markers such as SSEA-3, SSEA-4, Oct-3/4, Sox-2, Rex-1, nanog, Klf-4, FGF-4 or frizzled family receptor- 9 (FZD-9) (Kim et al., 2007; Bilic et al., 2008; Fatimah et al., 2013; Ryan et al., 2013). AMSCs have multilineage differentiation potential, superior proliferation ability, immunosuppressive, and anti-inflammatory potential, which makes them suitable for research and clinical use.

## Amniotic membrane and its clinical potential

Biological and mechanical properties directly predispose AM for clinical use (Pogozhykh et al., 2018). Placenta is a waste product after birth and can be utilized for graft preparation without any ethical controversy. AM graft is transparent, lack immunogenicity, reduces pain and contain active substances that accelerate and support wound healing. AM promotes granularization, re-epithelialization, reduces fibrosis, angiogenesis, pain, and inflammation, and it has antimicrobial and anti-viral features (Jirsova and Jones, 2017).

AM is thin, elastic, air-permeable and adheres well to the wound surface, providing an effective covering of exposed nerve endings (Hajiiski, 1990). It leads to pain relief and keeps

wound moisturized (Talmi et al., 1990; Mohammadi et al., 2017). It speeds up healing, protects wound against infections, promotes leukocyte invasion of wound bed and reduces the exudation of interstitial fluid and hematoma formation (Park and Tseng, 2000; Shimmura et al., 2001; Li et al., 2005; Baradaran-Rafii et al., 2007).

AM promotes epithelialization by production of numerous growth factors: EGF, HGF, keratinocyte growth factor (KGF), and the two growth factor receptors (KGFR, HGFR) (Koizumi et al., 2000; Insausti et al., 2010). These active substances remain present in AM even after the tissue preservation (Shimazaki et al., 1998; Dua and Azuara-Blanco 1999).

The AM suppress fibrosis (scar formation) by downregulation of the TGF-β signaling cascade with reduced expression of TGF-β-1,2,3 and TGF-receptor II isoforms in cells in contact with AM. This leads to suppression of fibroblast and myofibroblast differentiation along with a decrease in the expression of biochemical markers of this differentiation, namely α-SMA, fibronectin and integrin α5 (Tseng et al., 1997).

The antimicrobial effects of AM are ensured by the expression of bactricidin, betalysin, lysozyme and transferrin. The cells of AM produce antimicrobial peptides, such as β-defensins (Mao et al., 2017), elafin, secretory leucocyte proteinase inhibitor (King et al., 2003; Buhimschi et al., 2004) and anti-virotics, such as cystatin E (Ni et al., 1997) and interferon-γ (Franco et al., 1999). The most importantly, it seems that some antibacterial properties of the AM are maintained even after storage (Tehrani et al., 2013). Some studies showed that AM alone is not that efficient in eliminating viral replication, thus a new concept of using AM as a sponge, soaked with antiviral drugs, which are gradually released into infected wound bed after grafting, have been successfully tested (Mencucci et al., 2011).

Inhibition of angiogenesis is another essential function of the AM. In ophthalmology, vascularization of the cornea is undesirable phenomenon, resulting from an inflammatory response to infection and trauma of the cornea. Vascularization of the cornea extending to the center of the cornea significantly reduces visual acuity. Potential keratoplasty has a significantly lower success rate in long-term graft survival in recipients with vascularized corneas. The AM was found to suppress neovascularization in corneas due to its action as a physical barrier to growth and migration of vascular endothelial cells, as well as due to release of anti-angiogenic factors, such as endostatin, thrombospondin-1, heparin sulphate proteoglycan, interleukin-10, tissue inhibitors of metalloproteases (TIMP-1 to -4), and pigment epithelium-derived factor (Kim and Tseng, 1995; Hao et al., 2000; Kobayashi et al., 2002; Shao, 2004). However, the AM seems to have also pro-angiogenic effects, as it

produces pro-angiogenic factors, such as angiopoietin 1, vascular EGF, basic FGF or platelet-derived growth factor-BB (Duan-Arnold et al. 2015). The angiogenic effect is most probably modulated by mesenchymal side of the AM (Niknejad and Yazdanpanah, 2014).

**Amnion in healing of ophthalmic wounds**

As the first field, where the AM has become an "established" treatment was ophthalmology in reconstruction of conjunctiva (de Rotth, 1940). The resurgence in use AM occured in the 1990s when it was reported by Kim and Tseng as an effective scaffold for ocular surface reconstruction (Kim and Tseng, 1995). Since then, the AM has become a helper for the treatment of the corneal and conjunctival defects, where the AM was used as a scaffold or as a bandage, Figure 7 (Dua et al., 2004; Meller et al., 2011).

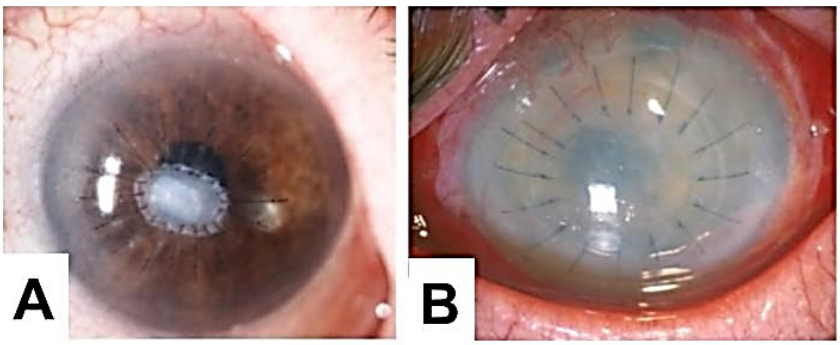


**Figure 7.** Transplantation of AM for treatment of corneal defects: (A) corneal ulcers (inlay technique); (B) non-healing condition after keratoplasty (overlay technique). Source: laboratory archive.

The BM of AM can provide a surface for growth of epithelium in cases where a spontaneous healing is difficult due to missing epithelial BM and BL, e.g. in persistent corneal epithelial defects (Lee and Tseng, 1997), infectious and neurotrophic ulcers (Chen et al. 2000), chemical and thermal burns of the cornea (Shimazaki et al., 1997). AM can be used as a filler to replace the missing corneal stroma in corneal ulcers. In these cases, it is possible to transplant AM in several layers and thus replace the stroma in its entire thickness, increasing the mechanical resistance of the damaged area of the cornea (Kruse et al., 2000).

Other ophthalmic indications include the possibility of conjunctival reconstruction, e.g. after pterygium surgery (Rosen, 2018), ocular scar pemphygoid or Steven-Johnson syndrome (Lee and Tseng, 1997). In patients with bullous keratopathy and low vision, coverage of cornea with AM is used for symptomatic pain relief (Chen et al., 2000).

**Amnion in healing of skin and other wounds**

AM represents almost an ideal biological dressing for treatment of skin wounds. In dermatology, the cryopreserved, air-dried or lyophilized (freeze-dried) AM was used as an alternative treatment for skin burns, diabetic foot ulcers, venous leg ulcers, pressure sores, and for patients with epidermolysis bullosa (Ilic et al., 2016; Haugh et al., 2017; Ahuja et al., 2019). Recent emergence of commercial AM products prompted its use in growing range of indications, especially treatment of chronic non-healing wounds (Ilic et al., 2016).

The use of AM grafts in the treatment of human wounds was started by Davis using both AM and CM to treat burned and ulcerated skin (Davis, 1910). AM is a near ideal temporary biological dressing for superficial (dermal) partial-thickness burns (Mohammadi et al., 2013). In extensive skin burns, the AM can be used as temporary skin cover and replacement, until the skin graft Tx (Fraser et al., 2009; Eskandarlou et al. 2016). Novel skin burns treatment methods include hydrogels or powders derived from AM (Murphy et al., 2019), which are easy to apply and show high healing efficacy (Rahman et al., 2019).

AM has been used in treatment of chronic non-healing wounds. Numerous clinical studies have demonstrated that AM increase frequency and probability of wound closure, compared to application of standard of care (SOC) methods (Haugh et al., 2017; Kogan et al., 2018; Serena et al., 2020). Many of these clinical trials used some of the commercially available products that are composed of both AM and CM, e.g. EpiFix, Grafix, AmnioExcel, etc. The presence of CM is likely to increase the amount of active ingredients beneficial to the treatment of chronic wound, as well as the longer duration of action, due to the slower degradation of the transplanted graft (McQuilling et al., 2017; Kirsner et al., 2020).

**Use of amnion in tissue-engineering**

The AM can be used as a scaffold for expansion of various cell types and as valuable source of cells that can be used in tissue-engineering and regenerative medicine. The AM can be used as a scaffold in form of intact membrane or as a decellularized carrier. More often, denuded AM is used as a scaffold for engineering of ocular surface (Lee et al., 2018b), blood vessel tissue (Lee et al., 2012), urothelium (Jerman et al., 2014) or bone (Tang et al., 2018) and cartilage regeneration (Keeley et al., 2014) regeneration. The mechanical properties of AM can be improved by chemical cross-linking, production of multilayer constructs or preparation of composites from AM and other materials, e.g. poly (lactic-co-glycolic acid), poly(L-lactide-co-ε-caprolactone), fibrin, silk fibroin, poly(ester) urethane or collagen and glycosaminoglycans (Arrizabalaga and Nollert, 2018).

## The preparation and storage of amnion grafts

The preparation of AM was first described by Lee and Tseng in 1997. The standard protocol includes donor selection, screening for transmissible diseases (HIV-1/2, hepatitis B and C, syphilis, etc.), collection of AM after caesarian section to avoid AM contamination by vaginal pathogens and processing AM under sterile conditions (Adds et al., 2001; Dua and Azuara-Blanco, 1999). Each AM from a single donor is processed as one batch of grafts.

### Preparation and decontamination of amnion for grafting

AM is obtained from the placenta, which is taken after a caesarean section at the end of a full-term pregnancy from a healthy mother who has signed an informed consent. The mother is carefully selected and serologically examined (hepatitis B and C, syphilis, HIV). The collected placenta is placed in a sterile container in the delivery room and transported dry or poured with physiological saline or decontamination solution into a tissue bank, where it should be processed into AM grafts within 24 hours (Keitel, 2019).

Standardly is the AM peeled off the placenta by blunt dissection, Figure 8, starting either from the placental edge towards the UC or in opposite direction. AMs are properly rinsed from blood clots and any remnants and the thin AM is transferred onto a proper carrier for better manipulation and side orientation. Such carrier can be either as the nitroacetate cellulose membrane (NCM) (Kim et al., 2001) or non-woven polyester mesh Sanatyl® (Tylex, Czech Republic). AM is placed usually with the epithelial side up, while stromal part adheres well onto carrier. AM is then cut into pieces and stored (Malhotra and Jain, 2014).

To ensure safety of AM grafts for future recipients, any remaining potential pathogens must be removed from the AM by proper decontamination. First, the placenta alone, then the separated placental membranes (AM, CM) are repeatedly rinsed with physiological saline (PS) and decontamination solution (DS). The DS is composed of an antibiotic–antimycotic (AA) cocktail often consisting of penicillin, streptomycin, neomycin, and amphotericin B, based on previously described methods (Kim et al., 2001; Malhotra and Jain, 2014). However, each laboratory can use its own (in-house made) DS if it is approved by local authorities. The only available tissue DS with certification based on European Directive 93/42/EEC is the BASE128 (Alchimia, Italy), which contains amphotericin B, cefotaxime, gentamicin, and vancomycin in RPMI 1640 medium (Gatto et al., 2013).

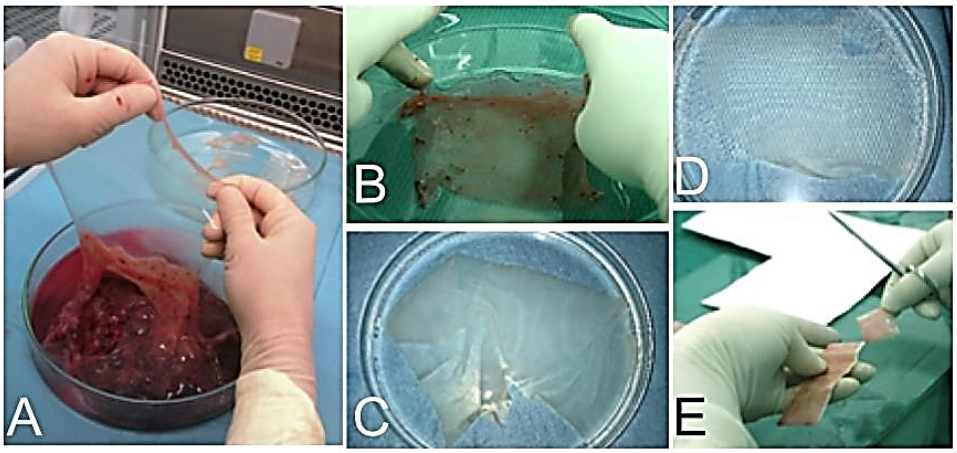


**Figure 8.** Preparation of AM grafts from placenta under aseptic conditions. (A) The AM is peeled off the decontaminated placenta; (B) blood clots are removed from AM by repeated washing; (C) after decontamination of AM, the tissue is transferred onto medical non-woven polyester mesh Sanatyl® (D) or NCM (E) and cut into smaller grafts that are then cryopreserved (-80 °C), lyophilized or air-dried (RT). Source: laboratory archive.

Alternatively, the sterilization of AM can be performed via gamma radiation (25 kGy), which is often used after freeze-/air-drying (Singh et al., 2003; Gajiwala and Gajiwala, 2004). However, the gamma radiation leads to irreversible morphological changes and loss of active substances in AM, thus its use is limited (Paolin et al., 2016). The negative effects of irradiation on AM may be diminished by bathing AM in glycerol (Ab Hamid et al., 2014).

**Storage of amnion**

In most countries, it is not possible to use a fresh (non-preserved) AM grafts clinically due to the legislative requirement to repeat the serological test examination of the living donor at least 180 days after tissue collection in order to cover the time (diagnostic) window for the potential transmission of communicable diseases. AM is thus stored by various methods. It can be stored in a dried state, as the air-dried AM or freeze-dried (lyophilized) AM, or frozen at low temperatures (-80°C), i.e. cryopreserved, Figure 9. These storage methods do not preserve cell viability well (Hennerbichler et al., 2007), but the presence of living AM cells is not essential for the success of Tx. The method of AM storage influences also structural integrity and content of bioactive substances in AM (Johnson et al., 2017).

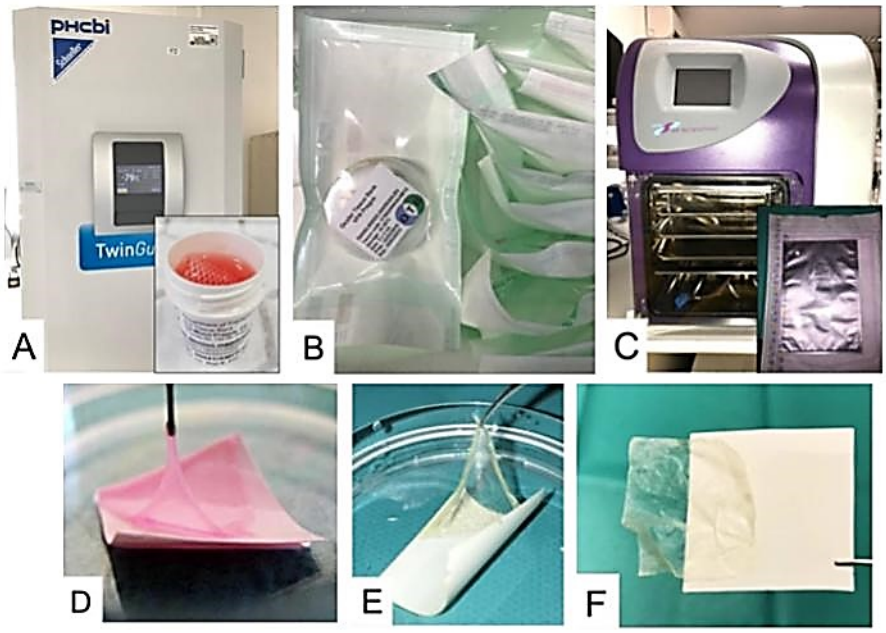


**Figure 9.** Storage of amnion (AM). (A) Cryopreserved AM is stored in DMEM/glycerol (1:1) medium at -80°C; (B) air-dried AM is stored in a sterile package at room temperature after drying in a biosafety cabinet; (C) lyophilized AM is prepared in a specialized machine (lyophilizer) and stored in a sterile package at RT. (D-F) AM grafts on NCM carrier either intact (D), re-hydrated (E) or dry (F). Source: laboratory and author's archive.

The most used storage method for AM is cryopreservation (Kim and Tseng, 1995), which is safe and effective for a long-term storage (Thomasen et al., 2009). AM samples are usually stored in a DMEM medium with glycerol (ratio 1:1) at -80 °C up to 5 years. Frozen AM excels with its high elasticity, good adhesion and simple handling. A structure of such AM closely resembles fresh AM (Wagner et al., 2018). Cell viability in cryopreserved AM decreases during storage but some vital cells can be recovered in thawed samples (Hennerbichler et al. 2007). The major drawbacks of cryopreservation are variations from the preparation process and the requirement of a deep-freezing facility.

Other common method of AM preservation includes air-drying. AM stretched on a support, such as an NCM, is usually dried overnight to 24 h at room temperature (RT) in a biosafety cabinet (Singh, 2003). After drying, gamma sterilization may follow (Baradaran-Rafii et al., 2007). Then, the AM is stored in a sealed package at RT until use. After rehydration, dried AM is less elastic than cryopreserved AM, which makes it difficult to handle it during surgery. The air-drying devitalizes AM cells and cause degradation of ECM, which is further enhanced by gamma sterilization (Ab Hamid et al., 2014).

The freeze-drying (lyophilization) is a process that prevents massive damage of sample caused by the direct transition of water from a liquid to a gaseous state (Burgos, 1983). The AM is freezed at -50 to -80 °C and dried under a high vacuum using lyophilizer, until 5–10% of residual water. This is followed by gamma irradiation of AM (Allen et al., 2013). Or AM can be chemically decontaminated and packaged into sterile bags before lyophilization (Dhall et al., 2018). Lyophilization allows storage and shipment of AM at RT but leads to devitalization of cells and partial deterioration of proteins (Rodríguez-Ares et al., 2009). Using saccharide lyoprotectans and controlled cooling rate, allow preparation of AM comparable to cryopreserved AM (Dhall et al., 2018).

**De – epithelialization of amnion**

Clinically, mostly intact AM (iAM) has been used for wound treatment. De-epithelialization of AM uncovers the BM, which may improve epithelial cell attachment and proliferation. Denuded AM (dAM) is used as a biological substrate on which various cell types can be seeded (Koizumi et al., 2007) or it can be applied directly into the wound bed to promote re-epithelialization. dAM supports growth of cells, such as LESCs, better than the iAM (Koizumi et al., 2007), suggesting that structural components of AM are more important for cellular growth that soluble factors in AM (Ilic et al., 2016). The iAM supports undifferentiated stem cell phenotype (Utheim et al., 2018).

# Hypotheses and aims of work

**Corneal endothelium (Hypothesis 1, H1):**

**Corneal endothelium contains stem/progenitor-like cells in the endothelial periphery, which allows preparation of endothelial graft from discarded corneas with preserved endothelial periphery; the endothelial cell phenotype can be confirmed with novel markers referred to be specific to corneal endothelium.**

Normal adult human corneal endothelium contains mitotically silent cells that are arrested in G1-phase of the cell cycle and stem/progenitor cells that are thought to reside in the corneal periphery and the transition zone between endothelium and trabecular meshwork. First, the expression of classical stem/pluripotent cell markers (Sox-2, Oct-3/4, nanog, nestin, etc.) has been detected in this region, and second, cells isolated from the periphery exhibit higher proliferation capacity *in vitro* than cells from the central part of cornea.

The transition zone is still poorly characterized and is uncertain if putative endothelial progenitors are sequestered in specific niches inside the transition zone or elsewhere in the endothelial layer. Some studies found stem/pluripotency marker expression mostly in corneas with incomplete or wounded endothelium.

Based on available research data, we hypothesized that we find a positive expression of selected stem/pluripotency markers in the periphery of corneal endothelium in both normal and wounded corneas. We also assumed that due to the expected existence of stem cells in the periphery of the endothelium, we would be able to prepare confluent endothelial cultures from discarded corneas and corneocleral rims with preserved corneal periphery, as a way for an increase of a pool of available donor endothelium for research or grafting.

Endothelial cell graft prepared by tissue engineering methods, as an alternative to deficient donor corneas, must be accurately identified via expression of specific phenotypic markers and correct functionality. A combination of several markers (Na+/K+-ATPase, ZO-1, NCAM, CD166, etc.) is used to confirm the phenotype of healthy corneal endothelium. Despite proposal of some endotehlial-specific markers, such as CD166, CD200, GPC4, PRDX6, none of these markers has been confirmed. We assume that novel endothelial markers will be expressed only in the endothelial layer of the native (healthy) and damaged corneas and will also be expressed in *in vitro* prepared endothelial cells and not in other corneal cells. This would confirm the specificity of these molecular markers and allow their use for identification of endothelial phenotype.

**Aims:**

- To detect stem/progenitor markers in the periphery of corneal endothelium and transition zone of corneas excluded from transplant program to confirm their specificity.
- To investigate the possibility of *in vitro* culturing endothelial cells isolated from donor corneas excluded from transplant program with preserved endothelial periphery under different conditions to find the best ratio between proliferation and endothelial phenotype.
- To characterize an expression of cell markers, reported to be specific to corneal endothelial cells in human corneal tissue and in *in vitro* endothelial cultures and confirm their potential use for identification of endothelial phenotype.

**Corneal endothelium (Hypothesis 2, H2):**

**Wounded corneal endothelium of corneas with preserved endothelial periphery containing stem/progenitor-like cells, will be repaired/regenerated faster than the endothelium of corneas lacking the endothelial periphery (Paper 1).**

In case of wounding, the corneal endothelium is primarily repaired by enlargement and migration of remaining CECs toward the lesion to cover the denuded area. It is known, that under physiological conditions, human CECs are arrested in the G1-phase of the cell cycle, but they retain their proliferative potential. As the most probable location of cells with proliferative activity and potential stem/progenitor cell-like character was suggested the periphery of the cornea, we supposed that these progenitor cells may participate in wound healing of centrally damaged corneal endothelium. Due to lack of human corneas for research, we decided to use some reliable mammalian model – the pig. The porcine tissue was suggested as a close equivalent of human tissue due to anatomical and biochemical similarities. Physiologically, the porcine corneal endothelial cells do not proliferate *in vivo*.

We presumed that centrally injured porcine corneal endothelium in corneoscleral tissue with preserved transition zone will be repaired/regenerated faster than that present in corneas lacking the transition zone. Based on our previous results we supposed that organ culture of tissue will allow more efficient wound healing compared to more frequently used hypothermic storage. We presumed that the healing will be positively influenced by serum concentration in organ culture medium.

**Aims:**

- To introduce mechanically damaged pig corneas as a mammalian model for assessment of corneal endothelial wound healing.
- To determine whether the endothelium of pig corneas with preserved corneal periphery and transition zone will repair faster and more efficiently than endothelium of corneas lacking the peripheral areas after a mechanically induced damage to central endothelium.
- To compare reparative capacity of corneal endothelium in corneas stored under various organ culture conditions (serum concentration, storage period) to find the best wound healing conditions (the most extensive and fastest reparation).

**Amniotic membrane (Hypothesis 3, H3):**

**In house-made decontamination solution has similar effect on amniotic cell viability, as well as antimicrobial efficiency and stability than the commercial decontamination solution (Paper 2 and 3).**

The amniotic membrane must be safe for patient. The safety of tissue is ensured by a collection of placentas from healthy mothers after elective caesarean section and following strict aseptic conditions during tissue processing. Despite that, there exists a risk of transmission of contamination to recipient originating from the donor or the operating/clean room environment. Therefore, the amnion intended for grafting must be chemically decontaminated or sterilized by radiation before storage of grafts. For grafting, we standardly prepare cryopreserved amnion, as this method preserves the biologically active substances in tissue better than other methods. Since the sterilization with radiation can destruct the structure of extracellular matrix components, we use chemical decontamination prior storage of amnion grafts. For that we can use the only commercially available and certified decontamination solution in Europe. Since this solution is not always available due to outages and its price is growing, we supposed that it would be possible to prepare a cheaper alternative to that solution, the laboratory decontamination solution, which could be approved by the national authority. We anticipated the similar antimicrobial activity, stability and cytotoxicity for our solution as the commercial solution possess.

**Aims:**

- To prepare tissue decontamination solution as an alternative to the only available certified commercial solution on European market, for its approval by national authority.

- To test our solution for its effect on amniotic (epithelial, stromal) cell viability and compare the results to commercial solution **(Paper 2)**.
- To compare the antimicrobial efficiency and stability of our solution with those reported for the commercial solution **(Paper 3)**.

**Amniotic membrane (Hypothesis 4, H4):**

**Using a gentle method for de-epithelialization of amniotic membrane, it is possible to obtain both, viable epithelium and intact denuded membrane simultaneously, for their further clinical/experimental use (Paper 4).**

The amniotic membrane can be used either with intact epithelium (intact amnion) or without it (denuded amnion). Clinically, the intact amnion is used for transplantation, as it contains higher levels of growth factors and its preparation is easier and faster than preparation of denuded amnion. However, due to favorable chemical composition of the basement membrane of amnion, the denuded amnion seems to be more suitable as a substrate for the re-epithelialization of exposed surfaces (eye, skin.) than intact amnion. In case of ocular surface reconstruction, the denuded amnion promotes faster growth of the ocular cells and suppresses local inflammatory and fibrotic response better than intact amnion. Amniotic epithelial cells that are released from amnion during de-epithelialization have a great clinical potential for use in the treatment of various diseases, as the cells are multipotent and nontumorigenic. They can be used also to produce cell-conditioned media.

Multiple de-epithelialization protocols for AM have been developed already, but the goal of such studies was to maintain either viable epithelial cells or intact matrix of amniotic membrane, especially intact basement membrane. We hypothesized that it is possible to develop a decellularization protocol where both, intact cells and intact amniotic membrane matrix can be obtained simultaneously, which would shorten the preparation of the denuded amnion and allow further use of the viable cells as well.

**Aims**:

- To develop an efficient, gentle and safe de-cellularization protocol to obtain both living epithelial cells and denuded amnion with intact structure in one step.

**Amniotic membrane (Hypothesis 5, H5):**

**Amnion grafts, prepared according to the protocol we use, stimulate and facilitates wound healing of non-healing skin wounds.**

Non-healing/chronic wounds present a substantial humanistic and economic burden to healthcare systems worldwide and have devastating effects on quality of life of patients. Treatment and care of such wounds can account for three percent of total healthcare expenditure in developed countries. The most prevalent form of non-healing wounds in the western world are low leg (lower limb) wounds that have various etiology (venous, arterial, diabetic, traumatic, other) and about 20-25 % of them become chronic. As using a standard-of-care method often leads to incomplete wound closure or its recurrence, the trend is to change standard-of-care method for biomedical, biological or hybrid wound care systems.

AM is considered as an ideal biological wound dressing because it promotes granulation and epithelialization, reduces the quantity of exudate, relieves pain, and provides moist environment for healing. In last decade its efficiency has been broadly confirmed in other fields, such as dermatology, plastic surgery or genitourinary medicine. Nowadays, the cryopreserved, air-dried or lyophilized AM allografts are available from tissue banks or from companies, offering commercial products. In the Czech Republic therapy using amnion is standardized only for reconstruction of ocular surface.

We used the cryopreserved or air-dried amnion allografts in a pre-clinical study on human patients, suffering from frequent non-healing wounds, to study the benefits of the amnion application on wound healing. We hypothesized that amnion allograft will induce wound healing, shorten the time of wound closure and reduce pain more than standard-of-care method. We also hypothesized that cryopreserved amnion will be more efficient in wound healing than dry AM, due to higher concentration of biologically active substances.

**Aims:**

- To prepare amnion graft for healing of chronic wounds in Czech Republic.
- To assess the benefits of amnion application in diverse groups of frequent non-healing wound, particularly, venous leg ulcers and diabetic foot ulcers, via measuring the size of the non-healing wounds in time until complete healing and observation of patient for possible recurrence of wound during a follow-up period.

## Material and methods

To achieve the aims of our work, a wide spectrum of methods was used. Individual material and methods are described in the appended publications or within a following paragraphs, regarding papers and hypotheses (H1 -H5). Author managed following steps:

**Paper 1 (H2): Endothelial wound repair of the organ-cultured porcine corneas**

- Processing of porcine tissue, mechanical tissue damage, cultivation of damaged tissue;
- Monitoring the repair of damaged endothelium - histological staining, microscopy;
- Evaluation of endothelial parameters (cell density, hexagonality, coefficient of variation) from taken photographs of the samples;
- Immunohistochemical (immunofluorescence) analysis of porcine tissue;
- Statistical analysis.

**Paper 2 (H3): Comparison of cytotoxicity of two decontamination solutions**

- Processing of placentas and preparation of amnion samples;
- Monitoring the cell vitality (live/dead assay, trypan blue staining) in tissue before and after decontamination – histological staining, microscopy, immunofluorescence;
- Evaluation of cell vitality from taken photographs of the samples;
- Statistical analysis.

**Paper 3 (H3): Antimicrobial efficiency and stability of two decontamination solutions**

- Preparation of decontamination solutions;
- Analysis of stability (pH changes, osmolality) during cold storage of the solutions;
- Data analysis and statistical analysis.

**Paper 4 (H4): The enzymatic de-epithelialization technique for amnion**

- Processing of the placenta and preparation of amnion samples;
- De-epithelialization of amnion and isolation and culture of the amnion cells;
- Preservation of denuded amnion and histological and immunohistochemical staining of the tissue.

**H1 (not published): Preparation of corneal endothelial cell culture and analysis of corneal tissue for stem/progenitor cells and endothelial-specific markers**

- Preparation of *in vitro* corneal endothelial cell cultures from discarded cadaverous tissue and monitoring the growth of the corneal endothelial cells – microscopy;
- Preparation of corneal tissue for immunohistochemical analysis – cryosectioning, flat-mounted corneas, *in vitro* cultures, cell imprints and immunohistochemistry
- Data analysis and statistical analysis.

**H5 (not published): Amnion grafts for healing of chronic wounds.**

- Preparation of amnion allografts from placentas in clean room facility;
- Evaluation of wound healing from taken photographs by software analysis;
- Preparation of amnion/chorion samples for biochemical and histological analysis.

**Material and methods regarding H1 (corneal endothelium)**

**Material**

Human endothelial serum free medium + L- glutamine (**h-SFM**), Opti-MEM I 1X medium with HEPES, 2,4 g/L Sodium Bicarbonate and L-Glutamine (**Opti-MEM I**), medium M199 with GltaMAX-I and Earle's Salts (**M199**), F-12 1X with L-Glutamine (**F12**), DMEM - high glucose, GlutaMAX(TM), HEPES (**DMEM**), Insulin-Transferrin-Selenium 100X (**ITS**), Fetal Bovine Serum (**FBS**), Phosphate buffered Saline 100X (**PBS**), TrypLE Express without Phenol red (**TrypLE**), Collagenase Type I (**Col I**), MEM Vitamins Solution 100X (**vitamin mix**), Antibiotic-Antimycotic 100X (**AA**), Bovine Pituitary Extract (**BPE**), Recombinant Human Epidermal Growth Factor (**EGF**), Recombinant Human β-NGF (**NGF**), heat-stable Recombinant Human FGF-β (**FGF**) (all from Gibco); L-Glutathione reduced, Chondroitin Sulfate A sodium salt from bovine trachea (**ChS**), Chemically Defined Lipid Mixture 1 (**lipids**), Trypan Blue, L-ascorbate, Triton X-100 surfactant, bovine serum albumin (**BSA**), paraformaldehyde (**PFA**), Tween 20 (all from Sigma-Aldrich), Penicillin – Streptomycin 100X (**Pen-Strep**, Serana), Gentamicin Sulfate (Biosera), ROCK-inhibitor Y-27632 (Wako Chemicals GmbH), Human FNC coating (**FNC**) (Athena Enzyme Systems), VISCOAT® Intraocular Viscoelastic Injection (Alcon), normal goat serum (Serotec, Bio-Rad), 4′,6-Diamidine-2′-phenylindole dihydrochloride (**DAPI**) or propidium iodide (**PI**) – Vectashield anti-fade mounting medium (Vector Laboratories), Millicell 0,4 μm cell culture inserts (Merck Millipore Ltd.), optimal cutting temperature (**OCT**) medium for frozen tissue

specimens Cryomount® (Histolab Products AB), Mouse and Rabbit Specific HRP/AEC (ABC) detection kit (ab93705, Abcam), BASE128 (Alchimia), Glycerolum 85% (Dr. Kulich Pharma s.r.o), Piperacilin/tazobactam 4500 mg (Fresenius Kabi s.r.o.), Fungizone Squibb, 50 mg (Bristol Myers), Vancomycin, 500mg (Mylan), Gentamycin, 80 mg/2ml (Sandoz).

**Research-grade human cadaver corneal tissues**

The human corneal tissue was collected by the National Cell and Tissue Centre (Brno, Czech Republic) and Eye Bank Prague (Prague, Czech Republic). The whole corneas were excluded from transplantation process due to slight corneal haziness or missing epithelial layers. The corneoscleral rims without central CE were obtained as a surplus after eye surgery performed in either General University Hospital in Prague (Prague, Czech Republic) or University Hospital Královské Vinohrady (Prague Czech Republic). The average surface area of the CE was 104.9 $mm^2$ (whole corneas, diameter 11.5 mm) and 54.6 $mm^2$ (corneoscleral rims), Figure. 10. The donated research-grade tissue was stored under hypothermia (4-8 °C) in Eusol-C storage medium, Figure 10.

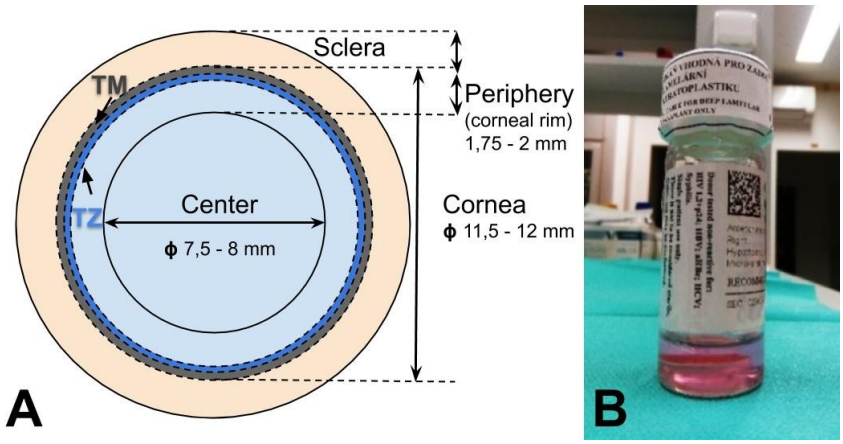


**Figure 10** (A) A scheme of the regions found in cornea (*en face* view from posterior side) and their sizes; TZ = transition zone, TM = trabecular meshwork. (B) The corneal tissue stored in Eusol medium prior their experimental use. Source: author's archive.

**Cell isolation and cell culture**

For isolation and culture of CECs, a total of 59 donor corneal tissues (40 rims and 19 whole corneas) were procured. Donors' age ranged from 23 to 78 years; the endothelial cell density was 2,200 cells/$mm^2$ at least. Before use, the tissue was rinsed with PBS and the quality of CE was examined by 0.2% (v/v) TB in PBS staining (2 min.) and response of cells to 1.8% (v/v) sucrose in PBS. Then tissue was rinsed with 1X Pen-Strep and 50 µg/ml gentamicin in M199/F12 medium.

A two-step, peel-and-digest method was applied for primary CEC isolation, as described elsewhere (Choi et al., 2014). Briefly, CE-Descemet's membrane (CE-DM) lamellas were carefully peeled under a dissecting microscope and incubated overnight at 37 °C in stabilization medium (SM1), Table 1. Next day, the tissue was incubated with 2 mg/ml Col I and 20mg/ml $CaCl_2$ in SM1 for 2 hours at 37 °C, followed by centrifugation at 550 x g for 8 min., with washing steps using PBS. The cells were further dissociated with 1X TrypLE for 10 min., at 37 °C, stopping the reaction with a selected PM, Table 1.

**Table 1.** Stabilization and proliferation media used for endothelial culture.

| | | | |
|---|---|---|---|
| **Stabilization media (SM)** | | | |
| **Acronym** | **Basal medium** | **FBS** | **Supplements** |
| SM1 | h-SFM | 15% | 1X ITS, 50 µg/ml gentamicin and 0,1X Pen-Strep |
| SM2 | h-SFM | 5% | 1X ITS, 50 µg/ml gentamicin and 0,1X Pen-Strep |
| | | | |
| **Proliferation medium (PM)** | | | |
| **Acronym** | **Basal medium (reference)** | **FBS** | **Supplements** |
| PM1 | Opti-MEM I (Zhu and Joyce, 2004) | 8% | 5 ng/ml EGF, 20 ng/ml NGF, 10 ng/ml FGF, 200 mg/l $CaCl_2$, 0,005% lipids, 1X AA, 50 µg/ml gentamicin, 1X vitamin mix, 20 µg/ml L-ascorbate, 0,08 % chondroitin sulfate, 0,5 mM L-glutathion |
| PM2 | Opti-MEM I (Zhu and Joyce, 2004, modified) | 8% | 100 µg/ml BPE, 5 ng/ml EGF, 10 ng/ml FGF, 10 µM Y-27632, 200 mg/l $CaCl_2$, 1X Pen-Strep, 50 µg/ml gentamicin, 20 µg/ml L-ascorbate |
| PM3 | M199/F12 (1:1) (Peh et al. 2013) | 5% | 10 ng/ml FGF, 10 µM Y-27632, 1X ITS, 20 µg/ml L-ascorbate, 1X AA, 50 µg/ml gentamicin, 0,5 mM L-glutathion |
| PM4 | M199/F12 (1:1) (Peh et al. 2013, modified) | 5% | 100 µg/ml BPE, 10 ng/ml FGF, 5 ng/ml EGF, 10 µM Y-27632, 1X ITS, 20 µg/ml L-ascorbate, 1X Pen-Strep, 50 µg/ml gentamicin |

Propagation of CECs was achieved using a dual media culture system (Peh et al., 2015; Bartakova et al., 2018), with slight modifications. For cell propagation, two types of basal media were used, either Opti-MEM I, or M199/F12 (1:1), varying in supplements, Table 1. The cells were seeded onto 8-well Lab-Tek chamber slides or Thermanox coverslips (Nunc), coated with FNC. In some cases, the cells, seeded at approx. 110 – 180 cells/mm$^2$ were covered by 50 µl of the viscoelastic solution (Viscoat®). PM was exchanged every other day and the cell culture progress was observed by phase contrast microscopy until confluence (4 weeks on average). After the CEC reached confluence, cells were incubated in SM2, until their hexagonal morphology was restored (5-7 days on average). The cell density was measured from photo-documentation with NIS Analysis Software. Another (rather minor) approach used in the study was an explant culture, culturing whole CE-DM lamellae, instead of isolated cells. The isolation and culture method used was the same as for the single cells, omitting the lamella digestion steps and use of Viscoat.

**Indirect immunofluorescence, enzyme immunohistochemistry**

Protocols used for indirect immunofluorescence staining of tissue (whole corneas/rims, CE imprints and cryosectioned tissue) are summarized in Table 2. The original protocols were slightly modified. The specimens were examined using Nikon Eclipse Ni-U H600L microscope and images were taken using Nikon DS-Fi3 camera (both Nikon Corporation, Tokyo, Japan). Corneal cryosections/cross-sections (7-µm thin) were prepared by slicing a liquid nitrogen-frozen tissue embedded in OCT and stored at -80°C until use. Some molecular markers were detected in tissue cryosections by enzyme immunohistochemistry, using Mouse and Rabbit Specific HRP/AEC (ABC) detection kit, by fixing the corneal cryosecions with cold acetone (10 min.) and staining the samples according to the kit manufacturer's protocol.

**Table 2.** Protocols used for immunofluorescence staining of corneal tissue in this study.

| Step | Flat mount | CE imprints on Millicell membranes | Cryosections | Primary cells |
|---|---|---|---|---|
| **Reference** | Hirata-Tominaga et al. 2013; Yam et al. 2019 | Merjava et al. 2009 | Merjava et al. 2008; Forest et al. 2015 | Frausto et al. 2015; Peh et al. 2017 |
| **Reaction vessel** | 24-well culture dish | Sample placed CE side up on a glass coverslip | Glass slide | 8-well chamber slide |
| **Fixation** | 2% PFA, 30 min., RT | cold acetone, 10 min | 0,5% PFA, 30 min., RT | 0,5% PFA in PBS, 30 min., RT |
| **Permeabilisation** | 1% Triton X, 10 min, RT | - | 0,2% Triton X-100, 10 min | 0,5% Triton X-100, 30 min., RT |
| **Non-specific binding block** | 2% BSA+ 5% normal goat serum, 30 min, 37°C | 2,5% BSA, 30 min., RT | 5% goat serum in PBS, 1h, RT | 5% goat serum in PBS, 1h, RT |
| **Primary antibody* (ATB) – see Table 3.** | 1h, 37°C; ATB diluted in 1% BSA | 1h, RT; ATB diluted in 1% BSA | 1h, RT, or overnight, 4°C, solvent: 5% goat serum | 1h, RT, or overnight, 4°C, solvent: 5% goat serum |
| **Secondary ATB - See Table 3** | 1h, 37°C; solvent: in 1% BSA | 1h, RT; solvent: 1% BSA | 1h, RT, solvent: 10% goat serum | 1h, RT, solvent: 10% goat serum |

*Primary antibody was omitted in negative control (NK) tissues.

The primary and secondary antibodies used for immunofluorescence or immunohistochemistry in this study are summarized in Table 3. Each antibody was diluted in either BSA in PBS or blocking buffer (FBS + BSA + PBS) solution.

**Table 3.** Primary and secondary antibodies used in the study. Rb = rabbit, Ms = mouse.

| **Primary antibody** | **Source and clone** | **Cat. No.** | **Dilution** | **Company** |
|---|---|---|---|---|
| 5HT1D Receptor | Rb poly | ab140486 | 1:40 | Abcam |
| Alpha smooth muscle actin | Ms mon (1A4) | ab7817 | 1:100 | Abcam |
| CD44/HCAM | Ms mon (DF1485) | sc-7297 | 1:50 | Santa Cruz Biotechnology |
| Anti-CD166 | Ms mon (TAG-1A3) | MABN1785 | 1:100 | Merck, Sigma Aldrich |
| Keratin 7 | Rb mon (D1E4) | 4465 | 1:100 | Cell Signaling |
| Keratin 19 | Rb mon (EP1580Y) | ab52625 | 1:500 | Abcam |
| Glypican 4 | Ms mon (51E3) | NBP2-49892 | 1:50 | Novus Biologicals |
| LGR5 | Ms mon (OTI2A2) | TA503316 | 1:25 | OriGene Technologies |
| MRGX3 | Rb poly | ab140863 | 1:50 | Abcam |
| Nanog | Ms mon (NNG-811) | ab62734 | 1:50 | Abcam |
| Oct4 | Rb mon (EPR17929) | ab181557 | 1:100 | Abcam |
| Prdx6 | Ms mon (TAG-2A12) | MABN1797 | 1:50 | Merck, Sigma Aldrich |
| Sox2 | Rb poly | ab97959 | 1:100 | Abcam |
| ZO1 | Ms mon (ZO1-1A12) | 33-9100 | 1:100 | Thermo Fisher Scientific |
| ZP4 | Rb poly | LS-C160968 | 1:50 | LSBio |
| Ki67 | Ms mon (MIB-1) | M7240 | 1:100 | Agilent, Dako |
| Na/K-ATPase-α1 | Ms mon (C464.6) | 05-369 | 1:100 | Merck, Sigma Aldrich |
| | | | | |
| **Secondary antibody** | | **Cat. No.** | **Dilution** | **Company** |
| Alexa Fluor 488-conjugated goat anti-mouse IgG | | A-11029 | 1:400 | Thermo Fisher Scientific |
| Alexa Fluor 594-conjugated goat anti-rabbit IgG | | A11037 | 1:400 | Thermo Fisher Scientific |

**Material and methods in experimental part regarding H5 (amnion):**

Human AM grafts for transplantation were prepared by manual dissection of the tissue from placentas of healthy donors, obtained after caesarean section delivery. The donors signed informed consent and their blood was screened for common transmissible diseases (hepatitis B and C, syphilis, HIV). The tissue was prepared under strictly aseptic conditions

following standardized protocols, approved by the State Institute for Drug Control. The AM intended for cold storage (-80°C) or air-drying were prepared within 24 hours after birth.

Briefly, each placenta was stored in a decontamination solution BASE128 until the next day from the date of birth. Then, the placenta was delivered to clean room and processed aseptically. AM was peeled off by blunt dissection. The AM sheets were repeatedly rinsed with sterile saline and BASE128 solution until the tissue was clean and then it was decontaminated with in-house made decontamination solution. After decontamination for at least 2 hours, the tissue was repeatedly rinsed with BASE128 and sterile saline and placed on the Sanatyl fabric, epithelial side up. The grafts of appropriate size were cut out and either stored in DMEM/glycerol (1:1) storage medium and immediately cryopreserved or air-dried inside of the biosafety cabinet for 24 hours, then packed into sterile bags and stored at RT.

**Application of amnion grafts onto chronic wounds**

AM grafts approved for transplantation, i.e. released after min. 6 months since graft preparation and re-testing the donor blood for transmissible disease, were applied by collaborating doctors at the clinic to patients selected according to predefined project criteria (age ≥ 18 years, the presence of resistant non-healing wounds for longer than 6 weeks, a wound size between 6 $cm^2$ to 105 $cm^2$, etc.). The wound treatment included regular wound care in the sense of debridement, cleaning the wound. The AM was applied epithelial side towards the wound bed, a good adherence assured (air bubbles removed) and covered by dressings to assure the wet environment. The wound bandage was done once a week.

**Analysis of the wound healing score**

The wound healing rate was observed on a regular basis and photographs of the wound were taken. The following parameters were assessed: the change of wound size/area/volume, granulation and epithelialization progress (%), curve of closure progress (wound area/volume change per week), and the time to complete healing (if applicable). The wound area was determined by semiautomatic analysis of images from photo-documentation, using NIS Analysis software (Nikon). The information collected in Wound-Quality-of-Life (QoL) questionnaire were continuously evaluated. The final values included statistical report on healing progress and QoL improvement. Wounds were defined as healed if a complete closure (100% re-epithelialization) occurred without drainage and need for dressing. Durable closure was assessed at a follow-up visit scheduled two weeks and 6-12 months after the complete healing/or three-month treatment.

# Results

In the following text, the most important published results (Paper 1 - 4) and yet unpublished data (Hypothesis 1, 5) are summarized. For more details, please see the appended publications.

## Part I: Corneal endothelium

### Results regarding H1: Preparation of an *in vitro* cultured corneal endothelium

Donor corneal tissue (n = 59), either whole corneas (n= 19) or corneoscleral rims (n=40) with a mean age of 57.78 ± 12.88 years, male:female ratio of 51:8 were used for this study. The most serious obstacles to endothelial cultivation due to quality of donor tissue were: the insufficient number or areas of dead CECs in donated corneoscleral rims, DM folds with the presence of dead CECs (mostly in whole corneas), areas with detached or denuded DM, and the presence of iris residues, Figure 11.

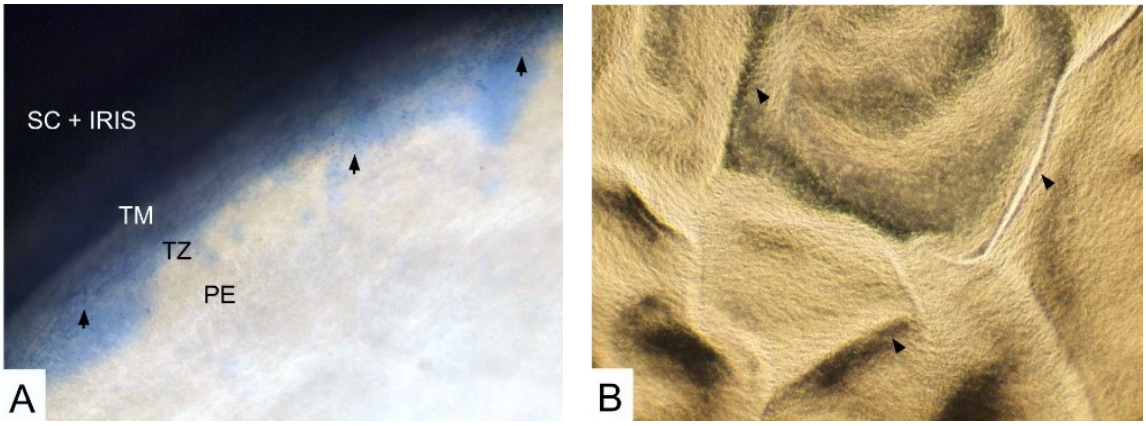


**Figure 11.** The most common issues with endothelium in donated research-grade corneas, used in this study. A) Areas of dead cells (arrows) within PE, TZ and TM; B) DM folds (arrows) where dead cells are present. SC = sclera, TM = trabecular meshwork, TZ = transition zone, PE = peripheral endothelium. Source: author's archive. Magnification 40x.

The confluent CE monolayers could be prepared by either the explant method or peel-and-digest method, the second being slightly more successful, Table 4. In average, 38.98% (23/59) of all prepared cultures were considered as successful, i.e. if the CE covered 80-100 % of one 0.8 $cm^2$ well of the Lab-Tek II 8-well chamber slide (0.64 – 0.80 $cm^2$) and the cells had a cobblestone-like morphology after incubation in SM2, Figure 12 and 13.

**Table 4.** Success of CEC *in vitro* culture. Overall, 59 donor tissues - 19 whole corneas and 40 corneoscleral rims (rims) were processed. The CECs were isolated either as explant tissue or using peel-and-digest method (PD).

| **Successful *in vitro* corneal endothelial cultures** | | | |
|---|---|---|---|
| **Method** | **Success ratio** | **Donor age (years)** | **Hypothermic storage (days)** |
| Explant method | 28.5% (2/7) | 76.0 ± 1.41 (75-77) | 7.50 ± 0.71 (7-8) |
| PD method | 40.38% (21/52) | 54.90 ± 12.80 (28-71) | 15.14 ± 4.87 (6-23) |
| Both isolation methods | 38.98% (23/59) | 56.82 ± 13.67 (28-77) | 14.68 ± 5.19 (6-23) |
| Rims vs. successful cultures<br>Rims vs. all rims<br>Rims vs. all PD rims<br>Rims vs. all cultures | 52.17% (12/23)<br>30.0% (12/40)<br>30.30% (10/33)<br>20.34% (12/59) | 55.10 ± 14.08 (28-71) | 12.08 ± 4.14 (6-18) |
| Corneas vs. successful cultures<br>Corneas vs. all corneas<br>Corneas vs. all PD corneas<br>Corneas vs. all cultures | 47.82% (11/23)<br>57.89% (11/19)<br>57.89% (11/19)<br>18.65% (11/59) | 54.70 ± 12.15 (35-70) | 17.80 ± 4.69 (11-23) |
| | | | |
| **Failed *in vitro* corneal endothelial cultures** | | | |
| **Method** | **Failure ratio** | **Donor age (years)** | **Hypothermic storage (days)** |
| Explant method | 71.43 % (5/7) | 61.20 ± 9.07 (49-69) | 8.80 ± 5.02 (4-16) |
| PD method | 59.62 % (31/52) | 59.0 ± 12.77 (23-78) | 18.07 ± 7.64 (9-41) |
| Both isolation methods | 61.02% (36/59) | 59.33 ± 12.19 (23-78) | 16.67 ± 7.99 (4-41) |
| Rims vs. successful cultures<br>Rims vs. all rims<br>Rims vs. all PD rims<br>Rims vs. all cultures | 47.82% (11/23)<br>70.0% (28/40)<br>69.7% (23/33)<br>47.45% (28/59) | 59.63 ± 12.66 (23-78) | 13.75 ± 4.21 (4-21) |
| Corneas vs. successful cultures<br>Corneas vs. all corneas<br>Corneas vs. all PD corneas<br>Corneas vs. all cultures | 45.0 % (9/20)<br>42.11% (8/19)<br>42.11% (8/19)<br>13.56% (8/59) | 58.56 ± 11.52 (34-69) | 24.44 ± 10.51 (10- 41) |

In a case of the peel-and-digest method, the CEC were isolated either by 0.2% EDTA, dispase or collagenase treatment, with the latest being the most successful method. EDTA or dispase treatment did not release the adequate amounts of CECs from DM, compared to collagenase treatment, which led to digestion of DM into fragments, after reaction time of at least two hours at 37 °C. Thus, this enzyme was implemented in a standard cell isolation protocol. Further digestion of cell isolated with 1X TrypLE Express (for 10 -15 min.) led to an increased number of single cells, but in all the cases, a portion of cell clusters remained after the second digestion.

The CEC were cultured in various media, Table 1, and observed daily for morphology, growth pattern, and proliferation rate. Standard pattern of cell culture is shown in Figure 12 (64 years old donor) and Figure 13 (36 years old donor). Up to 3.2 $cm^2$ or 6.4 $cm^2$ of CE were prepared from a single rim or cornea, respectively. The final cell densities were on average 848.5 ± 443.5 cells/$mm^2$ and were slightly higher in cultures derived from younger donors. The overnight stabilization of manually peeled CE-DM lamellae in SM1 improved the success of ongoing *in vitro* culture, compared to the culture without stabilization step, and thus this step was implemented in a standard protocol. The SM2 improved the morphology of CECs, propagated in PM, as it reduced the portion of fibroblast-like cells within culture, however the final CE monolayers contained up to 10% of these cells.

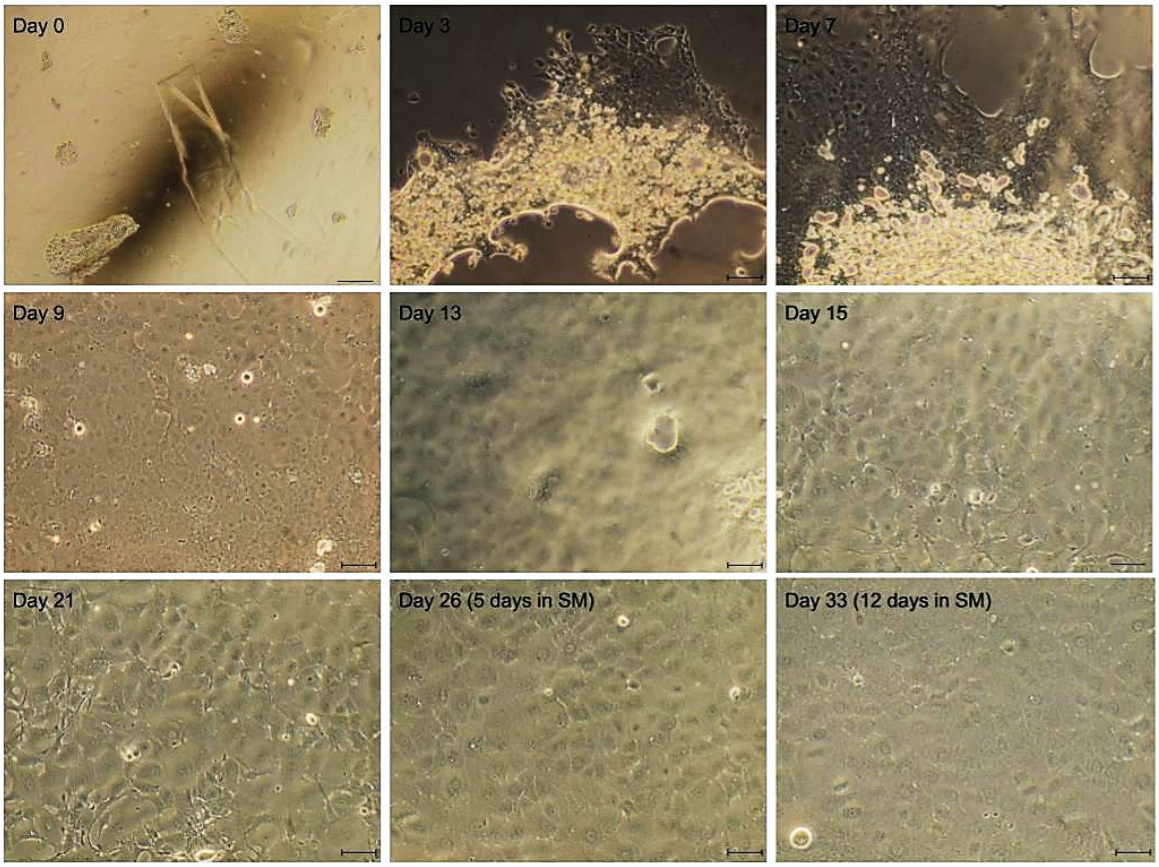


**Figure 12.** *In vitro* propagation of primary CECs in dual-media system (phase contrast microscopy). CEC were isolated from a whole cornea (64 years old donor), stored hypothermically for 11 days and stabilized overnight in SM1 prior processing. CEC were propagated in proliferation medium (PM4) in 8-well chamber slides until confluence (21 days), followed by stabilization medium (SM2) for 12 days to observe changes in monolayer. Endothelial cell density (at day 33) was 603.5 ± 309.1 cells/$mm^2$, i.e. 48277 ± 31212 cells/0.8 $cm^2$ culture area. The portion of fibroblast-like cells after SM2 culture was 7.0 ± 3.0 %/$mm^2$. Scale bar: 100 μm.

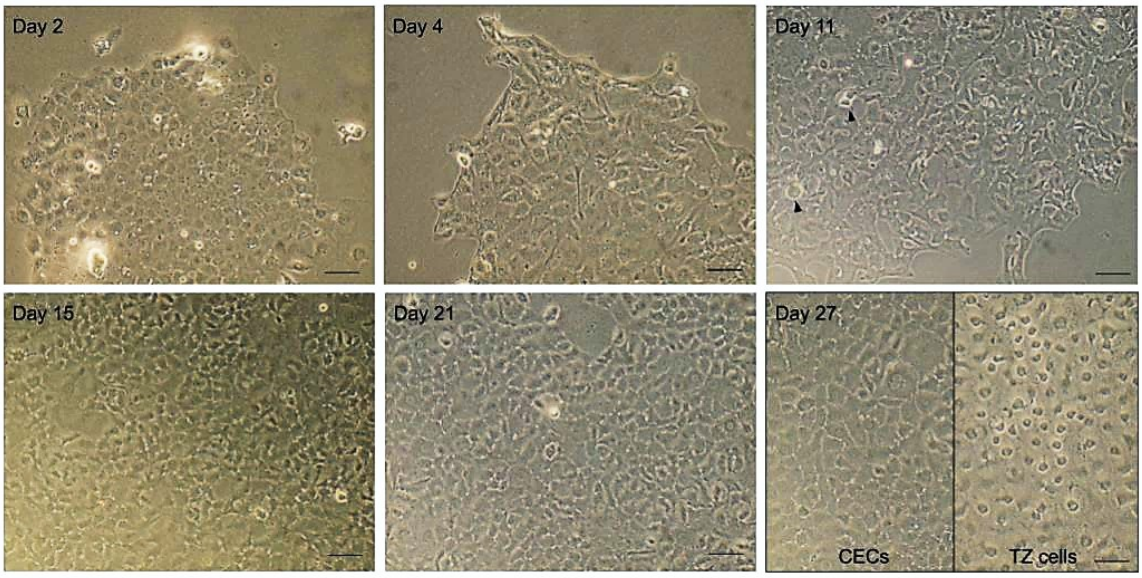


**Figure 13.** *In vitro* propagation of primary endothelial cells in dual-media system (phase contrast microscopy). CEC from a corneal rim (38 years, female), stored at 4 °C for 18 days, stabilized overnight in SM1 prior processing and propagated in 8-well chamber slides in proliferation medium (PM4), until confluence (27 days). Two types of cells were observed, the CECs and probably the transition zone (TZ) cells. Endothelial cell density (at day 27) was 1050.2 ± 255.6 cells/mm$^2$, i.e. 84018 ± 20445 cells/0.8 cm$^2$ culture area culture area. The portion of fibroblast-like cells at day 27 was 1.5 ± 0.7 %/mm$^2$. The incubation of SM2 was not included due to CECs hexagonality. Scale bar: 100 µm.

The unsuccessful cultures (61.02%) were characterized as those without attached cells after cell seeding, with no mitosis, but with a presence of apoptosis, senescent cells, or with irreversible fibroblastic changes of majority of CECs, Figure 14. The average age of donors and hypothermic storage length of unsuccessful cultures are summarized in Table 4.

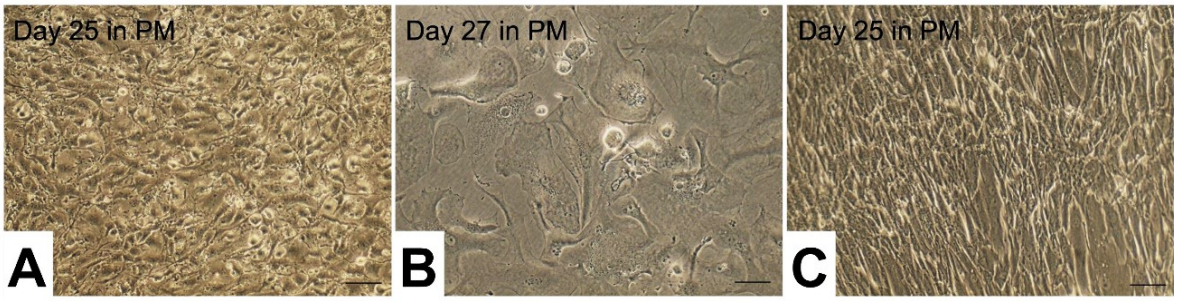


**Figure. 14** The unsuccessful corneal endothelial cultures (phase contrast). A) Fibroblastic (endothelial-to-mesenchymal) transformation of CEC; B) Senescent CECs C) Stromal fibroblasts or trabecular meshwork cell contamination. Scale bar: 100 µm.

In the end, we expanded CECs in two media – PM2 and PM4 that led to the most successful cultures. The most successful medium was the PM2 (60%), followed by PM4 (58.33%), i.e. the Opti-MEM I or M199/F12 based media supplemented with BPE, EGF,

FGF and ROCK inhibitor Y-27632. These were followed by PM3 (47.06%), i.e. M199/F12 supplemented with FGF and Y-27632 and the PM1 (20%), which was the least efficient. Slightly more mitotic cells (observed by phase contrast microscopy) and Ki-67 positive cells (observed by immunofluorescence) were detected in CE grown in PM2 (14.17%) than in PM4 (11.76%), Figure 15. However, the PM4 produced less K7-positive CECs than PM2.

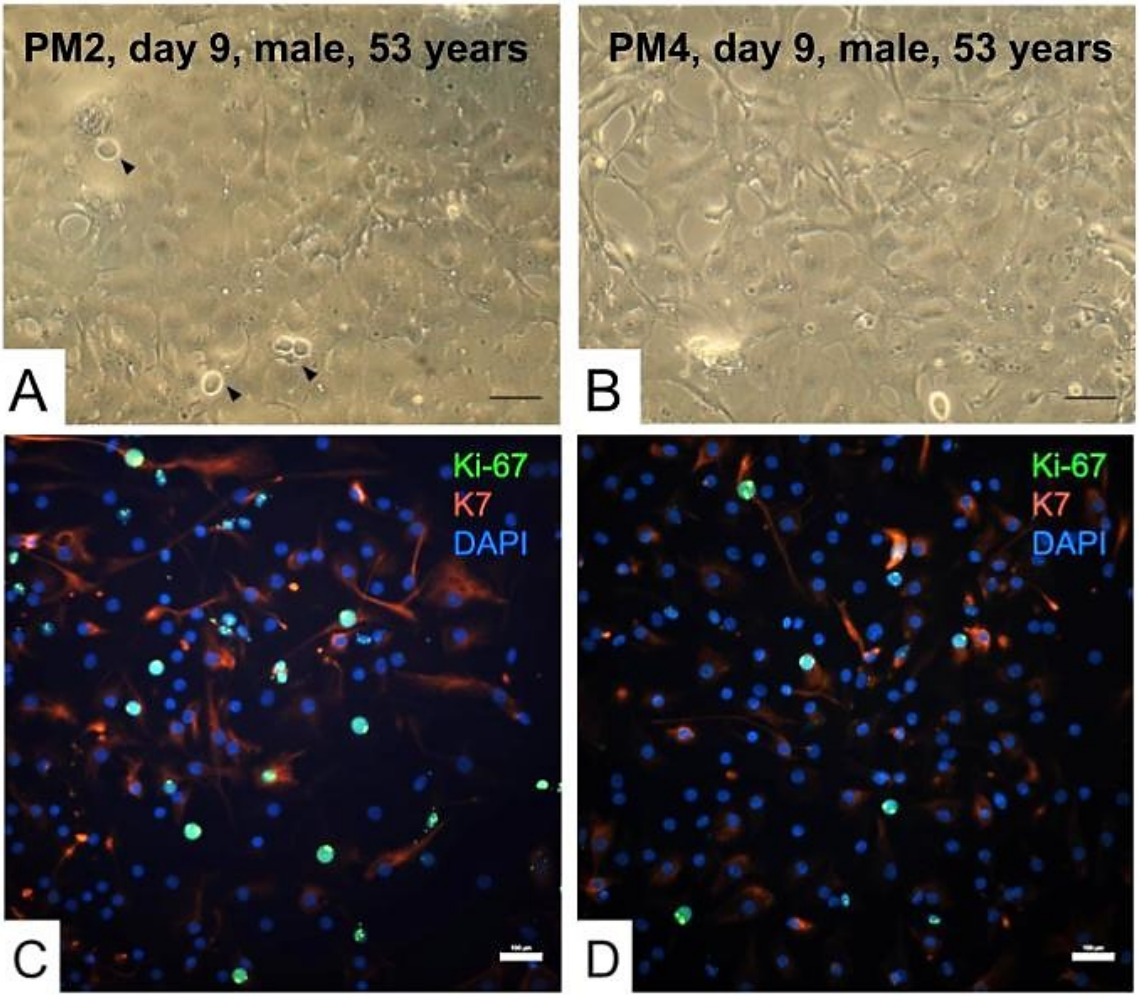


**Figure. 15** Immunofluorescent detection of Ki-67 and keratin 7 (K7) in CECs, derived from 53 years old donor, cultured for nine days in either PM2 (A, C) or PM4 (B, D). More mitotic (arrows) and Ki-67 positive (green) cells were detected in a monolayer cultured in PM2 (23.72%) than in PM4 (10.73%), and slightly less K7 positive (red) cells were detected in a CE cultured in PM4 (46.89%) than in PM2 (51.28%). Scale bar: 100 μm.

The change of CECs to fibroblast-like cells at various time points was recognized under all tested conditions. None of the selected PM (and their supplements) were able to inhibit fibroblast-like changes that regularly affected up to 10% of cells within the monolayer. The signs of starting fibroblast-like morphological change of CECs within expanding cell layer were detectable under phase contrast light microscope approximately one week (7.56 ± 2.25 days) from the day of primary culture start. After exposure to the SM2

for a sufficiently long time (3-14 days), most of the CEC that acquired a fibroblast-like phenotype during culture in the PM returned to polygonality and mitosis ceased. The resulting primary culture (monolayer) was composed of a mixture of polygonal cells and large cells with irregular cell shape, expressing endothelial markers Na+/K+-ATPase, ZO-1, Figure 16. If the cells undergone a massive irreversible phenotypic change, even a prolonged (> 5 day) culture in SM2 did not lead to a return to the hexagonal cell shape.

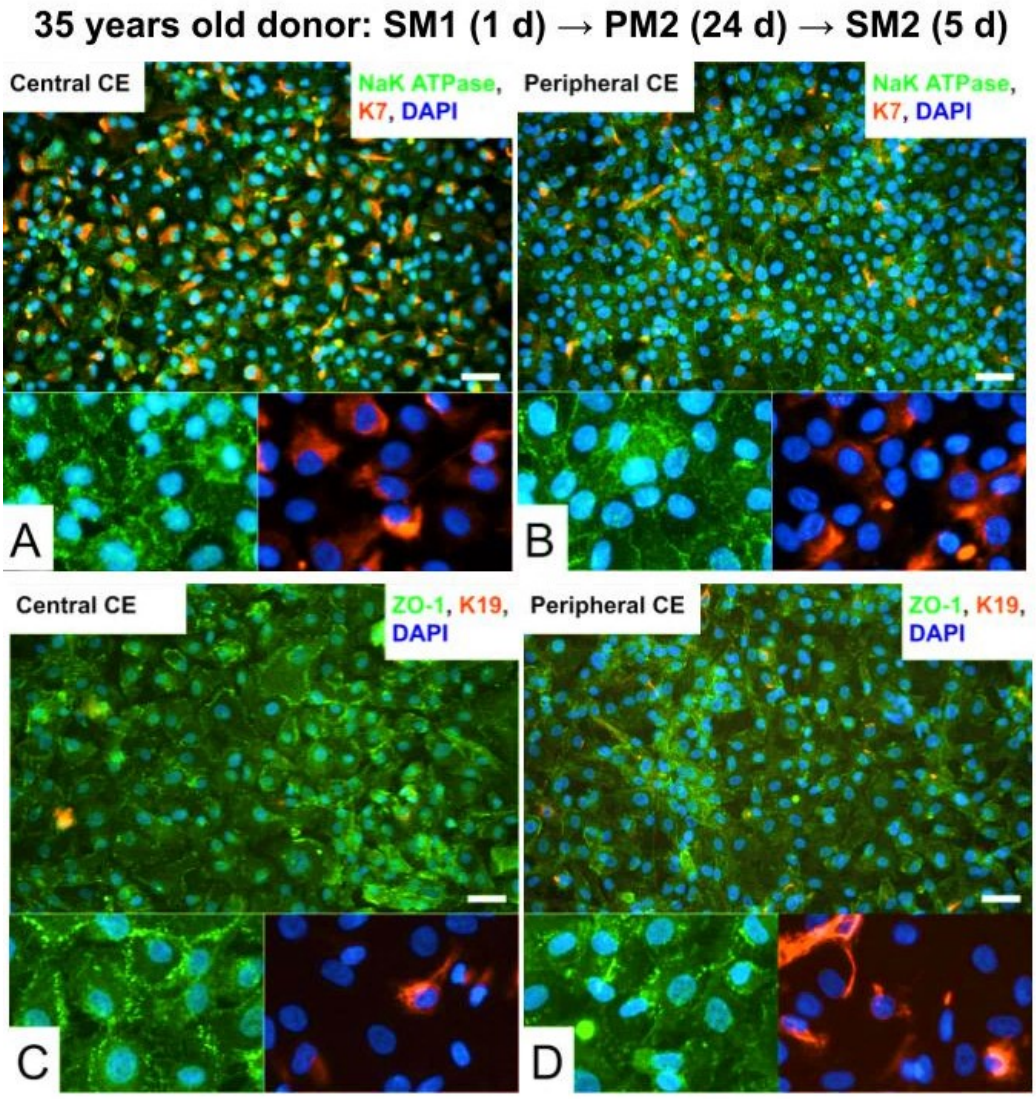


**Figure 16.** Immunofluorescent detection of Na+/K+-ATPase, ZO-1, keratin 7 and 19 expression in CECs, derived from 35 years old donor, cultured *in vitro* for 30 days. CECs isolated from central CE and peripheral CE were cultured separately, under same conditions. More CEC were obtained from peripheral CE (1212.7±178.2 cells/mm$^2$), compared to central CE (986.4 ±273.1 cells/mm$^2$). The CECs stained positively for all selected markers: Na+/K+-ATPase and ZO-1, predominantly in cytoplasmic membrane, and keratins in cell cytoplasm. CECs were more positive for K7 than K19, without significant differences between central and peripheral CE. Scale bar: 50 µm.

An increased expression of K7 was observed in *in vitro* expanded CECs during the whole culture period (observed on Day 9 and Day 30). The K19 was expressed in a few CECs of *in vitro* cultured CE – Figure 16.

The expression of endothelial markers, CD166 and Prdx6, occurred predominantly in the cytoplasm of cultured CECs at the end of culture period, Figure 17.

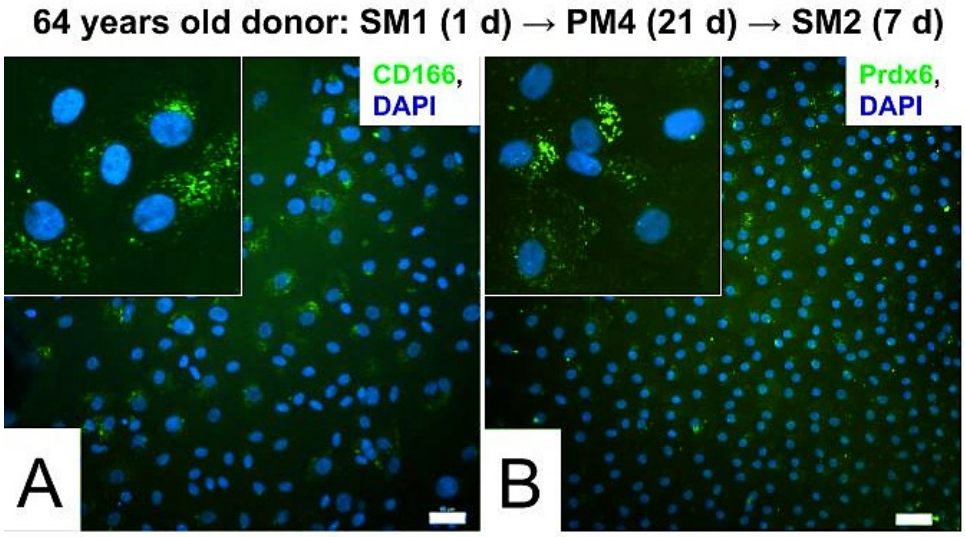


**Figure 17**. Immunofluorescent detection of CD166 (A) and Prdx6 (B) expression in CECs, derived from 64 years old donor, cultured *in vitro* for 29 days in 8-wells of Lab-Tek chamber slides. Average cell density: 669.1± 420.8 cells/mm$^2$. Scale bar: 50 µm.

**Results regarding H1: Molecular markers found in native and *in vitro* cultured endothelial cells**

The expression pattern of a panel of markers that have been reported to be specific to human corneal endothelium was examined by immunohistochemical (IHC) and immunofluorescence (IF) methods. None of the proposed molecules was found to be specific marker of CE, using standard IHC/IF methods and the antibodies summarized in Table 3 (Material and methods section). In all protocols, at least three corneal tissues/cultures from different donors were analyzed. Negative controls (primary antibody omitted), were negative for all antibodies used.

The staining patter of the two common endothelial markers, the Na+/K+-ATPase and ZO-1, in corneal endothelium and epithelium is shown in Figure 18.

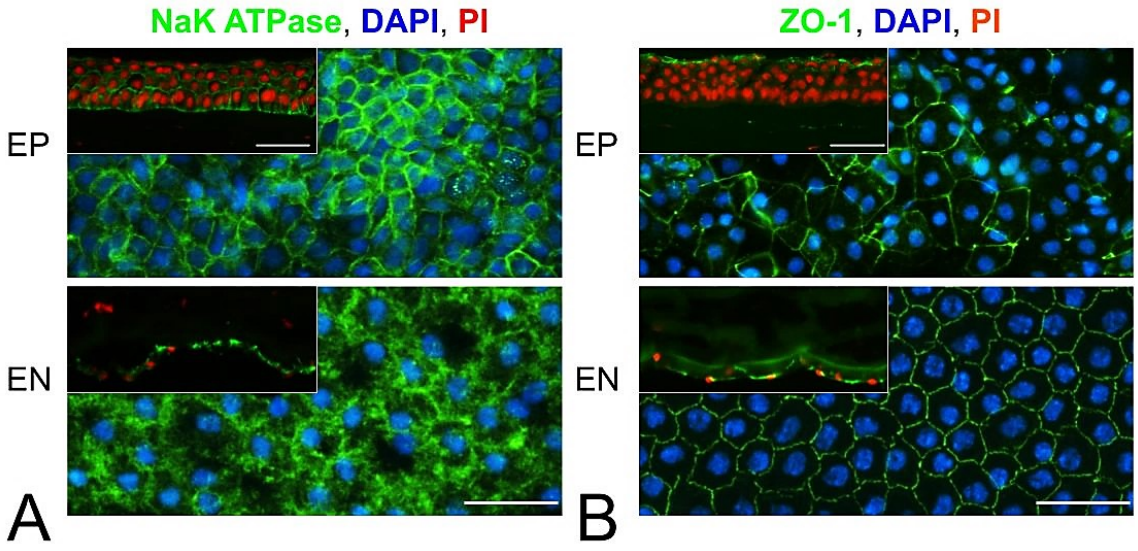


**Figure 18**. Immunofluorescent detection of Na+/K+-ATPase (A) and ZO-1 (B) expression in native CE-cell imprints; corneal cross-sections are shown in picture inserts. EP = epithelium, EN = endothelium, PI = propidium iodide (red). Scale bar: 50 µm.

The CD166 (ALCAM) was found to be expressed in CE, keratocytes and limbus. The Prdx6 and GPC4 were found to be expressed in all corneal cells, Figure 19. Compared to CD166, the Prdx6 signal was slightly weaker in all samples. The Prdx6 expression was found predominantly in limbal area of epithelium, and in some epithelial cells on *en face* cell imprints. The GPC4 expression by endothelium was stronger than the expression of Prdx6, but weaker than CD166.

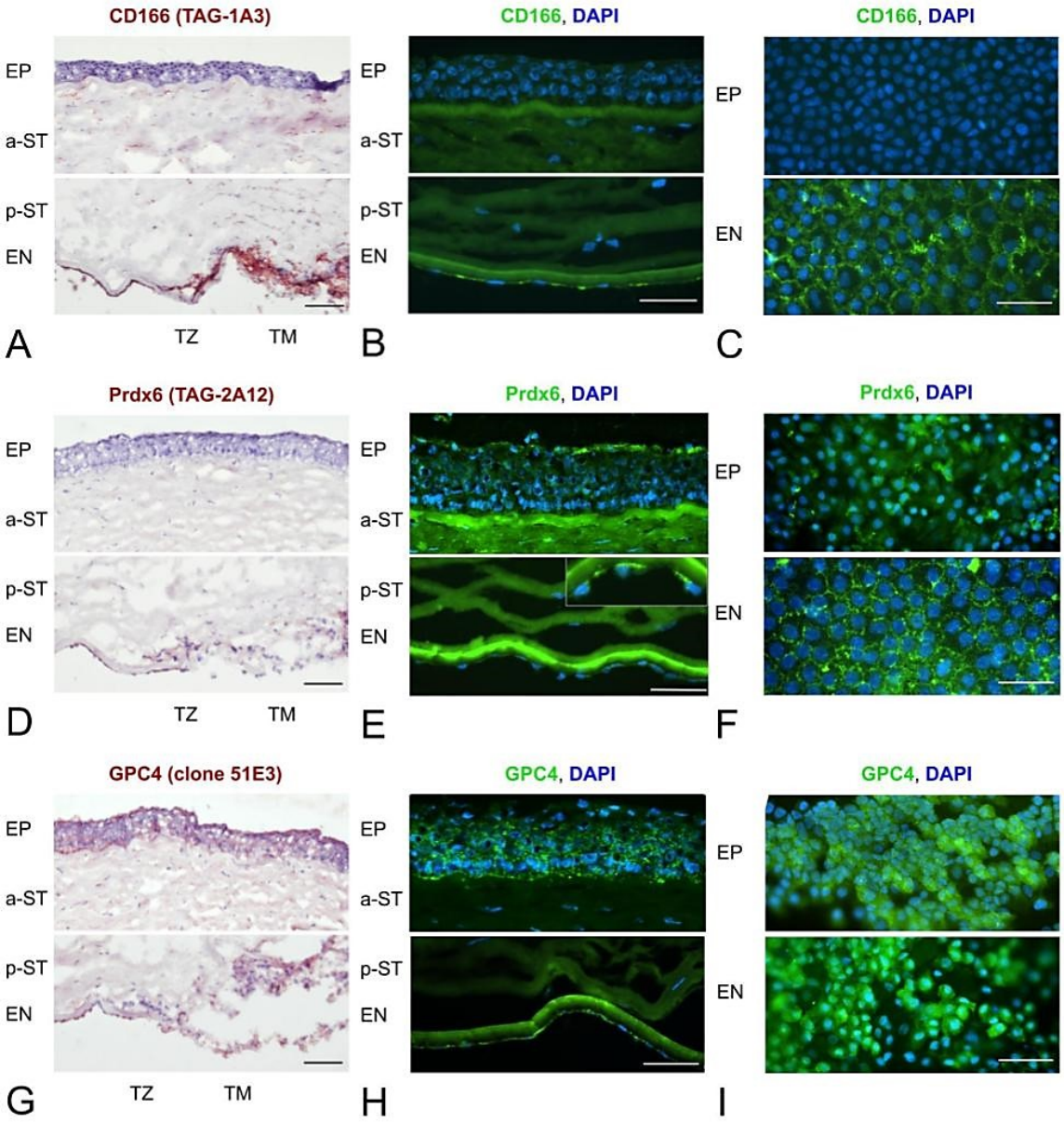


**Figure. 19** The expression of proposed CEC-specific markers CD166/ALCAM (A-C), Prdx6 (D-F), GPC4 (G-I) in normal human cornea. (A, D, G) Enzyme IHC, tissue cross-sections; (B, E, H) The IF, tissue cross-sections; (C, F, I) The IF, cell imprints. EP = epithelium, a-ST = anterior stroma, p-ST = posterior stroma, EN = endothelium, TZ = transition zone, TM = trabecular meshwork. Negative controls are not shown. Counterstains: hematoxylin and DAPI. Scale bar: 50 µm. Source: author's archive.

Another group of proposed endothelial-specific markers, the MRGX3, ZP4 and 5HT1D were found to be expressed in all corneal cells, Figure 20.

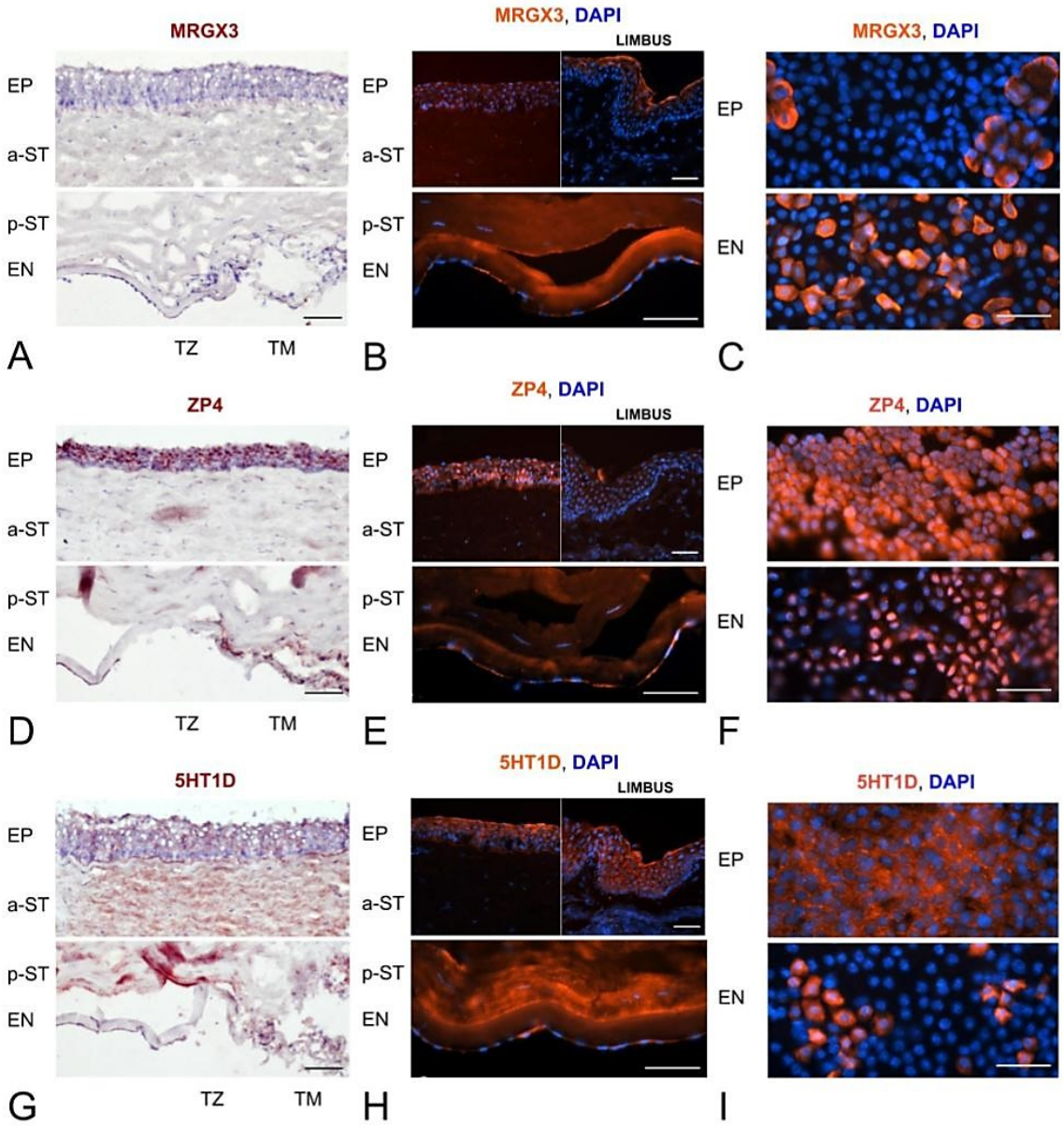


**Figure 20.** The expression of another proposed CEC-specific markers. (A-C) MRGX6, (D-F) ZP4, (G-I) 5HT1D in normal human cornea. (A, D, G) Enzyme IHC, tissue cross-sections; (B, E, H) The IF, tissue cross-sections; (C, F, I) The IF, cell imprints. EP = epithelium, a-ST = anterior stroma, p-ST = posterior stroma, EN = endothelium, TZ = transition zone, TM = trabecular meshwork. All three molecules were expressed in EN, EP, ST and corneal limbus with varying staining intensities. Negative controls are not shown. Counterstains: hematoxylin and DAPI. Scale bar: 50 µm. Source: author's archive.

Immunostaining of Lgr5 showed expression in both, CE and epithelium. However, the staining signal of used antibody was weak. Using increased antibody concentration, the positive expression of Lgr5 was found in some epithelial cells and peripheral CE, and to a lesser extent also in the central CE, Figure 21. The Sox2 was found to be expressed in both, central and peripheral CE and EP. Clusters of Sox2-positive CECs were found throughout

the whole CE monolayer, but prominently in the far periphery of CE. The Sox2 was expressed also in the epithelium and was found in cell nuclei and cytoplasm, Figure 21.

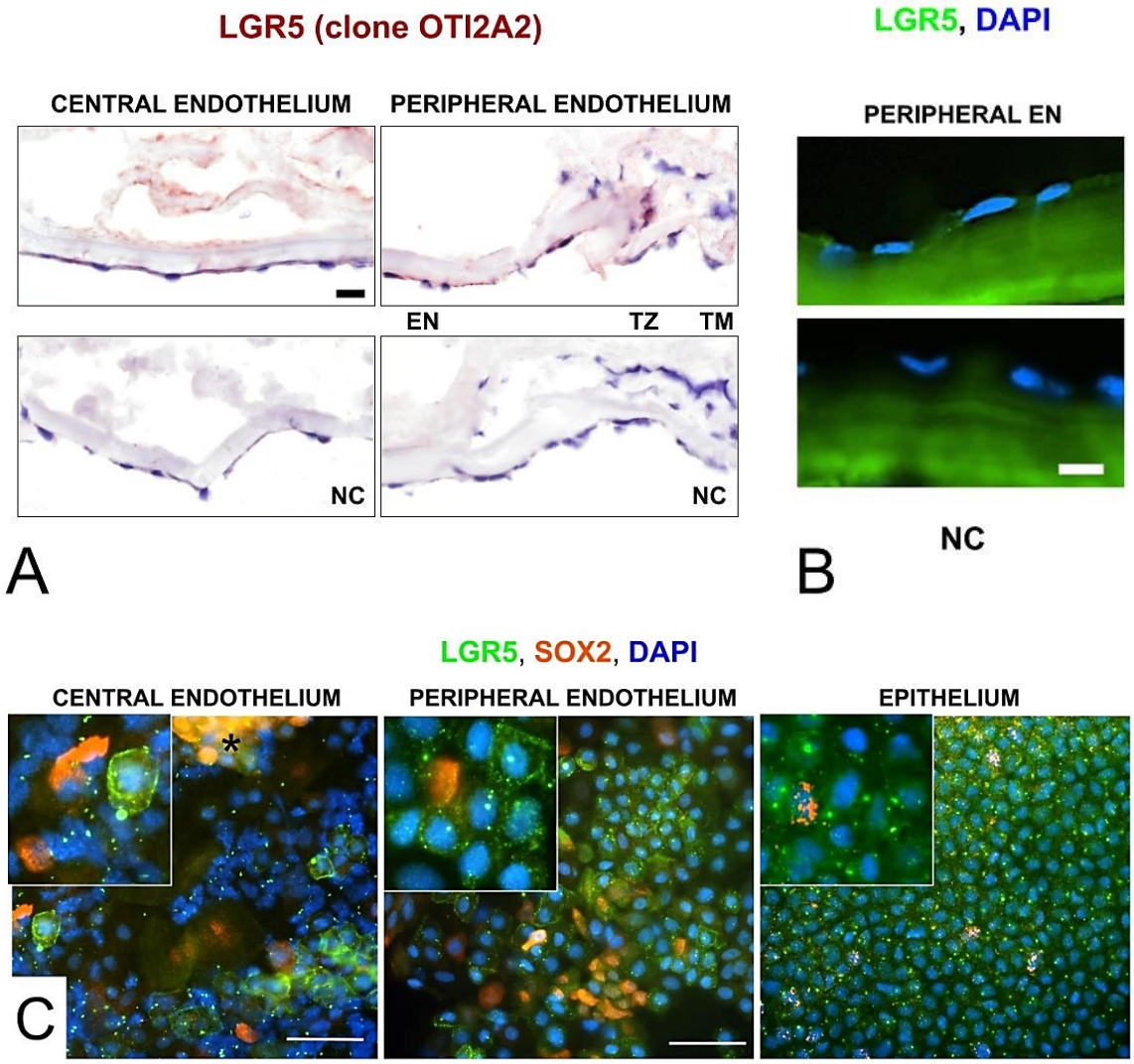


**Figure 21.** The expression of Lgr5 and Sox2 in normal human cornea. (A) Enzyme IHC, tissue cross-sections; (B) The IF, tissue cross-sections; (C) The IF, cell imprints; detail of EN is shown in inserts. NC = negative control. NCs are not shown for cell imprints. Counterstains: hematoxylin, DAPI. Scale bar: 10 μm (A, B) and 50 μm (C).

The CD44 was expressed in EP and stroma, with a weak CD44 expression found in some CECs of cell imprints. The α-SMA was expressed in limbus and a very weak signal was observed in some epithelial cells. Both, endothelial and epithelial cells were positive for K7 and K19, Figure 22. Immunostaining of cell imprints revealed some single cells or island of CECs stained with K7 and K19, with more abundant expression of K19 in CEC compared to K7. Positive staining of CECs for K7 was less obvious from staining of cross-sections. The two keratins were abundantly expressed in corneal epithelium and limbus.

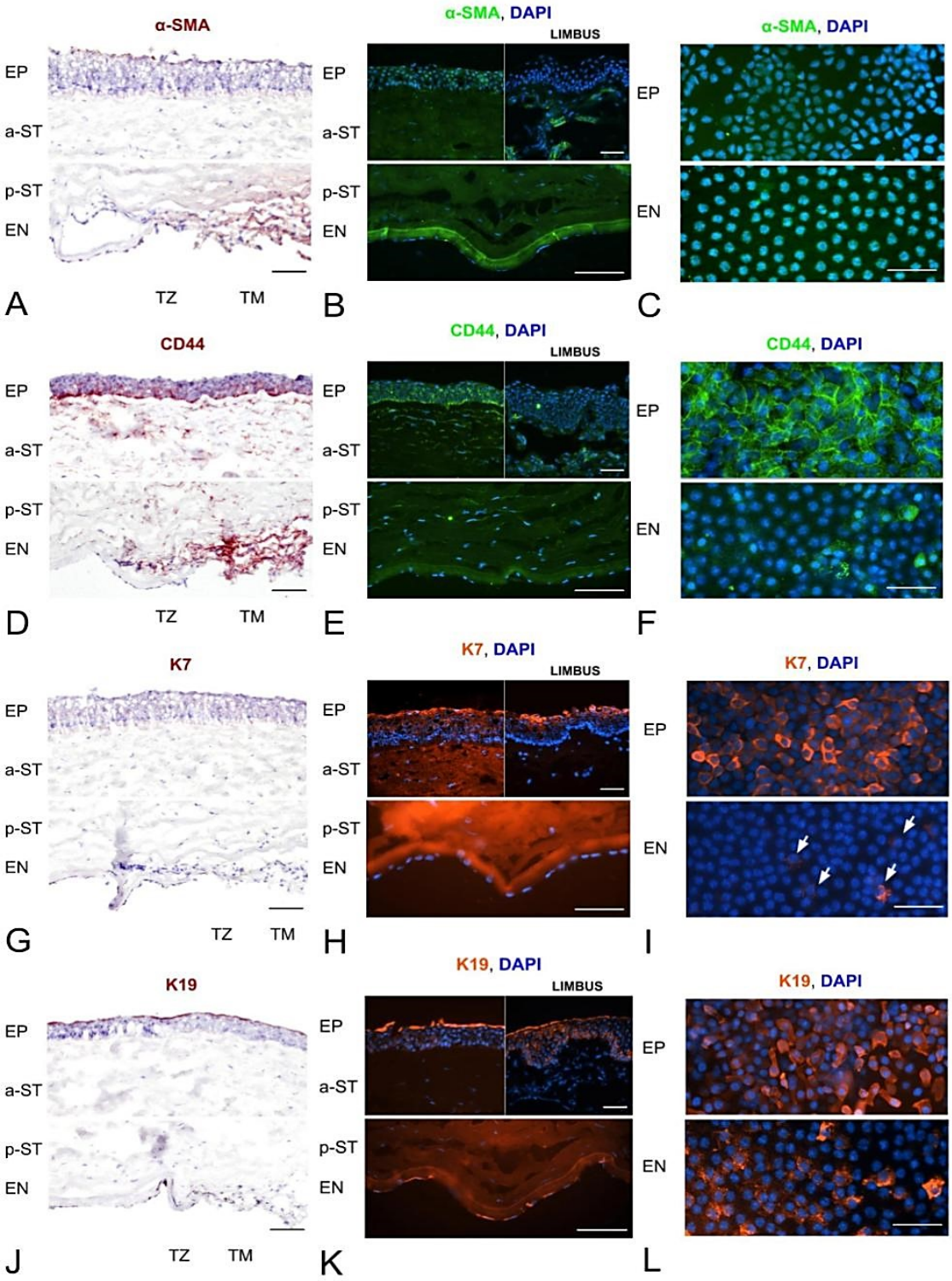


**Figure 22.** The expression pattern of α-SMA (A-C), CD44 (D-F), K7 (G-I) and K19 (J-L) in normal human corneas. (A, D, G, J) Enzyme IHC, tissue cross-sections; (B, E, H, K) The IF, tissue cross-sections; (C, F, I, L) The IF, cell imprints. EP = epithelium, a-ST = anterior stroma, p-ST = posterior stroma, EN = endothelium, TZ = transition zone, TM = trabecular meshwork. The expression of K7 (I) was very weak in EN (arrows). EP = epithelium, a-ST = anterior stroma, p-ST = posterior stroma, EN = endothelium, TZ = transition zone, TM = trabecular meshwork. Scale bar: 50 μm

The Ki-67 positive cells were found very occasionally in the TM, TZ, peripheral CEC and central CECs, neighboring the site of denuded DM regions in flat mounted control corneas, Figure 24. The Sox2 expression was detected in TM regions, and in TZ or peripheral and paracentral CE regions of 80% of analyzed corneas, Figure 23. We observed that culturing the control cornea in SM1 for three days at 37°C increased the number of Ki-67 positive cells, compared to untreated control corneas.

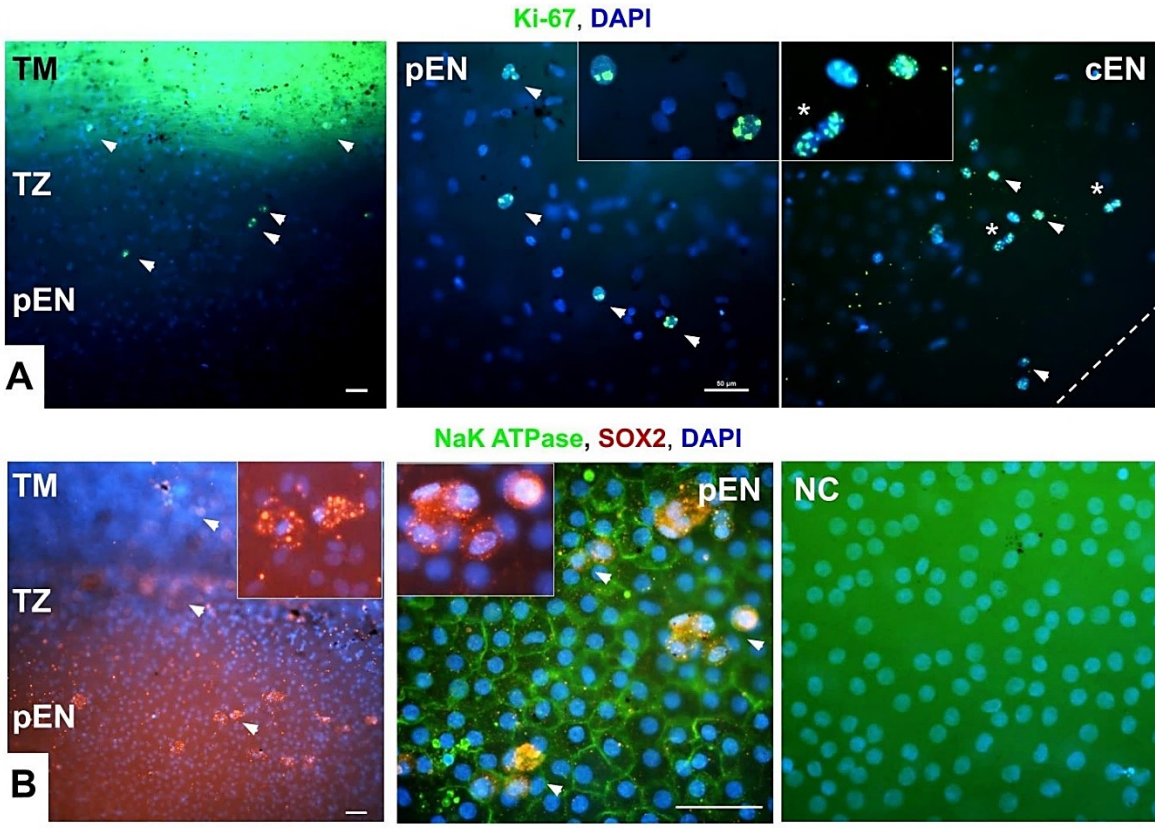


**Figure 23.** Immunofluorescence detection of the proliferation marker Ki-67 (A) and stem cell marker Sox2 (B) in CE of normal human corneas. Rare positivity is marked (arrowheads). In (A) the cell nuclei undergoing division can be seen (asterisks). TM = trabecular meshwork, TZ = transition zone, pEN = peripheral CE, cEN = central CE, NC = negative control. Scale bar: 50 µm.

The expression of other stem cell markers such as nanog or Oct3/4 was not confirmed by our immunocytochemical analysis, as the strong background signal or a weak positivity in CECs prevented the signal from being evaluated correctly. Dotted signal in cytoplasm of some CECs was achieved staining the tissue with Oct4 antibody. Nanog signal could be seen in the cytoplasm of come CECs, but it was very weak and due to repeatedly obtained strong background signal its positivity could not be confirmed, Figure 24.

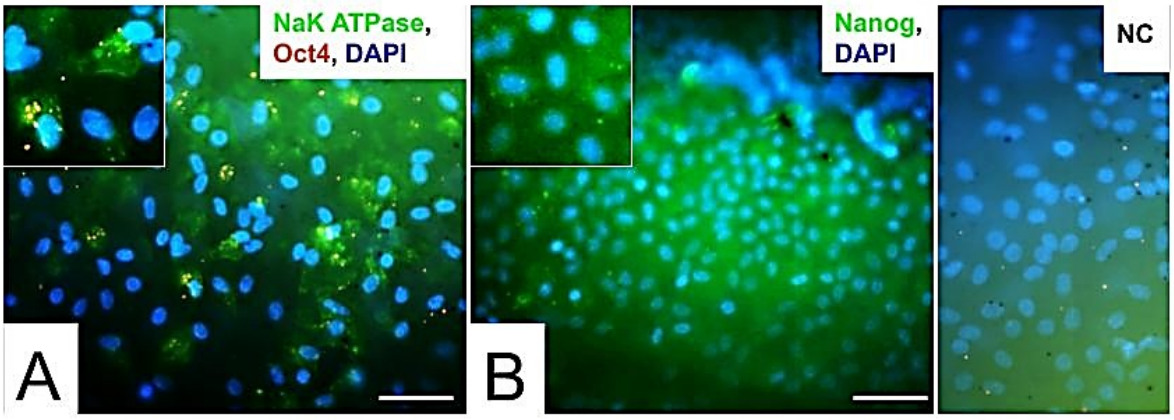


**Figure 24**. Immunofluorescence detection of the Oct4 (A) and Nanog (B) in CE of normal human peripheral CE – flat mounts. NC = negative control. Scale bar: 50 μm.

**Repair and regeneration of corneal endothelium – a porcine model**

Porcine model was used to assess repair/regeneration capacity of CE after injury, as the porcine tissue is a close equivalent of human tissue. Porcine CE does not proliferate *in vivo* under normal conditions, but retain proliferative capacity, similarly to human CE. The first goal of this study was to determine whether after a mechanical damage of central CE the pig corneas with the presence of TZ (large discs, diameter of 17.5 mm) will repair more quickly than corneas without TZ (small discs, diameter of 12.0 mm). The second goal was to compare the reparative capacity of CE when stored under various organ culture (OC) conditions: serum concentration (2% or 10% v/v FBS) and storage period (5- or 9-day).

The reparative capacity of the CE was assessed by a computer-aided measurement of the common CEC parameters, such as endothelial cell density of live cells (LECD, cells/mm$^2$), the percentage of dead cells (%DC) obtained after trypan blue staining, the percentage of hexagonal cells (6A) and the coefficient of variation (CV) in the central (C) and paracentral (PC) endothelium, i.e. the 2 mm wide ring of CE, surrounding the central lesion (wound area of 6.8 mm$^2$) in samples, obtained after Alizarin red S dying of cell borders. The parameters were assessed also in fresh (non-cultured) discs (n = 42) and cultured discs (n = 124), either intact (control) or injured discs, i.e. with mechanically induced lesion. One injured disc and its respective control always came from one pair of porcine eyes. The final mean values for 16 culture conditions assessed are summarized in Table 5. CE imprints were collected from some representative corneas and immunoassayed for the proliferation marker Ki-67 and the nucleolar marker fibrillarin to assess cell proliferation associated with healing of CE in both large and small corneas.

**Table 5.** The CEC parameters and statistical significance between the groups. LECD = endothelial cell density of live cells, %DC = percentage of dead cells, 6A = percentage of hexagonal cells, CV = coefficient of variation in the central (C) and paracentral (PC) endothelium of corenoscleral discs (controls, intact, injured), cultured under four different OC conditions. Statistical significance (P-value): *P ≤ 0.05; **P ≤ 0.010; ***P ≤ .005

| Cond. (days, FBS) | Small (S), large (L), injured (+), intact (–) | Group | *N* | LECD (C) (cells/mm$^2$ ± SD) | LECD (PC) (cells/mm$^2$ ± SD) | DC (C) (%) | DC (PC) (%) |
|---|---|---|---|---|---|---|---|
| 5d, 2% | S(–) | C1 | 7 | 4203.5 ± 248.0 | 4110.8 ± 245.7 | 0.4 ± 0.9 | 0.4 ± 0.6 |
| | S(+) | C2 | 7 | 229.7 ± 201.8 | 2957.3 ± 807.5 | 78.2 ± 16.2 | 2.7 ± 4.9 |
| | L(–) | C3 | 9 | 4193.0 ± 341.1 | 4117.2 ± 322.1 | 0.4 ± 0.6 | 0.6 ± 0.6 |
| | L(+) | C4 | 8 | 351.0 ± 390.1 | 3425.7 ± 266.1 | 63.7 ± 31.8 | 2.2 ± 4.7 |
| 5d, 10% | S(–) | C5 | 7 | 4024.3 ± 447.8 | 3970.9 ± 185.5 | – | 0.1 ± 0.1 |
| | S(+) | C6 | 9 | 404.1 ± 275.2 | 3156.6 ± 477.8 | 48.0 ± 29.9 | 1.1 ± 1.8 |
| | L(–) | C7 | 8 | 4004.9 ± 547.6 | 4165.0 ± 368.2 | 0.3 ± 0.9 | 0.1 ± 0.1 |
| | L(+) | C8 | 8 | 742.0 ± 502.0 | 3236.4 ± 833.7 | 29.7 ± 16.9 | 0.5 ± 0.8 |
| 9d, 2% | S(–) | C9 | 7 | 3778.7 ± 395.8 | 3729.7 ± 275.0 | 0.3 ± 0.4 | 0.6 ± 0.9 |
| | S(+) | C10 | 8 | 1657.3 ± 597.8 | 3431.8 ± 400.7 | 13.9 ± 25.9 | 1.0 ± 1.7 |
| | L(–) | C11 | 7 | 4065.4 ± 621.3 | 3977.7 ± 229.6 | 0.5 ± 0.2 | 0.4 ± 0.3 |
| | L(+) | C12 | 6 | 1902.1 ± 700.0 | 3867.8 ± 316.0 | 13.4 ± 21.7 | 0.6 ± 0.6 |
| 9d, 10% | S(–) | C13 | 6 | 3996.2 ± 604.1 | 4096.0 ± 379.1 | 0.4 ± 0.6 | 0.1 ± 0.1 |
| | S(+) | C14 | 8 | 2409.4 ± 881.8 | 3949.5 ± 275.5 | 6.8 ± 17.9 | 0.6 ± 0.9 |
| | L(–) | C15 | 8 | 4375.3 ± 297.9 | 4033.3 ± 313.8 | 0.1 ± 0.2 | 0.4 ± 0.8 |
| | L(+) | C16 | 8 | 2555.0 ± 347.0 | 4007.5± 261.2 | 1.7 ± 2.8 | 0.1 ± 0.1 |

Cond., storage condition; d = days of organ culture, incl. 24-36-h deswelling in cultivation medium with dextran; FBS, concentration (v/v) of fetal bovine serum in storage medium; S, small corneoscleral discs with a diameter 12 mm; L, large corneoscleral discs with a diameter 17.5 mm; C, central endothelium; PC, paracentral endothelium (adjacent to former lesion); SD, standard deviation; (+) injured disc (sample); (–) intact disc (control); LECD, endothelial cell density of live cells; DC, percentage of dead cells.

| Cond. (days, FBS) | Small (S), large (L), injured (+), intact (–) | | 6A (C) (%) | 6A (PC) (%) | CV (C) | CV (PC) |
|---|---|---|---|---|---|---|
| 5d, 2% | S(–) | C1 | 51.0 ± 4.6 | 51.0 ± 4.0 | 14.1 ± 1.9 | 15.8 ± 2.2 |
| | S(+) | C2 | 35.1 ± 16.6 | 47.5 ± 5.6 | 22.8 ± 10.8 | 34.5 ± 23.1 |
| | L(–) | C3 | 48.7 ± 2.2 | 49.2 ± 2.0 | 14.4 ± 1.2 | 17.6 ± 3.8 |
| | L(+) | C4 | 37.1 ± 14.2 | 51.3 ± 3.4 | 31.4 ± 17.5 | 25.7 ± 9.2 |
| 5d, 10% | S(–) | C5 | 50.6 ± 4.2 | 51.3 ± 3.5 | 15.4 ± 3.5 | 17.3 ± 2.1 |
| | S(+) | C6 | 42.4 ± 4.6 | 49.2 ± 3.1 | 31.7 ± 8.6 | 35.2 ± 19.6 |
| | L(–) | C7 | 54.0 ± 5.1 | 52.2 ± 3.3 | 19.8 ± 11.7 | 17.1 ± 4.0 |
| | L(+) | C8 | 42.0 ± 5.8 | 48.8 ± 3.2 | 33.2 ± 13.9 | 26.7 ± 17.3 |
| 9d, 2% | S(–) | C9 | 51.3 ± 4.0 | 48.7 ± 4.1 | 16.4 ± 3.5 | 17.9 ± 1.9 |
| | S(+) | C10 | 44.2 ± 4.5 | 47.4 ± 3.2 | 28.4 ± 6.6 | 21.4 ± 5.5 |
| | L(–) | C11 | 49.6 ± 5.3 | 47.8 ± 5.3 | 18.0 ± 8.9 | 18.2 ± 4.8 |
| | L(+) | C12 | 44.1 ± 3.4 | 47.7 ± 3.3 | 33.2 ± 10.1 | 20.0 ± 4.3 |
| 9d, 10% | S(–) | C13 | 48.1 ± 4.0 | 50.1 ± 3.9 | 19.8 ± 6.6 | 17.8 ± 4.8 |
| | S(+) | C14 | 40.2 ± 4.2 | 46.8 ± 3.4 | 28.8 ± 5.2 | 20.1 ± 3.7 |
| | L(–) | C15 | 50.4 ± 4.5 | 48.3 ± 3.4 | 14.4 ± 1.6 | 17.0 ± 1.4 |
| | L(+) | C16 | 37.2 ± 3.9 | 45.8 ± 3.3 | 29.2 ± 6.0 | 17.6 ± 2.5 |

| | Inj. | | LECD (C) | LECD (PC) | %DC (C) | %DC (PC) |
|---|---|---|---|---|---|---|
| S:L | – | C1:C3 | 0.947 | 0.966 | 0.964 | 0.557 |
| | + | C2:C4 | 0.443 | 0.154 | 0.265 | 0.863 |
| | – | C5:C7 | 0.942 | 0.184 | – | 0.770 |
| | + | C6:C8 | 0.101 | 0.809 | 0.148 | 0.377 |
| | – | C9:C11 | 0.224 | 0.198 | 0.628 | 0.530 |
| | + | C10:C12 | 0.678 | 0.621 | 0.722 | **0.036*** |
| | – | C13:C15 | 0.146 | 0.740 | 0.313 | 0.315 |
| | + | C14:C16 | 0.674 | 0.672 | 0.455 | 0.112 |
| 2:10% | – | C1:C5 | 0.373 | 0.252 | – | 0.143 |
| | + | C2:C6 | 0.161 | 0.539 | **0.023*** | 0.428 |
| | – | C3:C7 | 0.400 | 0.764 | 0.719 | **0.027*** |
| | + | C4:C8 | 0.091 | 0.555 | **0.017*** | 0.308 |
| | – | C9:C13 | 0.443 | 0.079 | 0.931 | 0.135 |
| | + | C10:C14 | 0.066 | **0.009**** | 0.533 | 0.578 |
| | – | C11:C15 | 0.140 | 0.759 | 0.203 | 0.894 |
| | + | C12:C16 | **0.040*** | 0.382 | 0.244 | 0.076 |
| 5:9 d | – | C1:C9 | **0.027*** | **0.024*** | 0.859 | 0.608 |
| | + | C2:C10 | **1.550E−04***** | 0.159 | **3.500E−05***** | 0.398 |
| | – | C3:C11 | 0.533 | 0.436 | 0.836 | 0.424 |
| | + | C4:C12 | **9.532E−05***** | **0.012*** | **0.005***** | 0.333 |
| | – | C5:C13 | 0.925 | 0.454 | – | 0.861 |
| | + | C6:C14 | **2.408E−04***** | **0.001***** | **0.004***** | 0.504 |
| | – | C7:C15 | 0.113 | 0.420 | 0.520 | 0.352 |
| | + | C8:C16 | **7.693E−07***** | **0.036*** | **0.002***** | 0.163 |

inj- injury of endothelium: intact (-) or injured (+)

In fresh corneas, the LECD/mm$^2$ (mean ± standard deviation) were 3998.0 ± 215.4 (central area) and 3888.2 ± 363.1 (paracentral area). The mean %DC (±SD) was 0.5 ± 0.9 (C) and 3.5 ± 7.8 (PC). The mean 6A (±SD) was 50.7 ± 4.3 (C) and 51.1 ± 3.1 (PC); and the mean CV (±SD) was 13.3 ± 1.7 (C) and 13.7 ± 1.4 (PC). Cultured (intact) controls had stable LECD in C, as seen in Table 5; %DC reached 0.6% at maximum, the 6A ranged between 47.8% and 54.0%, and CV varied from 14.1 to 19.8. In contrast, most of the CEC parameters worsened in injured cultured discs – lower values of LECD and 6A and higher %DC and CV, compared to control discs. After OC (all conditions) of injured discs, 6A was slightly lower in C (35.1–44.2%) than in PC (45.8–51.3%) and mean CV values varied in C (22.8–33.2) and in PC (17.6–35.2).

No significant difference of CEC parameters was found between small and large cultured control discs. The mean values of LECD of large injured discs were numerically higher than in small injured discs, but the difference was not statistically significant, Table 5. Compared to small discs, the mean values of %DC were numerically lower in large discs in all conditions, gradually decreasing in direction from C2 to C16 i.e., with prolonged culture and increased FBS concentration. The only significant difference in %DC ($P = 0.036$) was found between paracentral %DC of small and large disc cultured for 9 days in medium with 2% FBS. When we compared the CEC parameters between intact and injured corneas with respect to the serum concentration (2% vs. 10% FBS) we found higher LECD in 75% of discs cultured in medium with 10% FBS with two statistically significant differences.

In general, the prolonged storage (9d) considerably improved CEC parameters of injured discs, when compared to shorter storage (5d). After 5-day culture, the lesions were partially repaired in 95% of discs, while after 9 days, complete reparation was observed in 99% of discs. The CECs expressing the Ki-67, a marker of proliferation, and fibrillarin, a nucleolar marker, were detected in organ cultured corneas, with more Ki-67 positive cells detected in the discs stored for 9 days compared to those stored for 5 days. No significant difference in Ki-67 expression was observed between small and large discs or between the two OC media. The Ki-67 positive CECs, repopulating central part of cornea, were observed in samples after 9-day incubation. After 5-day culture, the Ki-67 signal was detected in few individual cells scattered throughout the area of cell imprints. Fibrillarin staining showed mostly two to five irregularly shaped nucleoli per nucleus. Round, relatively large nucleoli, reflecting cells with high metabolic activity, were present particularly in central parts of the cornea with no differences related to the employed conditions. The factors that influenced

the improvement of the CE parameters (and wound closure) of injured disc the most significantly were the prolonged culture time and the higher serum concentration in medium.

## Part II: Amniotic membrane

### Effect of decontamination on vitality of human amniotic membrane cells (Paper 2)

The aim of this study was to compare the toxic effect of the commercial solution BASE128 and laboratory decontamination solution (LDS), with analogous composition of antibiotics (AA) on human amniotic epithelial (AECs) and stromal cells (AMCs). The percentage of dead AECs (%DEC) in fresh (control) and decontaminated AM was assessed by trypan blue staining of AM samples incubated in either BASE128 or LDS under three protocols: (1) 6 h, 37 °C, (2) 24 h, at RT or (3) 24 h, 4 °C. Additionally, we stained the AECs and AMCs, in fresh and cryopreserved decontaminated AMs, for apoptotic features via terminal deoxynucleotidyl transferase (TdT) dUTP nick-end labelling (TUNEL) method.

The mean %DEC (±SD) values in fresh (control) AM samples and decontaminated AM samples are summarized in Figure 25.

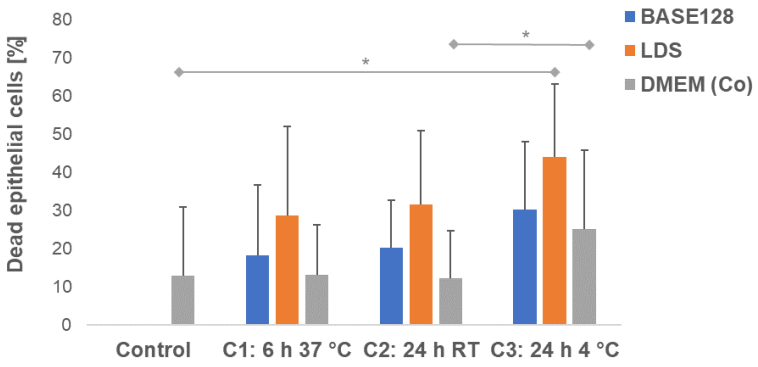


**Figure 25.** The mean percentage of the dead epithelial cells (%DEC ± SD) in control (fresh) and decontaminated AM, from six placentas. The BASE128, LDS or DMEM as a control solution (Co) were used. The AM specimens were incubated for 6 h at 37 °C (C1), for 24 h at room temperature (RT) (C2), or for 24 h at 4 °C (C3). The asterisks represent statistically significant difference (*P < 0.05) (Student´s t-test).

Due to the fact that relatively high variability in %DEC was present already in samples of fresh AM (12.9 ± 18.1), we compared the mean %DEC of decontaminated AM to the mean %DEC of the fresh AM and expressed it as n-fold increase/decrease in %DEC for individual placentas and conditions (C1 - C3; BASE128, LDS, DMEM), Table 6. Comparing the values of n-fold increase in %DEC among LDS, BASE128 and DMEM in each condition (C1 - C3), the increase was highest for LDS in 15 out of 18 cases, with the highest values in C3. The difference in n-fold increase in %DEC between BASE128 and DMEM of each

respective group was minimal. The slight decrease in %DEC, compared to the fresh AM, was observed in some cases of cultivation of AM in DMEM.

**Table 6.** The n-fold increase/decrease in %DEC in decontaminated AM, expressed for six analysed placentas (P1 - P6). Comparison of mean %DEC was done between decontaminated AM vs. fresh AM of respective placenta. P-value (Student´s t-test, unpaired, two-tailed): P < 0.05*; P < 0.01**; P < 0.005*** (in brackets).

| | C1: 6 h 37 °C | | | C2: 24 h RT | | | C3: 24 h 4 °C | | |
|---|---|---|---|---|---|---|---|---|---|
| | BASE·128 | LDS | DMEM | BASE·128 | LDS | DMEM | BASE·128 | LDS | DMEM |
| P1 | 1.2 (0.637) | 2.2 (5.26E−07)*** | 0.8 (0.344) | 1.9 (2.77E−04)*** | 2.7 (6.78E−13)*** | 0.7 (0.207) | 1.9 (6.93E−04)*** | 2.6 (2.46E−10)*** | 0.8 (0.430) |
| P2 | 2.2 (0.062) | 4.5 (2.475E−04)*** | 0.9 (0.725) | 1.4 (0.178) | 3.6 (8.29E−04)*** | 2.1 (0.044)* | 1.6 (0.120) | 4.3 (2.15E−05)*** | 1.8 (0.076) |
| P3 | 1.3 (0.162) | 2.1 (0.003)*** | 1.2 (0.213) | 0.8 (0.357) | 1.3 (0.306) | 1.5 (0.053) | 1.9 (0.004)*** | 1.6 (0.042)* | 2.4 (3.78E−04)*** |
| P4 | 2.1 (1.581E−04)*** | 2.4 (3.792E−04)*** | 1.6 (0.011)* | 1.0 (0.897) | 2.9 (5.56E−06)*** | 1.4 (0.096) | 1.1 (0.336) | 5.3 (2.76E−20)*** | 2.4 (1.34E−06)*** |
| P5 | 1.0 (0.994) | 1.8 (0.052) | 1.0 (0.937) | 1.3 (0.226) | 2.9 (4.26E−09)*** | 0.7 (0.267) | 4.8 (7.18E−14)*** | 7.0 (1.57E−31)*** | 4.2 (1.67E−15)*** |
| P6 | 1.4 (0.069) | 1.7 (0.003)*** | 0.9 (0.613) | 1.7 (0.002)*** | 1.8 (0.003)*** | 0.5 (0.013)* | 2.8 (8.50E−14)*** | 2.4 (1.10E−12)*** | 2.1 (2.22E−04)*** |

Compared to DMEM (control), an increase in the %DECs was observed after longer 24h decontamination period and after incubation of AM samples in LDS. The lowest %DEC was found after the treatment with BASE128 for 6 h at 37 °C. Storage for 24 hours and at low temperature was less beneficial to the quality of the tissue than storage for 6 hours, independent of the type of decontamination solution (BASE128, LDS).

The percentage of apoptotic AECs (%AEC) and AMCs (%AMC) determined by TUNEL assay, Figure 26, showed that the mean %AEC was less than 1% and the mean %AMC in fresh control was 42.0 ± 18.5 (16.1-59.7 %). In all specimens, the mean %AEC remained low, about 1-2 % and mean %AMC increased significantly (except for C3, BASE•128) up to 87.9% (C1), compared to control. Changes in the mean %AEC and %AMC among groups were not statistically significant.

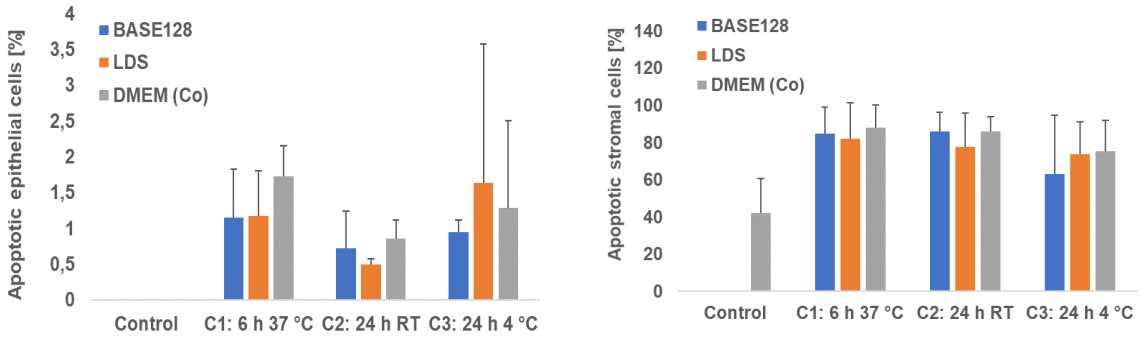


**Figure 26.** The percentage of apoptotic AECs and AMCs determined by TUNEL assay.

**Efficiency of decontamination solutions against selected pathogens (Paper 3)**

The two solutions used for decontamination of AM, the BASE128 and LDS, were compared in their antimicrobial efficiency against five human pathogens (*Staphylococcus aureus, Pseudomonas aeruginosa, Proteus mirabilis, Escherichia coli and Enterococcus faecalis*) via agar well diffusion method and their stability (pH, osmolarity) in time (1, 3 and 6 months of cold storage + fresh control) was determined by pH meter InoLAB pH 720 (WTW, Weilheim, Germany) and TearLAB® Osmometer (TearLAB Co., San Diego, CA).

The difference in the inhibition of bacterial growth was mostly not statistically significant. Both solutions were the most effective at elimination of *P. mirabilis* and the lowest antimicrobial activity was measured against *S. aureus*. The BASE128 had lower antimicrobial efficiency against *E. coli* and *E. faecalis* than LDS. The antimicrobial activity of both solutions against *S. aureus* slightly decreased with cold storage, Table 7.

Comparing the pH and osmolarity as indicators of a solution stability, the pH values for LDS were higher than those for BASE128 after cold storage, Table 8. The higher difference in pH was assessed between the two solutions after storage for 6 months, i.e. pH 7.72 ± 0.19 (LDS) vs. pH 7.58 ± 0.07 (BASE128). The osmolarity values for the LDS ranged between 277.50 units (T3) to 392.00 units (T0), while the values of BASE128 were mostly below the range of the TearLAB® Osmometer, Table 8.

**Table 7**. The effect of cold storage of two decontamination solutions, BASE128 and LDS, on their antimicrobial activity against five bacterial strains, expressed as a mean diameter (in mm) of the inhibitory zone (IZ) ± standard deviation (SD), Statistically significant difference between the IZ of the two solutions, cold-stored for a period of 0 (T0), 1 (T1), 3 (T2) or 6 months (T3), was counted—the P values: *P ≤ 0.05; **P ≤ 0.005; ***P ≤ 0.001. The P values ≤ 0.05 are indicated in brackets, below the numerically higher mean IZ value out of a pair of means, relevant to compared solutions.

| Organism | IZ (mm), mean ± SD | | | | | | | |
|---|---|---|---|---|---|---|---|---|
| | BASE•128 | | | | LDS | | | |
| | T0 | T1 | T2 | T3 | T0 | T1 | T2 | T3 |
| *P. mirabilis* | 49.8 ± 0.4 | 49.0 ± 0 | 49.0 ± 0 | 49.2 ± 0.8 | 49.8 ± 0.4 | 49.3 ± 0.5 | 50.0 ± 0 (0.001)*** | 49.0 ± 1.1 |
| *P. aeruginosa* | 39.6 ± 2.9 | 39.4 ± 3.1 | 39.7 ± 2.5 | 39.1 ± 3.8 | 40.3 ± 2.9 | 40.0 ± 2.5 | 39.5 ± 2.0 | 38.3 ± 3.3 |
| *S. aureus* | 30.5 ± 0.5 (0.015)* | 29.0 ± 0 | 27.3 ± 0.5 | 28.2 ± 0.1 | 29.2 ± 0.8 | 28.7 ± 0.5 | 27.2 ± 0.4 | 27.3 ± 0.5 |
| *E. coli* | 35.3 ± 0.5 | 36.7 ± 0.5 | 36.0 ± 0 | 35.3 ± 0.5 | 37.8 ± 0.4 (0.003)** | 37.8 ± 0.4 (0.007)* | 37.3 ± 0.8 (0.009)* | 36.5 ± 0.5 (0.013)* |
| *E. faecalis* | 32.3 ± 0.5 | 32.7 ± 0.5 | 31.5 ± 0.5 | 31.0 ± 0.6 | 37.0 ± 0 (0.002)** | 36.0 ± 0.6 (0.004)** | 36.7 ± 0.5 (0.004)** | 36.5 ± 0.5 (0.004)** |

**Table 8**. Stability of BASE128 and LDS, stored for different time-periods, i.e. 0 (T0), 1 (T1), 3 (T2) or 6 months (T3), expressed as changes in pH and osmolarity.

| Parameter | Mean ± SD | | | | | | | |
|---|---|---|---|---|---|---|---|---|
| | BASE•128 | | | | LDS | | | |
| | T0 | T1 | T2 | T3 | T0 | T1 | T2 | T3 |
| pH | 7.46 | 7.61 ± 0.03 | 7.52 ± 0.09 | 7.58 ± 0.07 | 7.36 ± 0.07 | 7.61 ± 0.07 | 7.60 ± 0.03 | 7.72 ± 0.19 |
| Osmol (mOsm/l) | BR | 288.50 ± 19.90 | BR | BR | 392.00 | 285.00 ± 4.24 | 285.00 ± 8.49 | 277.50 ± 2.12 |

*BR* below range of TearLAB® Osmometer

**De-epithelialization of human amniotic membrane for experimental use (Paper 4)**

The AM was successfully de-epithelialized using all three types of enzymatic methods, i.e. TrypLE Express, trypsin/EDTA, and thermolysin that had comparable efficiency. However, in case of treatment of AM with thermolysin the morphological changes in epithelial BM and underlying stroma occurred, suggesting aggressive proteolysis. The BM and stroma were preserved the best with trypsin/EDTA treatment. After use of TrypLE Express, partial damage to BM was observed. Collagen type IV and laminin α5 chain showed clear positivity in BM of all control specimens and specimens after TrypLE Express and trypsin/EDTA treatment, but in specimens after thermolysin treatment, inconsistent staining pattern was observed between amnions from different placentas, Figure 27. In three AMs, the collagen and laminin were localized almost exclusively in BM layer, and in other samples, the signal was scattered throughout the stroma, but not in BM.

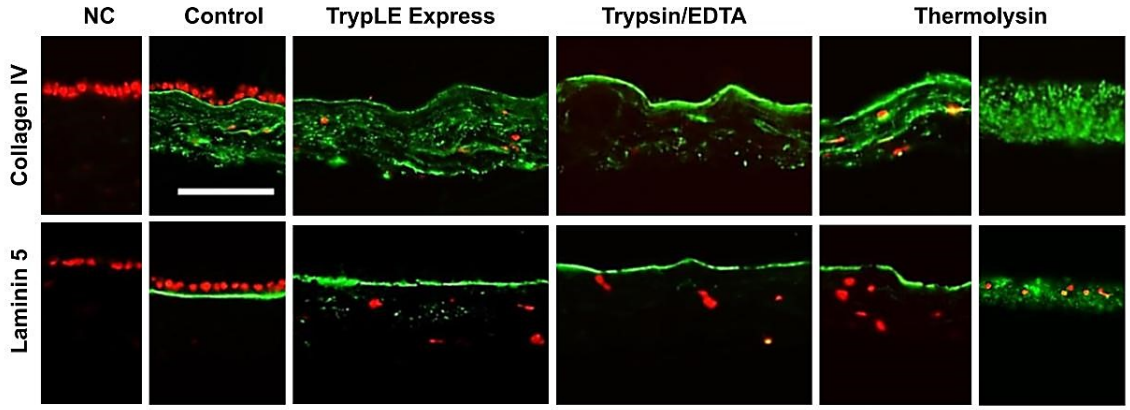


**Figure 27.** Distribution of collagen type IV (α2) and laminin α5 (green signal) in intact (Control) and denuded AM. NC = negative control. Cell nuclei were stained with the propidium iodide (red). Scale bar: 100 μm. Source: Trosan et al. (2018).

About 60% of cells remained viable using trypsin/EDTA, approximately 6% using TrypLE Express, and all cells were lethally damaged after thermolysin application. Thermolysin treatment caused loss of normal spindle-shaped cell morphology of AMCs that acquired round cell shape. The AECs isolated from AM after trypsin/EDTA treatment could be successfully cultured for several passages. The morphology of these cells changed from cuboidal at the primary culture to more mesenchymal-like shape in the 4$^{th}$ and 5$^{th}$ cell passage. In AECs of later passages, the higher proliferation activity was observed. In cultured AECs, the expression of stem cell markers SOX2 (up to 2$^{nd}$ passage), NANOG (up to 4$^{th}$ passage) and OCT-4 (all passages) was detected. However, the expression of OCT-4 was not confirmed by reverse transcription PCR, when primers for transcription variant specific for stem cells (OCT-4A) were used. The metabolic activity of AECs (determined by the WST-1 assay) was insignificantly increased when cells were co-cultured with EGF.

**Treatment of chronic wounds with human amniotic membrane (preliminary results)**

Ten patients (80 % of them polymorbid) with 17 chronic, non-healing wounds, Table 9, were treated by cryopreserved AM grafts (n=9) and air-dried AM graft (n=1), prepared by trained personnel in clean room in Motol University Hospital. The AM grafts were applied onto cleaned wounds once a week or less frequently and the wound healing was analyzed - the wound borders on taken photographs were marked and wound area was automatically counted by NIS analysis software. Data from accompanying QoL questionnaires were analyzed as well.

**Table 9.** Patients included in the study. SOC = standard-of-care (prior to a switch to AM application), M = male, F = female, d =dry AM, f=frozen/cryopreserved AM. All patients (P) besides one (asterisk) were treated exclusively by frozen AM. Pain rating scale: 0=no-pain, 10=the worst pain. VLU = venous leg ulcer, DLU = diabetic leg ulcer; W = wound.

| P No. | Sex + age | W type | W No. | SOC prior AM (weeks) | W size -start ($cm^2$) | Tratment with AM (weeks) | W closure (%) | AM used (No.) | AM used ($cm^2$) | Pain rating - start to end |
|---|---|---|---|---|---|---|---|---|---|---|
| **P1** | M, 67 | DLU | W1 | 120 | **62.8** | 6 | **14** | 4 | 81 | 4→2 |
| | | | W2 | 120 | **5.6** | 11 | **19** | 9 | 111 | 4→2 |
| **P2** | M, 77 | DLU | W3 | 72 | **2.6** | 10 | **100** | 8 | 45 | 1→0 |
| **P3** | M, 60 | VLU | W4 | 36 | **16.8** | 32 | **100** | 15 | 245 | 2→0 |
| | | | W5 | 36 | **4.5** | 17 | **100** | 11 | 84 | 2→0 |
| **P4** | M, 73 | DLU | W6 | 56 | **50.5** | 14 | **100** | 11 | 224 | 5→0 |
| | | | W7 | 56 | **1** | 8 | **100** | 2 | 29.5 | 5→0 |
| | | | W8 | 56 | **2.4** | 6 | **100** | 4 | 14.5 | 5→0 |
| | | | W9 | 56 | **13.8** | 34 | **100** | 10 | 142 | 5→0 |
| **P5** | M, 64 | VLU | W10 | 18 | **6.2** | 32 | **86.5** | 12 | 140.4 | 3→0 |
| | | | W11 | 18 | **2.9** | 17 | **98** | 12 | 59.6 | 3→0 |
| **P6*** | F, 86 | VLU | W12 | 27 | **20.2** | 19 | **96** | 26(d) + 3(f) | 428 | 2→1 |
| **P7** | M, 72 | VLU | W13 | 260 | **29** | 32 | **43.7** | 16 | 590 | 5→0 |
| | | | W14 | 260 | **1.6** | 32 | **94.5** | 16 | 196 | 5→0 |
| **P8** | M, 73 | DLU | W15 | 46 | **48** | 17 | **95.6** | 11 | 247 | 3→0 |
| **P9** | F, 66 | VLU | W16 | 24 | **16** | 7 | **100** | 5 | 120 | 0→0 |
| **P10** | F, 68 | DLU | W17 | 50 | **7.1** | 54 | **76.4** | 29 | 256 | 7→1 |

Photos of some of the treated wounds are shown in Figure 28.

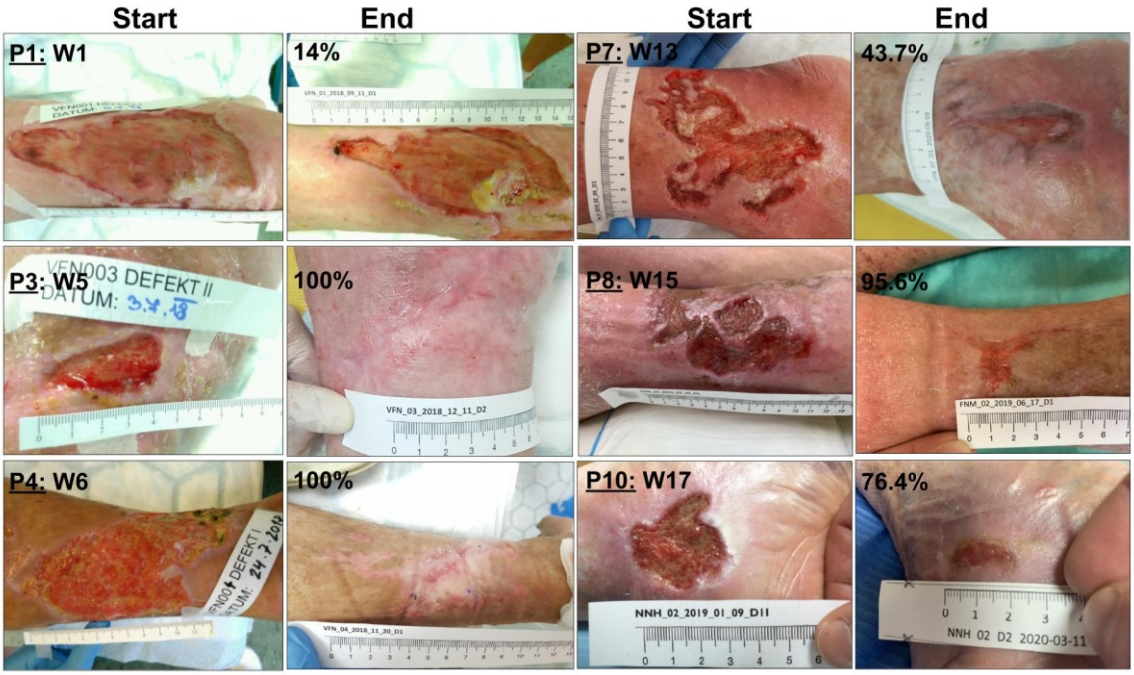


**Figure 28.** Some of the patients (P) with chronic wounds (W) treated with amnion are shown at the beginning and at the end of the AM application period. In all cases, the wound closure was initiated by AM and pain reduced. The % in up left corner represents the wound area reduction. Source: A. Svobodova, MD, General University Hospital in Prague; R. Fiala, MD, University Hospital Motol; V. Horvath, MD, Na Homolce Hospital.

In general, after application of AM onto wound, the wound healing was initiated, and pain reduced in all the treated wounds. The 47% (8/17) wounds were completely healed up to 9 months since first AM application, while 29% (5/17) wounds were healed from more than 80 % up to now. The average length of wound healing period using SOC prior AM application was 77.1 ± 74.9 weeks (18-260 weeks), and an average wound healing period using AM was 20.5 ± 13.4 weeks (6-54 weeks). In all cases there was a significant decrease in pain after five-ten weeks of AM application. The treatment of unhealed wounds continues.

The assessed wound healing rate measured as the size of the wound (in $cm^2$) and wound area reduction (in %) is summarized in Figure 29.

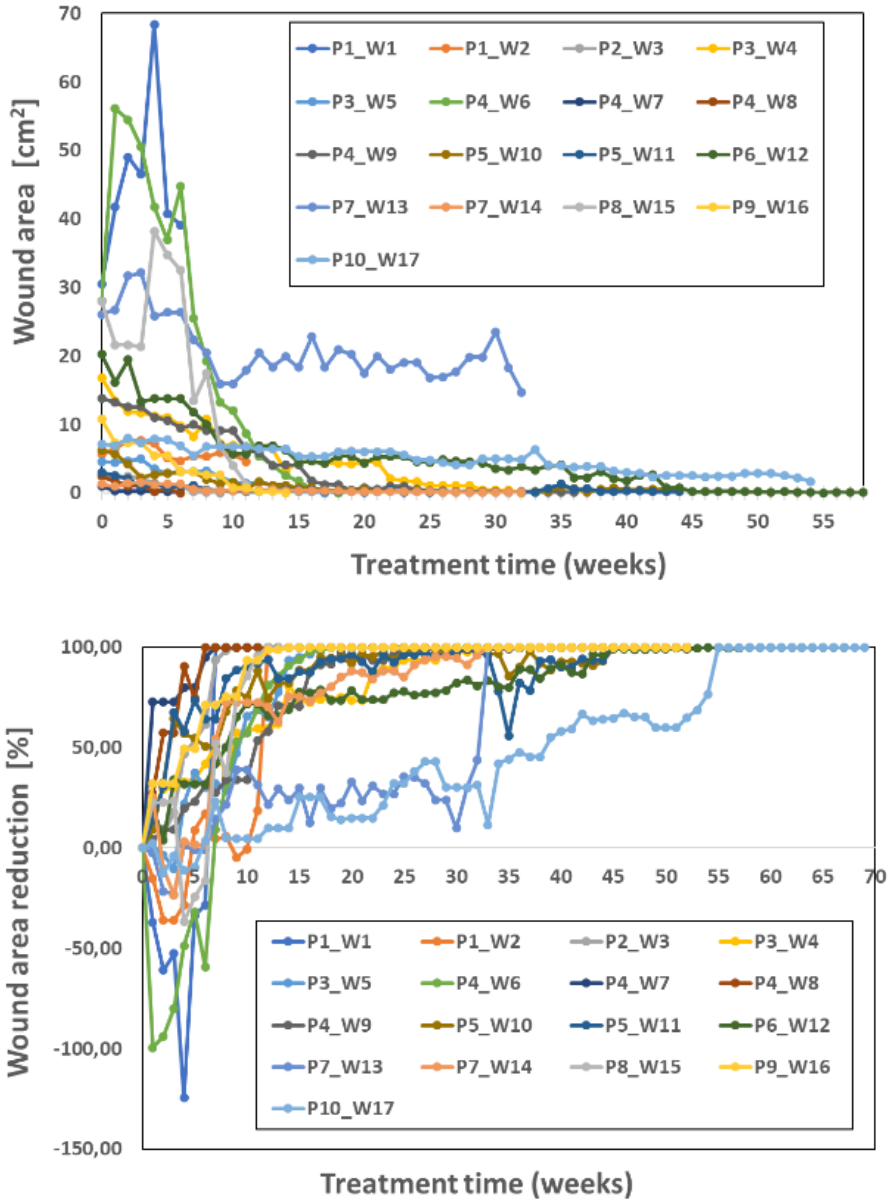


**Figure 29.** The graphical view of wound healing process measured as the size of the wound (in $cm^2$) and wound area reduction (in %) for ten patients with 17 treated wounds.

# Discussion

# Part I: Corneal endothelium

**Corneal endothelium (Hypothesis 1): Preparation of corneal endothelial cell culture.**

Due to the global shortage of donor corneas for endothelial keratoplasties, alternative therapies are being developed including tissue engineering construct and cell injection therapy (Chang et al., 2018). The current trend is to use a cadaveric CECs for graft preparation. In response to the lack of donor corneas, we focused on exploring the possibility of *in vitro* propagation of CECs from corneas deemed unsuitable for Tx or corneoscleral rims (surplus tissue after CE keratoplasty) to increase the supply of donor CE for research and potentially for grafting. Since our results have not been published yet, they are discussed in more detail in this section.

We prepared 38.98% (23/59) of successful monolayers of CECs from donor corneas or rims. These results suggest that CE cultures can be prepared not only from whole corneas, but also from rims that do not contain central CE but have preserved periphery, where stem/proliferating cells could reside. Considering only successful cultures (n=23), slightly more successful cultures were prepared from rims (52.17%, 12/23) than from whole corneas (47.82%, 11/23) by both cell isolation methods. Peel-and-digest method led to more successful cultures derived from corneas (57.89%, 11/19) than from rims (30.30%, 10/33), showing the whole corneas as better source of CECs, as expected. Peel-and-digest method was better method for cell expansion than explant culture method. These results are like that achieved by Choi et al. (2014), who derived the 31.97% (86/269) of successful cultures, with 47.06% (8/17) of cultures derived from whole cornea and 27.83% (64/230) from the rims.

Our results could be affected not only by donor-to-donor characteristics, but also by characteristics and sizes of tissue. Unlike the whole corneas, the rims contained less CECs due to lacking central CE, as well as they often contained areas of impaired/dead cells as a result of tissue processing and storage (Jirsova et al. 2017a). On the other hand, this could be balanced by a shorter storage period of rims (6-18 days), compared to whole corneas (11-23 days), which could minimize the negative effects of hypothermia on CE quality. Moreover, the presence of corneal periphery in rims, where the higher ECD than in central CE was observed, could compensate the loss of central CE in rims (He et al., 2012). Other factors that could possibly influence the outcomes of this study is cause of death (traumatic vs. non-traumatic) (Ventura et al., 1997), cancer or diabetes of the donor (Briggs et al., 2016), race or previous ocular surgery (cataract, refractive), duration from death to enucleation and

the time from preservation to establishment of culture affect quality of CE (Kwon et al., 2016; Parekh et al., 2019a). We did not analyze other factors than the age of donor and the length of storage on quality of CEC cultures and it will be examined in the future studies.

Prolonged storage of corneas in hypothermic conditions and higher donor age negatively affected the success of our CEC cultures, similarly to other studies (Corwin et al. 2013; Parekh et al., 2019a). The average age of donors in case of successful cultures was 56.82 ± 13.67 (28-77) years and 59.33 ± 12.19 (23-78) years in case of unsuccessful cultures. Slightly less successful cultures were derived from older donors (38.2%, 13/34, 60-77 years old) than from younger donors (40%, 10/25, 28-59 years old). Choi et al. (2014) prepared more successful cultures from younger donors (42.9%, 64/149, <60 years old) than from older donors (18.3%, 22/120, >60 years old). This shows the possibility to successfully expand CECs even from donors over 60 years old. Moreover, it was easier to peel CE lamella from older corneas than from younger ones. Similar observation was previously reported (Bennett et al., 2015). Due to lower thickness of DM at younger age, the CE-DM harvested from young corneas have also a tendency to form tighter scroll than lamella obtained from older donor, which may represent an additional stress to CECs (Bennett et al., 2015).

The average storage length of successful cultures was 14.68 ± 5.19 (6-23) days and 16.67 ± 7.99 (4-41) days in case of unsuccessful cultures. Recently it has been shown that hypothermia (for 7 days at 4 °C) negatively affects the growth capacity of CE, and thus success of CEC cultures, compared to organ-culture storage at 31°C (Parkeh et al., 2019a). Due to prolonged hypothermia, whole corneas often contained DM folds and largely sloughed off epithelium. Considering the already published positive effects of organ cultures on CE (Nejepinska et al., 2010; Spinozzi et al., 2018), donor tissue in our experiments was pre-incubated in medium with 15% FBS (overnight), and this increased the success of the cultures, compared to those derived from non-incubated tissue. In such stabilized corneas we detected more Ki-67 positive cells, in both, peripheral and central CE, than in HT corneas. Other factors that were found to positively influence the establishment of CEC cultures that scored as a success were the use of PM (preferably the Opti-MEM I), supplemented with FBS, BPE, EGF, bFGF and ROCK inhibitor, SM2 for 5-7 days, the use of FNC coating as a culture surface and Viscoat, which forced CECs to attach to surface (Parekh et al. 2019b). We did not analyze other factors than the age of donor and the length of hypothermic storage on quality of CEC cultures. The evaluation of other parameters will be one of the goals of the following studies.

We were able to prepare up to 3.2 and 6.4 $cm^2$ of confluent CE from one corneoscleral rim or cornea, respectively. Cell reached confluence after one month and had features of native CECs, i.e. they expressed endothelial markers Na+/K+-ATPase, ZO-1, CD166 and Prdx6. Despite all effort, the total CECs yields were small (LECD: 848.5 ± 443.5 cells/$mm^2$), which is still unsatisfactory for possible clinical use. The cultures represented a mixture of morphologically heterogeneous cells, with a portion (up to 10%/$mm^2$) of cells resembling fibroblasts. Higher cell yields were obtained when CECs derived from younger donors were propagated. None of the used culture media could revert severe EnMT or senescence, if they occurred. This is consistent with results published in other studies (Peh et al., 2015; Parekh et al., 2019b). Probable causes of a large cell loss during the culture were initial tissue quality, CECs isolation method, as well as activation of EnMT and senescence signaling pathways during prolonged culture in PM (Frausto et al., 2020). Therefore, this culture protocol will need to be significantly modified in the future, for example by adding inhibitors of senescence and EnMT. Due to lack of sufficient numbers of CECs we did not validate our results by PCR or western blot methods. Besides that, there is no consensus about a correct genotypic expression profile for healthy CECs (Van den Bogerd et al., 2019).

**Corneal endothelium (Hypothesis 1): Analysis of corneal tissue for stem/progenitor cells and corneal endothelium specific markers**

In response to the need to identify the CE phenotype *in vivo* and *in vitro*, for its possible clinical use, we examined healthy corneal tissue for the presence of a number of selected molecules that have been reported by recent studies as molecules expressed only by CECs and no other corneal cells. The CEC-specific markers are necessary for characterization of native/intact CECs as well as for *in vitro* prepared cultures.

Our relatively extensive immunocytochemical study, showed that none of the selected markers is specific for native CE and its close vicinity, where stem cell for CE could be located (TZ, TM) but can be found in other corneal regions. The following markers were examined (regions of their expression are summarized in brackets): CD166 (endothelium, TZ, TM, stroma, limbus), Prdx6 (epithelum, limbus), GPC4 (all three main corneal cell types, predominantly endothelium and epithelium), MRGX3, 5HT1D, ZP4 (all corneal cells), CD44 (epithelium, stroma), α-SMA (TM, stroma, limbus), K7 (endothelium, epithelium, limbus) and K19 (endothelium, epithelium, limbus). Positive staining for stem/progenitor markers Sox2 and Lgr5 was located predominantly at the periphery of CE, but also in some CECs of the central CE. The Ki-67 positive CECs were found

predominantly in the periphery of CE but also in the central CE, especially near the wounded CE or denuded DM. More Ki-67 positive CECs were detected in organ-cultured corneas than in hypothermically stored corneas. It was reported that the Ki-67 protein levels in a cell depends on the current cell-cycle phase and Ki-67 is undetectable at the G1/S transition in slowly cycling cells that spent a long time in quiescence before re-entering the cell cycle (Miller et al., 2018), the description that applies for CECs (Joyce, 2012a; Espana et al., 2015).

The CD166 (also known as ALCAM) was reported to be expressed in CECs and not keratocytes or epithelial cells, by three independent groups, using three different methods (Ding et al., 2014; Okumura et al., 2014; Dorfmueller et al. 2016). However, the CD166 was detected in other cell types, such as lung fibroblasts or embryonic stem cells (Ding et al., 2014; Dorfmueller et al., 2016). Other groups detected CD166 expression in corneal epithelial limbal stem cells (Albert et al., 2012), corneal stromal stem cells (Funderburgh et al., 2005; He et al., 2016) and corneal epithelium (He et al., 2016). The last finding is in accordance with our observation. The anti-Prdx6 monoclonal antibody TAG-2A12 developed by Ding et al. (2014) was reported to bind CECs only, but the recent transcriptomic study found Prdx6 also in *ex vivo* epithelial cells and keratocytes (Frausto et al., 2020), which is consistent with our observation. The GPC4 was originally reported as a surface-specific marker of CECs, discriminating them from stromal fibroblasts, together with CD200 (Cheong et al., 2013). Our data show that GPC4 is not specific to CECs, like observation of Frausto and colleagues (2020), who reported expression of GPC4 in *ex vivo* epithelial cells and keratocytes. They also detected expression of CD200 in all corneal cells.

In our study, none of the three CEC-specific markers, 5HT1D/HTR1D, ZP4 and MRGX3/MRGPRX3, originally reported by Yoshihara and colleagues (2015), was found exclusively in CECs by this study. The positivity was found throughout the all corneal layers. Weak expression of these three markers in *ex vivo* keratocytes and epithelium was reported also by Frausto et al. (2020). The CD44 and α-SMA are members of a panel of negative markers, i.e. molecules not expressed in CECs (reviewed by Van den Bogerd et al., 2020) which, together with positive markers, serve for characterization of CEC phenotype and their discrimination from other cell types. The CD44 was found to be expressed by corneal epithelium and keratocytes (Zhu et al., 1997; Okumura et al., 2014), which is like our observation. We detected weak expression of the α-SMA, highly conserved microfilament, in limbus, stroma and in some EP cells. As the α-SMA is usually found in stroma and

epithelium of wounded corneas (Esquenazi et al., 2009), more experiments are necessary to confirm or refute our results.

We also examined two cytoskeletal filaments, typical for epithelial cells, keratin 7 (K7) and keratin 19 (K19) and we detected their expression in native CE as well in *in vitro* cultured CECs. The expression of K19 was more prominent than K7, especially on endothelial imprints. The staining signal for K7 was very weak, showing positivity in minority of CECs. The expression of smaller keratins (K7, K8, K18, K19) was previously described in human CECs (Foets et al., 1990; Merjava et al., 2009; Nagymihály et al., 2017). The K7, is specifically expressed in the simple epithelia lining the cavities of the internal organs, in the gland ducts and blood vessels. The K19 is type I cytokeratin, specifically expressed in the developing epidermis, a conjunctiva and limbus (Jain et al., 2010). We also detected expression of K7 and K19 in our *in vitro* cultured CECs, during proliferative phase and after stabilization phase. The expression of K7, K8, K18 and K19 in normal CE shows that the CE has characteristics of a simple epithelia, which usually express these keratins during cell differentiation following cell division (Bragulla and Homberger, 2009). Recently, the K19 expression was associated with increased proliferation of breast cancer cells, where K19 regulates expression of transcription factor E2F1, which plays a key role in transition of cell into S phase of cell cycle (Sharma et al., 2019). Further examination of K7, K19, particularly those in *in vitro* expanded CE, is necessary.

The stem cell markers, Sox2 and Lgr5, were expressed especially in the peripheral CE, TZ and TM of control corneas. The expression of these markers was found by previous studies that have reported the presence of stem-like cells in peripheral parts of the CE (McGowan et al., 2007; Hirata-Tominaga et al., 2013; Epana et al., 2015; Yam et al., 2019). As the Sox2, which regulates other TFs (Oct4 and nanog), was shown to promote proliferation and maintain the stemness (Basu-Roy et al., 2015), as well as it is involved in differentiation and wound healing (McGowan et al., 2007; Han et al., 2014), question remains, if we detected the stem CECs or only the CECs responding to wound healing processes occurring after cell loss during hypothermic storage and after their transfer to organ culture (performed with some corneas). The Lgr5 positive staining of CECs in our samples is in accordance with other observations (Hirata-Tominaga et al., 2013; Espana et al., 2015; Yam et al., 2019). The Lgr5 is a well-established epithelial intestinal stem cell marker (Espana et al., 2015). It may suggest presence of Wnt-driven adult stem cell

populations within peripheral and central CE and putative TZ. As the selected antibody produced a weak signal, it is necessary to confirm our results using other antibody.

Although several markers have been proposed as endothelium-specific in the last twenty years or so (Engelman et al., 2001), none have been confirmed as such. When characterizing the endothelium in culture, it is best to use a non-specific Na+/K+-ATPase, which corresponds to the functionality of the endothelium and, at the same time, well displays its characteristic hexagonal shape. The N-cadherin (He et al., 2016), which was not investigated in this study, also appears to be a promising marker, as a growing number of studies demonstrate its specific expression in CECs and no other eye cells (Frausto et al., 2020). Thus, this marker, with several other will be examined in future studies.

**Corneal endothelium (Hypothesis 2): Endothelial wound repair of the organ-cultured porcine corneas (Paper 1)**

Due to lack of donor corneas for research, we introduced porcine CE as a substitute for scarce human tissue to study remodeling of CE layer after induced mechanical injury, as it has similar features as human CE, especially the non-proliferative nature (Nicholls et al., 2009; Fujita et al., 2013). We presumed that reparative/regenerative capacity of large discs will be more efficient compared to small ones, lacking the transition zone (TZ) between the peripheral CE and the trabecular meshwork, with the presence of putative CE stem cells that may participate in CE wound repair (reviewed by Van den Bogerd et al., 2018b**)**.

The results of the presented study indicate that the porcine CE of the large discs did not repair/regenerate significantly better compared to the smaller discs. No difference was observed between small and large control discs (with intact CE) neither in the central (C) nor in the paracentral CECs (PC), i.e. in the area around the wound, after OC. After injury, the LECD were numerically higher in all large discs, compared to small discs, but without statistical significance. This could be explained by participation of a higher number of CECs, surrounding the lesion in large discs, in wound closure, compared to small discs. As we did not assess CE parameters in far-periphery of CE, we could not confirm/exclude the participation of putative stem cells in TZ to increased LECD in large discs.

We assume that CEC parameters were negatively influenced by the softness of porcine cornea (Elsheikh et al., 2008). In contrast to human cornea, a porcine cornea is larger, and tend to flatten after trephination from porcine bulbus, which could affect the results of this study. Although all corneas with more than 5% of DC around induced lesion were excluded

from experiments, the consequent manipulation could lead to more DM folds in large discs than in small ones despite precautions taken during the tissue manipulation, as large discs bended more during handling.

In our study, the injured discs cultured in medium with 10% FBS had mostly higher values of LECD than those cultured in 2% FBS but statistically significant difference was found only in two cases. The positive effect of serum and its components on CE repair/regeneration, particularly on migration and proliferation of CECs, has been reported repeatedly in both human (Schultz et al., 1992; Nejepinska et al. 2010) and pig (Ayoubi et al., 1996). In contrast to serum concentration, the LECD values of all injured discs were statistically significantly improved after prolonged OC storage. The speed and quality of wound repair could be influenced by initial quality of corneal tissue, culture conditions, but also on type and size of the wound, as observed for human corneas (Waring et al., 1982; Bhogal et al., 2016). It was reported that in humans, the CE with lesion covering 4.4–11% surface of CE was completely closed after 5-7 days (Doughman et al., 1976; Hoppenreijs et al., 1992). In our porcine model, the wound with size of 6.8 $mm^2$, representing 5% of the CE surface was closed after 9 days of OC in most of the corneas. Thus, we can conclude that for endothelial repair the time is more important compared to serum concentration. As in humans, porcine corneal CECs spread out, proliferate and migrate quite slowly and thus need prolonged time for re-establishment of the CE monolayer. Nevertheless, the damage we induced could be too small for a successful activation of putative porcine CE stem cells.

In our experimental condition, the final LECD values in the central CE of injured corneas after 9-day (2409.4 ± 881.8 cells/$mm^2$) incubation did not reach those assessed in the central part of native corneas (3998.0 ± 215.4 cells/$mm^2$). It indicates that more than 9-day incubation period is needed for the full re-establishment of CE hexagonal mosaic, or that the CE proliferation/migration was slowed down by intercellular contact inhibition. Storage induced DM folds as well as natural CE loss during organ culture could counteract the positive effects of storage on regeneration of CE. It is possible that other not yet identified mechanisms might also prevent the full restoration of the ECD.

The proliferation capacity of porcine CEs has been confirmed by the presence of Ki-67-positive CECs in the C and PC endothelium of all injured discs particularly after 9-day OC. No expression was detected in control discs. This is in accordance with previous studies where no cells expressing Ki-67 were present in healthy human CE, but Ki-67 positive cells were detected at the border of healing lesions (Mimura and Joyce, 2006; Bhogal et al., 2016).

In summary, our results indicate that the reparative capacity of porcine corneas, expressed by the CE parameters, is maintained during OC. The CE of large discs tend to repair more rapidly compared to CE of small discs. Not only migration and cell surface enlargement but also proliferation of CECs contributes to the wound closure under experimental conditions used in this study. Our findings support the recent trend in tissue banks to store the large discs for ocular transplantations by OC, particularly for a lamellae preparation.

## Part II: Amniotic membrane

**Amniotic membrane (Hypothesis 3): In house-made decontamination solution have similar effect on amniotic cell viability, as well as antimicrobial efficiency and stability than the commercial decontamination solution (Paper 2 and 3)**

We optimized the AM graft preparation in conditions of tissue bank and prepared in-house made laboratory decontamination solution (LDS) with properties comparable to certified commercial solution (BASE128), which allowed us its use in a case of a supply failure (**Paper 2**). Additionally, this solution has been approved by the national authority, the State Institute for Drug Control.

In fresh AM, the percentage of dead amniotic epithelial cells (%AEC), varied between 4.8–28.1%. We suppose that this could be the result of the inherent tissue variability, the manipulation with placenta and environmental stress applied on AECs. Further epithelial damage during sample preparation was eliminated by using a perforated nitro acetate cellulose membrane as a carrier, to which the AM adhered well without tissue folding, and it was also possible to microscopically examine the vitality of AECs over the perforations. In general, our results are in accordance with other studies showing a good viability of cells (80%) in fresh AM after processing (Hennerbichler et al., 2007; Laurent et al., 2014).

We showed that there are only small differences in cell survival between the application of BASE128 and LDS. The viability of AECs was insignificantly higher after decontamination of AM with BASE128 compared to LDS. The lowest %DEC was found after the treatment with BASE128 for 6 h at 37 °C. Storage for 24 h was less beneficial to the quality of the tissue than storage for 6 h, independent of the type of decontamination solution. The worst survival rate (44.1 ± 19.0 % DEC) of the AECs was observed after storage of AM at low temperature (4 °C) in LDS. This observation is in accordance with some other studies (Jackson et al., 2016), where the best preservation of the cell/tissue

morphology was observed at temperatures between 12 and 24 °C. Further research on the effect of storage in various conditions on AM quality is necessary.

The LDS showed higher toxicity on cells, despite having the composition and concentration of antibiotics/antimycotics (AA) like BASE128. According to Gatto et al. (2013), the BASE128 is a mixture of AA and nutrients diluted in RPMI 1640 medium. Higher cytotoxicity of LDS can be explained by the lack of nutrients, such as glucose and vitamins, present in BASE128. It was shown that cells exposed to the stress, such as nutrient deprivation, accumulate reactive oxygen species and eventually die after a relatively short time (Altman and Rathmell, 2012; Cabodevilla et al., 2013).

Focused mainly on AA, we used LDS with simplified composition in the study to test impact of antibiotics (diluted in physiological saline) on AM, prior testing another additive. As we demonstrated, such solution has no dramatic impact on cell vitality and is simple to prepare at any time, when commercial solution is not available. The basic formula of LDS can be optimized by enrichment with nutrients to improve cell viability.

The viability of AECs was assessed via trypan blue staining. Nevertheless, in order to verify the efficiency and reliability of TB staining, we assessed the percentage of dead cells (%DEC) also via LIVE/DEAD Viability/Cytotoxicity test of the selected samples. The results were very similar (slightly lower) to those obtained by TB staining, however the tendency of increase in %DEC with prolonged incubation time and lower temperature was maintained. In our experiments, the fluorescent staining showed to be rather impractical and costly, as high number of samples had to be processed in limited time, and therefore, we decided to continue processing the samples by TB staining. Using TUNEL method we found higher portion of apoptotic stromal cells after decontamination (63–88%) than before decontamination (42%) suggesting that stromal cells are more susceptible to external stress stimuli than AECs where apoptosis remained constant during experiment (<2% apoptotic cells). This result could be explained by the fact, that AECs are continuously released from the basement membrane (Kumagai et al., 2001), whilst dead stromal cells remain in the stroma. The other plausible explanation is that the cells die by other, rather fast, mechanism than apoptosis (necrosis) and therefore cannot be identified using TUNEL assay. The potential effect of AA on induction of apoptotic cell death was thus not confirmed.

In conclusion, we introduced novel decontamination solution for AM decontamination, we examined various decontamination protocols and have shown that there are only small differences in cell survival between the application of BASE128 and LDS.

These findings may help to better understand the impact of conditions used for the processing and preservation of AM on the final quality of the potential tissue graft. Although the BASE128 expresses lower cytoxicity compared to LDS, the LDS has a satisfactory preservation of cell viability. The basic formula of LDS could be enriched with nutrient components, such as glucose or vitamins, to improve cell viability.

Once we prepared the laboratory decontamination solution which had cell toxicity comparable to commercial solution, we also had to verify its effectiveness with respect to the actual decontamination efficiency (**Paper 3**). The antimicrobial efficiency against five human pathogens (*Staphylococcus aureus, Pseudomonas aeruginosa, Proteus mirabilis, Escherichia coli, Enterococcus faecalis*) and stability (pH and osmolarity) of both decontamination solutions after 0, 1-, 3- and 6-months storage were examined. The difference in the inhibition of bacterial growth between the two decontamination solutions was mostly not statistically significant, with few exceptions. The most pronounced difference between the LDS and BASE128 was observed in their decontamination efficacy against *E. coli* and *E. faecalis*, where the LDS showed to be more efficient than BASE128. The lowest antimicrobial activity was measured against *S. aureus* in both solutions. The osmolarity value of LDS slightly decreased with cold storage, the osmolarity values of the BASE128 could not be measured as they were below the range of the osmometer. Slight changes were found in pH of the less stable LDS solution, whose pH increased from initial value $7.36 \pm 0.07$ to $7.72 \pm 0.19$ after 6 months-storage. We verified that BASE128 expresses similar efficiency in elimination of possible placental bacterial contaminants as LDS and both may be successfully used for decontamination of various tissues.

**<u>Amniotic membrane (Hypothesis 4):</u> Using a gentle method for de-epithelization of amnion, it is possible to obtain both, viable amniotic epithelium and intact denuded membrane simultaneously, for their further clinical/experimental use (Paper 4).**

The major goal of this study was to establish the conditions under which both undamaged basement membrane and viable AECs can be obtained. The denuded AM is more suitable as a substrate for expansion of various cell types, due to composition of basement membrane (Lee et al., 2018b), and amniotic cells contain populations of stem/pluripotent cell that can be further experimentally used (Insausti et al., 2014; Lim et al. 2009). As the results of this work were discussed in a Ph.D. thesis of the first author of this study, Peter Trošan, here we discuss the results very briefly.

We examined three enzymatic method (TrypLE Express, trypsin/EDTA, and thermolysin) for AM de-epithelialization and chose protocol, including Trypsin/EDTA treatment in combination with mechanical scraping as the most successful method for this purpose. Using this method, we obtained denuded AM with well-preserved BM, as well as about 60% viable multipotent AECs, which can be used for research purposes or tissue engineering (Miki et al., 2005). Treatment of AM with TrypLE Express did not disturb the BM significantly but led to only 6% of viable AECs obtained after enzyme treatment. The worst results, with respect to BM integrity and cell viability were observed with thermolysin treatment, which is in accordance to previous reports (Siu et al., 2008; Saghizadeh et al., 2013). Further propagation of isolated AECs led up to five successful passages of viable cells, with positive expression of stem cell markers (SOX2, NANOG), which decreased with passaging. The cell viability correlated well with level of BM damage. Therefore, we suggest that the trypsin/EDTA method is the method of choice when both intact AM and viable AECs are needed for subsequent use and are supposed to be isolated simultaneously.

**Amniotic membrane (Hypothesis 5): Amnion grafts, prepared according to the protocol we use, stimulate and facilitates wound healing of non-healing skin wounds.**

We have been observing the effect of prepared AM grafts on healing of chronic (non-healing) wounds of patients included in an ongoing multicenter study (Project No. NV18-08-00106: Amniotic membrane in the treatment of non-healing wounds) to assess the benefits of AM in diverse groups of non-healing wounds.

Preliminary data indicate that AM in most cases initiates the treatment of wounds in which standard treatment procedures (SOC) have failed. Up to now, the 41% (8/17) wounds were completely healed up to 9 months of AM application. From preliminary results we can clearly see that the application of cryopreserved AM was successful in the treatment of non-healing wounds. The application of AM to non-healing wounds led to an acceleration of healing, which on average started to slow down after 70% wound area reduction. Further healing then proceeded much more slowly. The rate of the treatment of a patient with air-dried AM was slow and after several weeks the treatment was discontinued and replaced with cryopreserved AM instead on the air-dried AM, which accelerated the wound healing. Despite the worse performance of air-dried AM, it is too early to make the conclusion, that cryopreserved AM is better for this purpose. As the clinical study is ongoing, the complete results will be published elsewhere and thus will not be further discussed in this study.

Finally, we are currently working on the analysis of AM from a biochemical point of view, with the aim of finding active substances that contribute to the therapeutic effects of AM, as the mechanism of the positive effect of AM on wounds has not yet been fully elucidated. We are also optimizing preparation of air-dried and lyophilized AM grafts for therapeutic use and examining the differences in wound healing ability and composition of these grafts, compared to standard, cryopreserved AM. The proper lyophilization method can lead to AM graft with comparable features and healing efficiency as observed in cryopreserved AM (Dhall et al., 2018). Moreover, dried grafts can be stored without special deep-freeze facility for long periods (years).

## Conclusion and future perspectives

I consider the following outputs as the main results of my work:

**Hypothesis 1**:

- Although we detected some markers of stem cells and proliferation in the periphery of the cornea, we could not definitively confirm the presence of stem/progenitor cells in the area. We found that corneoscleral rims with preserved peripheral endothelium are a sufficient source of cells to establish endothelial cell culture. The resulting cultures are equivalent to cultures derived from corneas with a complete (or intact) endothelium.
- We have established a protocol for *in vitro* propagation of corneal endothelial cells from discarded corneas or rims with preserved peripheral endothelium. Corneal tissue that would otherwise be discarded can thus be further used to increase pool of endothelial cell for research purposes or for grafting, as it still contains viable cells capable of proliferation. This protocol will be further optimized to maximize cell yields and to maintain their canonical phenotype during *in vitro* culture (hexagonal shape, endothelial marker expression).
- We have clarified the localization of some endothelial markers in the cornea. None of these markers were found to be specific for endothelial cells. The expression of the most promising markers, such as CD166, in *in vivo* and *in vitro* corneal endothelium will be verified in future research.

**Hypothesis 2**:

- No significant difference in endothelial parameters was found between small (corneal) and large (corneoscleral) porcine cultured discs, although the mean LECD values of large damaged and cultured discs were numerically higher than for small discs. Albeit the biochemical properties of the human and pig corneas are similar, the structure and strength of their cornea are different. The lower stiffness of the porcine cornea could adversely affect the results. It would be appropriate to repeat the presented type of experiments on a model of the human cornea, if a sufficient amount of tissue could be obtained in the future.

- We found that not only migration and flattening of endothelial cells but also their proliferation, which are supported by prolonged organ culture with higher serum levels, contribute to wound healing.
- We introduced the pig model as an *ex vivo* model suitable for research on endothelial repair/regeneration capacity.

**Hypothesis 3:**

- We developed our own solution for decontamination of amnion, which was introduced into the preclinical practice of a tissue bank. This solution has toxicity and antimicrobial efficacy similar to commercially available BASE128.

**Hypothesis 4**:

- We have developed and implemented a protocol in which an intact de-epithelialized amnion can be obtained in one step with viable amnion epithelial cell, and they can be further used in basic and preclinical research.

**Hypothesis 5:**

- We developed a protocol for the preparation of cryopreserved and air-dried amniotic grafts, which have been very successfully used to treat chronic long-term non-healing wounds of patients included in a multicenter preclinical study. This research will continue, including research into the mechanisms of action of individual amnion components on wound healing.

## Souhrn a další směrování projektu

Za hlavní výsledky své práce považuji následující výstupy:

**Hypotéza 1:**

- Přestože jsme detekovali některé markery kmenových buněk a proliferace na periferii rohovky, nemohli jsme definitivně potvrdit přítomnost kmenových/progenitorových buněk v dané oblasti. Zjistili jsme, že korneosklerální rimy se zachovaným periferním endotelem, jsou dostatečným zdrojem buněk pro založení kultury endotelových buněk. Vzniklé kultury jsou ekvivalentní kulturám vzniklým z rohovek s kompletním (nebo intaktním) endotelem.
- Zavedli jsme protokol pro *in vitro* propagaci endotelových buněk z rohovek vyřazených z transplantačního programu nebo rimů se zachovaným periferním endotelem. Tkáň, která by byla jinak vyřazena, může být takto dále použita ke zvýšení zásob endotelových buněk pro výzkumné účely nebo pro transplantaci, protože stále obsahuje funkční endotelové buňky schopné proliferace. Tento protokol bude dále optimalizován pro maximalizaci buněčných výtěžků a pro udržení jejich kanonického fenotypu během *in vitro* kultivace.
- Lokalizovali jsme řadu předpokládaných markerů endotelu v rohovce. Žádný z těchto markerů nebyl specifický pro buňky endotelu. Exprese nejslibnějších markerů, jako je CD166, v *in vivo* i *in vitro* CE tkáni, bude ještě studována.

**Hypotéza 2:**

- Nebyl nalezen signifikantní rozdíl v parametrech reparovaného endotelu mezi malými (rohovkovými) a velkými (korneosklerálními) prasečími kultivovanými disky, přestože průměrné hodnoty LECD velkých poškozených a kultivovaných disků byly numericky vyšší než u malých disků. I když biochemické vlastnosti rohovky člověka a prasete jsou podobné, struktura a tloušťka jejich rohovky se liší. Nižší tuhost (a tím indukované další poškození) prasečí rohovky mohla negativně ovlivnit získané výsledky. Prezentovaný typ experimentů by bylo vhodné v budoucnu zopakovat na modelu lidské rohovky.
- Zjistili jsme, že k zahojení rány přispívá nejen migrace a zvětšení plochy buněk endotelu, ale také jejich proliferace, které jsou stimulovány délkou kultivace s vyšším množství séra. V tkáňových bankách by mohla reparace rohovek s částečně poškozeným endotelem pomocí orgánové kultury zvýšit kvalitu a počet tkání pro transplantace.

- Zavedli jsme prasečí model jako *ex vivo* model vhodný pro výzkum reparační/regenerační kapacity endotelu.

**Hypotéza 3**:

- Vyvinuli jsme vlastní roztok pro dekontaminaci amnionu, který byl zaveden do preklinické praxe tkáňové banky. Tento roztok má obdobnou toxicitu a antimikrobiální účinnost jako komerčně dostupný roztok.

**Hypotéza 4**:

- Vyvinuli jsme a zavedli protokol, ve kterém lze v jednom kroku získat nepoškozený de-epitelizovaný amnion jako nosič pro kultivaci dalších typů buněk, například limbálních kmenových buněk, a také živé epitelové buňky amnionu, které budou dále použity v základním a preklinickém výzkumu.

**Hypotéza 5**:

- Vytvořili jsme protokol pro přípravu kryokonzervovaných a vzduchem sušených amniových štěpů, které byly velmi úspěšně použity k léčbě chronických dlouhodobě nehojících se ran pacientů doposud zahrnutých do multicentrické preklinické studie. Tento výzkum bude dále pokračovat, včetně výzkumu mechanismů účinku jednotlivých složek amnionu na hojení ran.

# References

Ab Hamid SS, Zahari NK, Yusof N, et al. (2014). Scanning electron microscopic assessment on surface morphology of preserved human amniotic membrane after gamma sterilisation. Cell Tissue Bank 15:15–24.

Adds PJ, Hunt CJ, Dart JK (2001). Amniotic membrane grafts,‘‘fresh’’ or frozen? A clinical and in vitro comparison. Br J Ophthalmol 85:905–907.

Ahuja N, Jin R, Powers C, et al. (2019). Dehydrated human amnion chorion membrane as treatment for pediatric burns. Adv Wound Care.

Albert R, Veréb Z, Csomos K, et al. (2012). Cultivation and characterization of cornea limbal epithelial stem cells on lens capsule in animal material-free medium. PloS one, 7(10), e47187.

Allen CL, Clare G, Stewart EA, et al. (2013). Augmented dried versus cryopreserved amniotic membrane as an ocular surface dressing. PloS One, 8(10).

Altman BJ, Rathmell JC (2012). Metabolic stress in autophagy and cell death pathways. Cold Spring Harb Perspect Biol, 4(9), a008763.

Arrizabalaga JH, Nollert MU (2018). Human amniotic membrane: a versatile scaffold for tissue engineering. ACS Biomater Sci Eng, 4(7), 2226-2236.

Ayoubi MG, Armitage WJ, Easty DL (1996). Corneal organ culture: effects of serum and a stabilised form of L-glutamine. Br J Ophthalmol, 80(8), 740-744.

Bahn CF, Glassman RM, MacCallum DK, et al. (1986). Postnatal development of corneal endothelium. Invest Ophtalmol Vis Sci, 27:44-51.

Baradaran-Rafii A, Arjmand B, Javadi M (2007). Amniotic membrane transplantation. Iran J Ophthal Res 2:58–75.

Barnett BP, Jun AS (2019). Corneal endothelial cell transplantation: Animal models. Corneal regeneration: Therapy and Surgery. J. L. Alió, J. L. Alió del Barrio and F. Arnalich-Montiel. Cham, Springer International Publishing: 437-454.

Bartakova A, Kunzevitzky NJ, Goldberg JL (2014). Regenerative cell therapy for corneal endothelium. Curr Ophthalmol Rep, 2(3): 81-90.

Bartakova A, Kuzmenko O, Alvarez-Delfin K, et al. (2018). A cell culture approach to optimized human corneal endothelial cell function. Invest Opthalmol Vis Sci, 59(3).

Basu-Roy U, Bayin NS, Rattanakorn K, et al. (2015). Sox2 antagonizes the Hippo pathway to maintain stemness in cancer cells. Nat Commun, 6(1), 1-14.

Bayyoud T, Rohrbach JM, Bartz-Schmidt KU, et al. (2019). Histopathology of a retrocorneal membrane after Descemet membrane endothelial keratoplasty: a case report. J Med Case Rep 13(1): 31.

Beaulieu Leclerc V, Roy O, Santerre K, Proulx S (2018). TGF-β1 promotes cell barrier function upon maturation of corneal endothelial cells. Sci Rep, 8(1).

Bednarz J, Rodokanaki-von Schrenck A, Engelmann K (1998). Different characteristics of endothelial cells from central and peripheral human cornea in primary culture and after subculture. In Vitro Cell Dev Biol Anim, 34(2): 149-153.

Benirschke K, Burton GJ, Baergen RN (2012). Anatomy and pathology of the placental membranes. In Pathology of the human placenta (pp. 249-307). Springer, Berlin, Heidelberg.

Bennett A, Mahmoud S, Drury D, et al. (2015). Impact of donor age on corneal endothelium-descemet membrane layer scroll formation. Eye Contact Lens, 41(4): 236-239.

Bhogal M, Lwin CN, Seah X-Y, et al. (2017). Allogeneic Descemet's membrane transplantation enhances corneal endothelial monolayer formation and restores functional integrity following Descemet's stripping." Invest Opthalmol Vis Sci, 58(10).

Bhogal M, Matter K, Balda MS, Allan BD (2016). Organ culture storage of pre-prepared corneal donor material for Descemet's membrane endothelial keratoplasty. Br J Ophthalmol, 100(11), 1576-1583.

Bilic G, Zeisberger SM, Mallik AS, et al. (2008). Comparative characterization of cultured human term amnion epithelial and mesenchymal stromal cells for application in cell therapy. Cell Transplant, 17(8), 955-968.

Bohnsack BL, Kasprick DS, Kish PE, et al. (2012). A zebrafish model of axenfeld-rieger syndrome reveals that pitx2 regulation by retinoic acid is essential for ocular and craniofacial development. Invest Ophthalmol Vis Sci, 53(1): 7-22.

Bonanno JA (2012). Molecular mechanisms underlying the corneal endothelial pump. Exp Eye Res, 95(1), 2-7.

Bourne G (1962). The foetal membranes: a review of the anatomy of normal amnion and chorion and some aspects of their function. Postgrad Med J, 38(438), 193.

Bragulla HH, Homberger DG (2009). Structure and functions of keratin proteins in simple, stratified, keratinized and cornified epithelia. J Anat, 214(4), 516-559.

Briggs S, Osuagwu UL, AlHarthi EM (2016). Manifestations of type 2 diabetes in corneal endothelial cell density, corneal thickness and intraocular pressure. J Biomed Res, 30(1), 46.

Buhimschi I, Jabr M, Buhimschi C, et al. (2004). The novel antimicrobial peptide β3- defensin is produced by the amnion: a possible role of the fetal membranes in innate immunity of the amniotic cavity. Am J Obstet Gynecol 191:1678–1687.

Bulmer JN, Johnson PM (1984). Macrophage populations in the human placenta and amniochorion. Clin Exp Immunol, 57(2), 393.

Burgos H (1983). Lyophilized human amniotic membranes used in reconstruction of the ear. J R Soc Med, 76(5), 433-433.

Cabodevilla AG, Sánchez-Caballero L, Nintou E, et al. (2013). Cell survival during complete nutrient deprivation depends on lipid droplet-fueled β-oxidation of fatty acids. J Biol Chem, 288(39), 27777-27788.

Corwin WL, Baust JM, Van Buskirk GR, Baust JG (2013). 47. In vitro assessment of apoptosis and necrosis following cold storage in human corneal endothelial cells. Cryobiology; 61:398-398.

Cvekl A, Tamm ER (2004). Anterior eye development and ocular mesenchyme: new insights from mouse models and human diseases. Bioessays, 26(4): 374-386.

Dai Y, Guo Y, Wang C, et al. (2014). Non-genetic direct reprogramming and biomimetic platforms in a preliminary study for adipose-derived stem cells into corneal endothelia-like cells. PLoS One, 9(10): e109856.

Davis J (1910). Skin transplantation with a review of 550 cases at the Johns Hopkins Hospital. Johns Hopkins Hospital Report 15: 3107.

De Rotth A (1940). Plastic repair of conjunctival defects with fetal membranes. Arch Ophthalmol, 23(3), 522-525.

Dhall S, Sathyamoorthy M, Kuang JQ, et al. (2018). Properties of viable lyopreserved amnion are equivalent to viable cryopreserved amnion with the convenience of ambient storage. PloS one, 13(10).

Ding V, Chin A, Peh G, et al. (2014). Generation of novel monoclonal antibodies for the enrichment and characterization of human corneal endothelial cells (hCENC) necessary for the treatment of corneal endothelial blindness. MAbs, Vol. 6, No. 6, pp. 1439-1452. Taylor & Francis.

Dorfmueller S, Ching Tan H, Xian Ngoh Z, et al. (2016). Isolation of a recombinant antibody specific for a surface marker of the corneal endothelium by phage display. Nat Publ Gr., 6(February):1-12.

Doughman DJ, Van Horn D, Rodman WP, et al. (1976). Human corneal endothelial layer repair during organ culture. Arch Ophthalmol, 94(10), 1791-1796.

Doutch JJ, Quantock AJ, Joyce NC, Meek KM (2012). Ultraviolet light transmission through the human corneal stroma is reduced in the periphery. Biophys J, 102(6): 1258-1264.

Drigeard Desgarnier MC, Zinflou C, Mallet JD, et al. (2016). Telomere length measurement in different ocular structures: A potential implication in corneal endothelium pathogenesis. Invest Ophthalmol Vis Sci, 57(13):5547-5555.

Dua HS, Azuara-Blanco A (1999). Amniotic membrane transplantation. Br J Ophthalmol 83:748–752.

Dua HS, Gomes JA, King AJ, Maharajan VS (2004). The amniotic membrane in ophthalmology. Surv Ophthalmol 49:51–77.

Duan-Arnold Y, Uveges TE, Gyurdieva A, Johnson A, Danilkovitch A (2015). Angiogenic potential of cryopreserved amniotic membrane is enhanced through retention of all tissue components in their native state. Adv Wound Care, 4(9), 513-522.

Dudakova L, Evans CJ, Pontikos N, et al. (2019). The utility of massively parallel sequencing for posterior polymorphous corneal dystrophy type 3 molecular diagnosis. Experimental eye research, 182, 160-166.

Elsheikh A, Alhasso D, Rama P (2008). Biomechanical properties of human and porcine corneas. Exp Eye Research, 86(5), 783-790.

Enders A, King B (1988). Formation and differentiation of extraembryonic mesoderm in the rhesus monkey. Am J Anat, 181:327–340.

Engelmann K, Bednarz J, Schäfer HJ, Friedl P (2001). Isolation and characterization of a mouse monoclonal antibody against human corneal endothelial cells. Exp Eye Res, 73(1), 9-16.

Engelmann K, Bohnke M, Friedl P (1988). Isolation and long-term cultivation of human corneal endothelial cells. Invest Ophthalmol Vis Sci 29(11): 1656-1662.

Engelmann K, Friedl P (1995) Growth of human corneal endothelial cells in a serum–reduced medium. Cornea 14:62–70.

Enomoto K, Mimura T, Harris DL, Joyce NC (2006). Age differences in cyclin-dependent kinase inhibitor expression and Rb hyperphosphorylation in human corneal endothelial cells. Invest Opthalmol Vis Sci, 47(10).

Eskandarlou M, Azimi M, Rabiee S, Rabiee MAS (2016). The healing effect of amniotic membrane in burn patients. World J Plast Surg, 5(1), 39.

Espana EM, Sun M, Birk DE (2015). Existence of corneal endothelial slow-cycling cells. Invest Ophthalmol Vis Sci, 56(6), 3827-3837.

Esquenazi S, Esquenazi I, Grunstein L, et al. (2009). Immunohistological evaluation of the healing response at the flap interface in patients with LASIK ectasia requiring penetrating keratoplasty. J Refract Surg, 25(8), 739-746.

Farazdaghi M, Adler J and Farazdaghi SM (2001). Electron microscopy of human amniotic membrane. In: Nather A (ed.) The Scientific Basis of Tissue Transplantation, World Scientific Publishing Co., New Jersey, USA pp. 149–171.

Fatimah SS, Tan GC, Chua K, et al. (2013). Stemness and angiogenic gene expression changes of serial-passage human amnion mesenchymal cells. Microvasc Res, 86:21–29.

Foets BJ, van den Oord JJ, Desmet VJ, Missotten L (1990). Cytoskeletal filament typing of human corneal endothelial cells. Cornea 9, 312–317.

Franco GR, De Carvalho AF, Kroon EG, et al. (1999). Biological activities of a human amniotic membrane interferon. Placenta, 20(2-3), 189-196.

Fraser JF, Cuttle L, Kempf M, et al. (2009). A randomised controlled trial of amniotic membrane in the treatment of a standardised burn injury in the merino lamb. Burns, 35(7), 998-1003.

Frausto RF, Chung DD, Boere PM, et al. (2019). ZEB1 insufficiency causes corneal endothelial cell state transition and altered cellular processing. PloS One, 14(6).

Frausto RF, Le DJ, Aldave AJ (2016). Transcriptomic analysis of cultured corneal endothelial cells as a validation for their use in cell replacement therapy. Cell Transplant, 25(6): 1159-76.

Frausto RF, Swamy VS, Peh GS, et al. (2020). Phenotypic and functional characterization of corneal endothelial cells during in vitro expansion. Sci Rep, 10(1), 1-22.

Fuchsluger TA, Jurkunas U, Kazlauskas A, Dana R (2011). Anti-apoptotic gene therapy prolongs survival of corneal endothelial cells during storage. Gene Ther, 18(8): 778-787.

Fujita M, Mehra R, Lee SE, et al. (2013). Comparison of proliferative capacity of genetically-engineered pig and human corneal endothelial cells. Ophthalmic Res, 49(3), 127-138.

Funderburgh ML, Du Y, Mann MM, et al. (2005). PAX6 expression identifies progenitor cells for corneal keratocytes. The FASEB journal, 19(10), 1371-1373.

Gage PJ, Rhoades W, Prucka SK, Hjalt T (2005). Fate maps of neural crest and mesoderm in the mammalian eye. Invest Ophthalmol Vis Sci, 46(11): 4200-4208.

Gajiwala K, Gajiwala AL (2004). Evaluation of lyophilised, gamma-irradiated amnion as a biological dressing. Cell Tissue Bank 5:73–80.

García-López G, Ávila-González D, García-Castro IL, et al. (2019). Pluripotency markers in tissue and cultivated cells in vitro of different regions of human amniotic epithelium. Exp Cell Res, 375(1), 31-41.

Garcin T, Gauthier A-S, Crouzet E, et al. (2019). Three-month storage of human corneas in an active storage machine. Transplantation, 104(6):1159-1165.

Gatto C, Giurgola L, D'Amato-Tothova J (2013). A suitable and efficient procedure for the removal of decontaminating antibiotics from tissue allografts. Cell Tissue Bank 14(1):107–115.

Gendron SP, Rochette PJ (2015). Modifications in stromal extracellular matrix of aged corneas can be induced by ultraviolet A irradiation. Aging Cell, 14(3): 433-442.

Goldberg MF, Bron AJ (1982). Limbal palisades of Vogt. Trans Am Ophthalmol Soc, 80, 155-171.

Gordon SR, Staley CA (1990). Role of the cytoskeleton during injury-induced cell migration in corneal endothelium. Cell Motil Cytoskeleton, 16(1): 47-57.

Grabska-Liberek I, Szaflik J, Brix-Warzecha M (2003). The importance of various factors relating to the morphological quality of corneas used for PKP by the Warsaw Eye Bank from 1996 to 2002. Ann Transplant, 8(2): 26-31.

Ha NT, Nakayasu K, Murakami A, Ishidoh K, Kanai A (2004). Microarray analysis identified differentially expressed genes in keratocytes from keratoconus patients. Curr Eye Res, 28:373–379; 2004

Hajiiski O (1990). Amniotic membranes for temporary burn coverage. Ann Burn Fire Disasters 9:88–92.

Hamrah P, Dana MR (2007). Corneal antigen-presenting cells. Chem Immunol Allergy, 92: 58-70.

Hamuro J, Ueno M, Toda M, et al. (2016). Cultured human corneal endothelial cell aneuploidy dependence on the presence of heterogeneous subpopulations with distinct differentiation phenotypes. Invest Ophthalmol Vis Sci, 57(10): 4385-92

Han SM, Han SH, Coh YR, et al. (2014). Enhanced proliferation and differentiation of Oct4-and Sox2-overexpressing human adipose tissue mesenchymal stem cells. Exp Mol Med, 46(6), e101-e101.

Hanna C, Bicknell DS, O'Brien JE (1961). Cell turnover in the adult human eye. Arch Ophthalmol, 65, 695-698.

Hao Y, Ma D, Hwang D, Kim W, Zhang F (2000). Identification of antiangiogenic and antiinflammatory proteins in human AM. Cornea 19:348–352.

Hara S, Kawasaki S, Yoshihara M, et al. (2019). Transcription factor TFAP2B up-regulates human corneal endothelial cell–specific genes during corneal development and maintenance. J Biol Chem, 294(7): 2460-2469.

Hassell JR, Birk DE (2010). The molecular basis of corneal transparency. Exp Eye Res, 91(3), 326-335.

Hatou S, Yoshida, S, Higa K, et al. (2013). Functional corneal endothelium derived from corneal stroma stem cells of neural crest origin by retinoic acid and Wnt/beta-catenin signaling. Stem Cells Dev, 22(5): 828-839.

Haugh AM, Witt JG, Hauch A, et al. (2017). Amnion membrane in diabetic foot wounds: a meta-analysis. Plast Reconstr Surg Glob Open, 5(4).

He Z, Campolmi N, Gain P, et al. (2012). Revisited microanatomy of the corneal endothelial periphery: new evidence for continuous centripetal migration of endothelial cells in humans. Stem Cells, 30(11), 2523-2534.

He Z, Forest F, Gain P, et al. (2016). 3D map of the human corneal endothelial cell. Sci Rep, 6:29047.

Hennerbichler S, Reichl B, Pleiner D, et al. (2007). The influence of various storage conditions on cell viability in amniotic membrane. Cell Tissue Bank, 8(1), 1-8.

Heuberger J, Birchmeier W (2010). Interplay of cadherin-mediated cell adhesion and canonical Wnt signaling. Cold Spring Harbor perspectives in biology, 2(2), a002915.

Hirata-Tominaga K, Nakamura T, Okumura N, et al. (2013). Corneal endothelial cell fate is maintained by LGR5 through the regulation of hedgehog and Wnt pathway. Stem Cells, 31(7): 1396-407.

Hoppenreijs VP, Pels E, Vrensen GF, Oosting J, Treffers WF (1992). Effects of human epidermal growth factor on endothelial wound healing of human corneas. Invest Ophthalmol Vis Sci, 33(6), 1946-1957.

Huppertz B (2008). The anatomy of the normal placenta. J Clin Pathol, 61(12), 1296-1302.

Chang YK, Hwang, JS, Chung TY, Shin YJ (2018). SOX2 activation using CRISPR/dCas9 promotes wound healing in corneal endothelial cells. Stem Cells, 36(12), 1851-1862.

Chen HJ, Pires RT, Tseng SC (2000). Amniotic membrane transplantation for severe neurotrophic corneal ulcers. Br J Ophthalmol, 84(8), 826-833.

Chen J, Li Z, Zhang L, et al. (2017). Descemet's membrane supports corneal endothelial cell regeneration in rabbits. Sci Rep, 7(1): 6983.

Chen X, Wu L, Li Z, et al. (2018). Directed differentiation of human corneal endothelial cells from human embryonic stem cells by using cell-conditioned culture media. Invest Ophthalmol Vis Sci, 59(7): 3028-3036.

Chen Y, Huang K, Nakatsu MN, et al. (2013). Identification of novel molecular markers through transcriptomic analysis in human fetal and adult corneal endothelial cells. Hum Mol Genet, 22(7): 1271-9.

Cheong YK, Ngoh ZX, Peh GSL, et al. (2013). Identification of cell surface markers glypican-4 and CD200 that differentiate human corneal endothelium from stromal fibroblasts. Invest Ophthalmol Vis Sci, 54(7), 4538-4547.

Chng Z, Peh GS, Herath WB (2013). High-throughput gene expression analysis identifies reliable expression markers of human corneal endothelial cells. PLoS One, 8:e67546.

Choi JS, Kim EY, Kim MJ, et al. (2014). Factors affecting successful isolation of human corneal endothelial cells for clinical use. Cell Transplant, 23(7): 845-54.

Choi JS, Williams JK, Greven M, et al. (2010). Bioengineering endothelialized neo-corneas using donor-derived corneal endothelial cells and decellularized corneal stroma. Biomaterials, 31(26): 6738-45.

Chowdhury UR, Madden BJ, Charlesworth MC, Fautsch MP (2010). Proteome analysis of human aqueous humor. Invest Ophthalmol Vis Sci, 51(10): 4921-4931.

Ickes R, Harris DL, Joyce NC (2002). "Classical" cadherin expression in corneal endothelium. Invest Ophthalmol Vis Sci, 43: U881-U881.

Ilic D, Vicovac L, Nikolic M, Lazic Ilic E (2016). Human amniotic membrane grafts in therapy of chronic non-healing wounds. Br Med Bull, 117(1), 59-67.

Insausti CL, Alcaraz A, García-Vizcaíno EM, et al. (2010). Amniotic membrane induces epithelialization in massive posttraumatic wounds. Wound Repair Regen, 18(4), 368-377.

Insausti CL, Blanquer M, García-Hernandez AM, et al. (2014). Amniotic Membrane-Derived Stem Cells: Immunomodulatory Properties and Potential Clinical Application. Stem Cells Cloning: Adv Appl, 7, 53−63.

Ishino Y, Sano Y, Nakamura T, et al. (2004). Amniotic membrane as a carrier for cultivated human corneal endothelial cell transplantation." Invest Opthalmol Vis Sci, 45(3).

Jackel T, Knels L, Valtink M, et al. (2011). Serum-free corneal organ culture medium (SFM) but not conventional minimal essential organ culture medium (MEM) protects human corneal endothelial cells from apoptotic and necrotic cell death. Br J Ophthalmol, 95(1): 123-130.

Jackson C, Eidet JR, Reppe S, et al. (2016). Effect of Storage Temperature on the Phenotype of Cultured Epidermal Cells Stored in Xenobiotic-Free Medium. Curr Eye Res 41, 757-768.

Jain R, Fischer S, Serra S, Chetty R (2010). The use of Cytokeratin 19 (CK19) immunohistochemistry in lesions of the pancreas, gastrointestinal tract, and liver. Appl Immunohistochem Mol Morphol, 18(1):9-15.

Jerman UD, Veranic P, Kreft ME (2014). Amniotic Membrane Scaffolds Enable the Development of Tissue-Engineered Urothelium with Molecular and Ultrastructural Properties Comparable to that of Native Urothelium. Tissue Eng., Part C, 20 (4), 317−327.

Jiang S, Nail SL (1997). Effect of process conditions on recovery of protein activity after freezing and freeze-drying. Eur J Pharm Biopharm,45:249–57.

Jirsova K, Clover J, Stoeger et al. (2017a) Light and Specular Microscopy Assessment of the Cornea for Grafting. In: Light and Specular Microscopy of the Cornea. Cham: Springer International Publishing; p. 75–100

Jirsova K, Jones GL (2017b). Amniotic membrane in ophthalmology: properties, preparation, storage and indications for grafting—a review. Cell and tissue banking, 18(2), 193-204.

Jirsova K, Merjava S, Martincova R, et al. (2007). Immunohistochemical characterization of cytokeratins in the abnormal corneal endothelium of posterior polymorphous corneal dystrophy patients. Exp Eye Res, 84(4): 680-86.

Jirsova K, Neuwirth A, Kalasova S, Vesela V, Merjava S (2010). Mesothelial proteins are expressed in the human cornea. Exp Eye Res, 91(5): 623-9.

Johnson A, Gyurdieva A, Dhall S, et al. (2017). Understanding the impact of preservation methods on the integrity and functionality of placental allografts. Ann Plast Surg, 79(2), 203-213.
Joseph A, Hossain P, Jham S, et al. (2003). Expression of CD34 and L-selectin on human corneal keratocytes. Invest Ophthalmol Vis Sci, 44:4689–92.
Joyce NC (2012a). Proliferative capacity of corneal endothelial cells. Exp Eye Res, 95(1): 16-23.
Joyce NC, Harris DL, Markov V, Zhang Z, Saitta B (2012b). Potential of human umbilical cord blood mesenchymal stem cells to heal damaged corneal endothelium. Mol Vis, 18, 547.
Kabosova A, Azar DT, Bannikov GA, et al. (2007). Compositional differences between infant and adult human corneal basement membranes. Invest Opthalmol Vis Sci, 48(11).
Keeley R, Topoluk N, Mercuri J (2014). Tissues Reborn: Fetal Membrane-Derived Matrices and Stem Cells in Orthopedic Regenerative Medicine. Crit Rev Biomed Eng, 42 (3−4), 249−270.
Keino H, Horie S, Sugita S (2018). Immune privilege and eye-derived T-regulatory cells. J Immunol Res, 2018: 1679197.
Keitel S (2019). Guide to the quality and safety of tissues and cells for human application, European Committee (Partial Agreement) on Organ Transplantation, European Directorate for the Quality of Medicines & HealthCare (EDQM), 4th edn. Council of Europe, Strasbourg, pp 227–233. https://www.edqm.eu/en/news/new-guide-quality-and-safety-tissues-and-cells-human-application (Accessed online: 5.5.2020).
Kennedy S, Lace R, Carserides C, et al. (2019). Poly-ε-lysine based hydrogels as synthetic substrates for the expansion of corneal endothelial cells for transplantation. J Mater Sci Med, 30(9).
Kim J and Tseng S (1995). The effects on inhibition of corneal neovascularization after human AM transplantation in severely damaged rabbit corneas. Korean J Ophthalmol 9:32–46.
Kim J, Kang HM, Kim H et al (2007). Ex vivo characteristics of human amniotic membrane derived stem cells. Cloning Stem Cells 9:581–594
Kim JS, Kim JC, Hahn TW, Park WC (2001). Amniotic membrane transplantation in infectious corneal ulcer. Cornea 20:720–726.
King A, Critchley H, Sallenave J, Kelly R (2003). Elafin in human endometrium: an antiprotease and antimicrobial molecule expressed during menstruation. J Clin Endocrinol Metab 88:4426–4431.
Kirsner RS, Margolis DJ, Baldursson BT, et al. (2020). Fish skin grafts compared to human amnion/chorion membrane allografts: A double-blind, prospective, randomized clinical trial of acute wound healing. Wound Rep Regen, 28(1), 75-80.
Kobayashi N, Kabuyama Y, Sasaki S, Kato K, Homma Y (2002). Suppression of corneal neovascularization by culture supernatant of human amniotic cells. Cornea 21:62–67.
Kogan S, Sood A, Granick MS (2018). Amniotic Membrane Adjuncts and Clinical Applications in Wound Healing: A Review of the Literature. Wounds: a compendium of clinical research and practice, 30(6), 168-173.
Koh SWM (2012). Corneal endothelial autocrine trophic factor VIP in a mechanism-based strategy to enhance human donor cornea preservation for transplantation. Exp Eye Res, 95(1), 48-53.
Koike C, Zhou K, Takeda Y, et al. T (2014). Characterization of amniotic stem cells. Cell Reprogram, 16(4), 298-305.
Koizumi N, Inatomi T, Sotozono C, et al. (2000). Growth factor mRNA and protein in preserved human amniotic membrane. Curr Eye Res 20:173–177.
Koizumi N, Rigby H, Fullwood NJ, et al. (2007). Comparison of intact and denuded amniotic membrane as a substrate for cell-suspension culture of human limbal epithelial cells. Graefes Arch Clin Exp Ophthalmol 245, 123-134.
Komai Y, Ushiki T (1991). The three-dimensional organisation of collagen fibrils in the human cornea and sclera. Invest Ophthalmol Vis Sci, 32:2244–58
Kremer I, Rapuano CJ, Cohen EJ, Laibson PR, Eagle RC (1993). Retrocorneal Fibrous Membranes in Failed Corneal Grafts. Am J Ophthalmol, 115(4): 478-483.
Kruse FE, Joussen AM, Rohrschneider K, et al. (2000). Cryopreserved human amniotic membrane for ocular surface reconstruction. Graefe's Arch Clin Exp Ophthalmol, 238(1), 68-75.
Kumagai K, Otsuki Y, Ito Y, et al. (2001). Apoptosis in the normal human amnion at term, independent of Bcl-2 regulation and onset of labour. Mol Hum Reprod, 7(7), 681-689.
Kwon JW, Cho KJ, Kim HK, et al. (2016). Analyses of factors affecting endothelial cell density in an eye bank corneal donor database. Cornea, 35(9), 1206-1210.

Laing RA, Sanstrom MM, Berrospi AR, Leibowitz HM (1976). Changes in the corneal endothelium as a function of age. Exp Eye Res 22(6): 587-594.
Lass JH, Sugar A, Benetz BA, et al. (2010). Endothelial cell density to predict endothelial graft failure after penetrating keratoplasty. Arch Ophthalmol 128(1): 63-69.
Laurent R, Nallet A, Obert L, et al. (2014). Storage and qualification of viable intact human amniotic graft and technology transfer to a tissue bank. Cell Tissue Bank, 15(2), 267-275.
Lee J, Jung E, Heur M (2019). Injury induces endothelial to mesenchymal transition in the mouse corneal endothelium in vivo via FGF2. Mol Vis, 25: 22-34.
Lee JG, Jung E, Heur M (2018a). Fibroblast growth factor 2 induces proliferation and fibrosis via SNAI1-mediated activation of CDK2 and ZEB1 in corneal endothelium. J Biol Chem 293(10): 3758-3769.
Lee HJ, Nam SM, Choi SK, et al. (2018b). Comparative study of substrate free and amniotic membrane scaffolds for cultivation of limbal epithelial sheet. Sci Rep, 8(1), 1-11.
Lee PH, Tsai SH, Kuo L, et al. (2012). A prototype tissue engineered blood vessel using amniotic membrane as scaffold. Acta Biomater, 8(9), 3342-3348.
Lee S-H, Tseng SCG (1997). Amniotic membrane transplantation for persistent epithelial defects with ulceration. Am J Ophthalmol, 123(3):303–12
Lehrer MS, Sun TT, Lavker RM (1998). Strategies of epithelial repair: modulation of stem cell and transit amplifying cell proliferation. J Cell Sci, 111 (Pt 19), 2867-2875.
Li C, Dong F, Jia Y, et al. (2013). Notch signal regulates corneal endothelial-to-mesenchymal transition. Am J Pathol, 183(3): 786-795.
Li H, Niederkorn J, Neelam S, et al. (2005). Immunosuppressive factors secreted by human amniotic epithelial cells. Invest Ophthalmol Vis Sci 46:900–907.
Li W, Sabater AL, Chen Y-T, et al. (2007). A novel method of isolation, preservation, and expansion of human corneal endothelial cells. Invest Opthalmol Vis Sci, 48(2).
Lim LS, Riau A, Poh R (2009). Effect of Dispase denudation on amniotic membrane. Mol Vis, 15: 1962–1970
Ljubimov AV, Saghizadeh M (2015). Progress in corneal wound healing. Prog Retin Eye Res, 49: 17-45.
Loh CY, Chai JY, Tang TF, et al. (2019). The E-cadherin and N-cadherin switch in epithelial-to-mesenchymal transition: Signaling, therapeutic implications, and challenges. Cells, 8(10), 1118.
Loh IP, Gaskin JCF, Sherwin T, McGhee CN (2018). Extreme Descemet's membrane rupture with hydrops in keratoconus: Clinical and histological manifestations. Am J Ophthalmol Case Rep, 10, 271-275.
Lovatt M, Adnan K, Peh GSL, Mehta JS (2018). Regulation of Oxidative Stress in Corneal Endothelial Cells by Prdx6. Antioxidants (Basel), 7(12).
Malhotra C, Jain AK (2014). Human amniotic membrane transplantation: different modalities of its use in ophthalmology. World J Transplant 4:111–121.
Mao Y, Hoffman T, Singh-Varma A, et al. (2017). Antimicrobial peptides secreted from human cryopreserved viable amniotic membrane contribute to its antibacterial activity. Sci Rep, 7(1), 1-8.
McGowan SL, Edelhauser HF, Pfister RR, et al. (2007). Stem cell markers in the human posterior limbus and corneal endothelium of unwounded and wounded corneas. Mol Vis,13:1984-2000.
McQuilling JP, Vines JB, Kimmerling K, et al. (2017). Proteomic comparison of amnion and chorion and evaluation of the effects of processing on placental membranes. Wounds, 29(6), E38-E42.
Meller D, Pauklin M, Thomasen H, et al. (2011). Amniotic membrane transplantation in the human eye. Dtsch Arztebl Int 108:243–248.
Mencucci R, Paladini I, Menchini U, et al. (2011). Inhibition of viral replication in vitro by antiviral-treated amniotic membrane. Possible use of amniotic membrane as drug-delivering tool. Br J Ophthalmol, 95(1), 28-31.
Merjava S, Neuwirth A, Mandys V, Jirsova K (2009). Cytokeratins 8 and 18 in adult human corneal endothelium. Exp Eye Res, 89(3): 426-31.
Miki T (2018). Stem cell characteristics and the therapeutic potential of amniotic epithelial cells. Am J Reprod Immunol 80, e13003.

Miki T, Lehmann T, Cai H, Stolz DB, Strom SC (2005). Stem cell characteristics of amniotic epithelial cells. Stem cells, 23(10), 1549-1559.

Miller I, Min M, Yang C, et al. (2018). Ki67 is a graded rather than a binary marker of proliferation versus quiescence. Cell Rep, 24(5), 1105-1112.

Mimura T, Joyce NC (2006). Replication competence and senescence in central and peripheral human corneal endothelium. Invest Ophthalmol Vis Sci, 47(4), 1387-1396.

Mimura T, Yamagami S, Amano S (2013). Corneal endothelial regeneration and tissue engineering. Prog Retin Eye Res, 35: 1-17

Miyai T, Maruyama Y, Osakabe Y, Nejima R, Miyata K, Amano S (2008). Karyotype changes in cultured human corneal endothelial cells. Mol Vis,14: 942-950.

Miyamoto T, Sumioka T, Saika S (2010). Endothelial mesenchymal transition: a therapeutic target in retrocorneal membrane. Cornea 29 Suppl 1: S52-56.

Mohammadi AA, Eskandari S, Johari HG, et al. (2017). Using amniotic membrane as a novel method to reduce post-burn hypertrophic scar formation: A prospective follow-up study. J Cutan Aesthet Surg, 10(1), 13.

Mohammadi AA, Jafari SMS, Kiasat M, et al. (2013). Effect of fresh human amniotic membrane dressing on graft take in patients with chronic burn wounds compared with conventional methods. Burns, 39(2), 349-353.

Muller LJ, Pels E, Schurmans LR, Vrensen GF (2004). A new three-dimensional model of the organization of proteoglycans and collagen fibrils in the human corneal stroma. Exp Eye Res, 78:493–501

Murphy C, Alvarado J, Juster R, Maglio M (1984). Prenatal and postnatal cellularity of the human corneal endothelium. A quantitative histologic study. Invest Ophthalmol Vis Sci, 25(3): 312-322.

Murphy SV, Skardal A, Nelson Jr RA, et al. (2019). Amnion membrane hydrogel and amnion membrane powder accelerate wound healing in a full thickness porcine skin wound model. Stem Cells Transl Med, 9(1):80-92.

Nagymihály R, Veréb Z, Albert R, et al. (2017). Cultivation and characterisation of the surface markers and carbohydrate profile of human corneal endothelial cells. Clin Exp Ophthalmol, 45(5), 509-519.

Navaratnam J, Utheim T, Rajasekhar V, et al. (2015). Substrates for expansion of corneal endothelial cells towards bioengineering of human corneal endothelium. J Funct Biomater, 6(3): 917-45.

Nejepinska J, Juklova K, Jirsova K (2010). Organ culture, but not hypothermic storage, facilitates the repair of the corneal endothelium following mechanical damage. Acta Ophthalmol, 88(4): 413-19.

Ni J, Abrahamson M, Zhang M, et al. (1997). Cystatin E is a novel human cysteine proteinase inhibitor with structural resemblance to family 2 cystatins. J Biol Chem 272:10853–10858.

Niehrs C (2012). The complex world of WNT receptor signalling. Nat Rev Mol Cell Biol 13(12): 767-779.

Nicholls S, Bailey M, Mitchard L, Dick AD (2009). Can the corneal endothelium of the pig proliferate in vivo? Acta Ophthalmol, 87.

Niknejad H, Peirovi H, Jorjani M, et al. (2008). Properties of the amniotic membrane for potential use in tissue engineering. Eur Cell Mater, 15:88–99.

Niknejad H, Yazdanpanah G (2014). Opposing effect of amniotic membrane on angiogenesis originating from amniotic epithelial cells. J Med Hypot Ideas, 8(1), 39-41.

Noh JW, Kim JJ, Hyon JY, et al. (2015). Stemness Characteristics of Human Corneal Endothelial Cells Cultured in Various Media. Eye & Contact Lens: Science & Clinical Practice 41(3): 190-196.

Okumura N, Hirano H, Numata R, et al. (2014). Cell surface markers of functional phenotypic corneal endothelial cells. Invest Ophthalmol Vis Sci. 2014;55(11):7610-7618.

Okumura N, Inoue R, Kakutani K, et al. (2017). Corneal endothelial cells have an absolute requirement for cysteine for survival. Cornea, 36(8): 988-94.

Okumura N, Kay EP, Nakahara M, et al. (2013). Inhibition of TGF-beta signaling enables human corneal endothelial cell expansion in vitro for use in regenerative medicine. PLoS One 8(2): e58000.

Okumura N, Koizumi N (2020). Regeneration of the corneal endothelium. Curr Eye Res, 45(3), 303-312.

Okumura N, Minamiyama R, Ho LT, et al. (2015a). Involvement of ZEB1 and Snail1 in excessive production of extracellular matrix in Fuchs endothelial corneal dystrophy. Lab Invest 95(11): 1291-1304.

Okumura N, Kusakabe A, Hirano H, et al. (2015b). Density-gradient centrifugation enables the purification of cultured corneal endothelial cells for cell therapy by eliminating senescent cells. Sci Rep, 5(1).

Palchesko RN, Funderburgh JL, Feinberg AW (2016). Engineered basement membranes for regenerating the corneal endothelium. Adv Healthc Mater, 5(22): 2942-2950.

Paolin A, Trojan D, Leonardi A, et al. (2016). Cytokine expression and ultrastructural alterations in fresh-frozen, freeze-dried and c-irradiated human amniotic membranes. Cell Tissue Bank 17:399–406.

Parekh M, Ahmad S, Ruzza A, Ferrari S (2017). Human corneal endothelial cell cultivation from old donor corneas with forced attachment. Sci Rep, 7(1): 142.

Parekh M, Peh G, Mehta JS, et al. (2019a). Effects of corneal preservation conditions on human corneal endothelial cell culture. Exp Eye Res, 179: 93-101.

Parekh M, Romano V, Ruzza A, et al. (2019b). Increasing donor endothelial cell pool by culturing cells from discarded pieces of human donor corneas for regenerative treatments. J Ophthalmol: 1-8.

Park W, Tseng S (2000). Modulation of acute inflammation and keratocyte death by suturing, blood, and amniotic membrane in PRK. Invest Ophthalmol Vis Sci 41:2906–2914.

Paull AC, Whikehart DR (2005). Expression of the p53 family of proteins in central and peripheral human corneal endothelial cells. Mol Vis, 11: 328-334.

Peh GS, Lee MX, Wu FY, et al. (2012). Optimization of human corneal endothelial cells for culture: the removal of corneal stromal fibroblast contamination using magnetic cell separation. Int J Biomater, 2012:601302

Peh GS, Toh KP, Wu FY, Tan DT, Mehta JS (2011). Cultivation of human corneal endothelial cells isolated from paired donor corneas. PLoS One, 6(12).

Peh GSL, Toh K-P, Ang H-P, et al. (2013). Optimization of human corneal endothelial cell culture: density dependency of successful cultures in vitro. BMC Research Notes 6(1).

Peh GS, Adnan K, George BL, Ang HP, Seah XY, Tan DT, Mehta JS (2015). The effects of Rho-associated kinase inhibitor Y-27632 on primary human corneal endothelial cells propagated using a dual media approach. Sci Rep, 5(1), 1-10.

Pfister RR (1973). The normal surface of corneal epithelium: a scanning electron microscopic study. Invest Ophthalmol, 12, 654-668.

Pistsov MY, Sadovnikova EY, Danilov SM (1988). Human corneal endothelial cells: Isolation, characterization and long-term cultivation. Exp Eye Res, 47(3): 403-414.

Pogozhykh O, Prokopyuk V, Figueiredo C, et al. (2018). Placenta and placental derivatives in regenerative therapies: experimental studies, history, and prospects. Stem cells Int, 2018:4837930.

Rahman MS, Islam R, Rana MM, et al. (2019). Characterization of burn wound healing gel prepared from human amniotic membrane and Aloe vera extract. BMC Complement Altern Med, 19(1), 115.

Reneker LW, Silversides DW, Xu L, Overbeek PA (2000). Formation of corneal endothelium is essential for anterior segment development-a transgenic mouse model of anterior segment dysgenesis. Development, 127(3), 533-542.

Rodríguez-Ares MT, López-Valladares MJ, Tourino R, et al. (2009). Effects of lyophilization on human amniotic membrane. Acta Ophthalmol, 87(4), 396-403.

Rosen R (2018). Amniotic membrane grafts to reduce pterygium recurrence. Cornea, 37(2), 189.

Roy O, Leclerc VB, Bourget JM, et al. (2015). Understanding the process of corneal endothelial morphological change in vitro. Invest Ophthalmol Vis Sci, 56(2): 1228-1237.

Ryan JM, Pettit AR, Guillot PV, et al. (2013). Unravelling the pluripotency paradox in fetal and placental mesenchymal stem cells: Oct-4 expression and the case of the emperor's new clothes. Stem Cell Rev Rep, 9:408–421.

Saghizadeh M, Winkler MA, Kramerov AA, et al. (2013). A simple alkaline method for decellularizing human amniotic membrane for cell culture. PloS one, 8(11), e79632.

Scott JE, Bosworth TR (1990). A comparative biochemical and ultrastructural study of proteoglycan-collagen interactions in corneal stroma. Functional and metabolic implications. Biochem J, 270:491-7.

Senoo T, Joyce NJ (2000). Cell cycle kinetics in corneal endothelium from old and young donors. Invest Ophthalmol Vis Sci, 41(3):660-7.

Serena TE, Yaakov R, Moore S, et al. (2020). A randomized controlled clinical trial of a hypothermically stored amniotic membrane for use in diabetic foot ulcers. J Comp Eff Res, 9(1), 23-34.

Shamsuddin AK, Nirankari VS, Purnell DM, Chang SH (1986). Is the corneal posterior cell layer truly endothelial? Ophthalmology, 93(10): 1298-1303.

Shao C (2004). Suppression of corneal neovascularization by PEDF release from human amniotic membranes. Invest Ophthalmol Vis Sci 45:1758–1762.

Shao C, Fu Y, Lu W, Fan X (2011). Bone marrow-derived endothelial progenitor cells: a promising therapeutic alternative for corneal endothelial dysfunction. Cells Tissues Organs 193(4): 253-263.

Sharma P, Alsharif S, Bursch K, et al. (2019). Keratin 19 regulates cell cycle pathway and sensitivity of breast cancer cells to CDK inhibitors. Sci Reports, 9(1), 1-12.

Shen L, Sun P, Zhang C, et al. (2017). Therapy of corneal endothelial dysfunction with corneal endothelial cell-like cells derived from skin-derived precursors. Sci Rep, 7(1): 13400.

Shimazaki J, Shinozaki N, Tsubota K (1998). Transplantation of amniotic membrane and limbal autograft for patients with recurrent pterygium associated with symblepharon. Br J Ophthalmol 82:235–240.

Shimazaki J, Yang HY, Tsubota K (1997). Amniotic membrane transplantation for ocular surface reconstruction in patients with chemical and thermal burns. Ophthalmology, 104(12), 2068-2076.

Shimmura S, Shimazaki J, Ohashi Y, Tsubota K (2001). Antiinflammatory effects of amniotic membrane transplantation in ocular surface disorders. Cornea, 20:408–413.

Schmidt A, Morales-Prieto DM, Pastuschek J, et al. (2015). Only humans have human placentas: molecular differences between mice and humans. Journal of reproductive immunology, 108, 65-71.

Schultz G, Cipolla L, Whitehouse A, et al. (1992). Growth factors and corneal endothelial cells: III. Stimulation of adult human corneal endothelial cell mitosis in vitro by defined mitogenic agents. Cornea, 11(1), 20-27.

Singh JS, Haroldson TA, Patel SP (2013). Characteristics of the low density corneal endothelial monolayer. Exp Eye Res, 115:239-45.

Singh R, Gupta P, Kumar P, et al. (2003). Properties of air-dried radiation processed amniotic membranes under different storage conditions. Cell Tissue Bank 4:95–100.

Siu CK, Ke Y, Orlova G, Hopkinson AC, Siu KM (2008). Dissociation of the N-Cα bond and competitive formation of the [zn− H]•+ and [cn+ 2H]+ product ions in radical peptide ions containing tyrosine and tryptophan: The influence of proton affinities on product formation. J Am Soc Mass Spectrom, 19(12), 1799-1807.

Slettedal JK, Lyberg T, Røger M, et al. (2008). Regeneration with proliferation of the endothelium of cultured human donor corneas with extended postmortem time. Cornea 27(2): 212-219.

Soh YQ, Peh GS, Mehta JS (2016). Translational issues for human corneal endothelial tissue engineering. J Tissue Eng Regen Med, 11(9): 2425-42.

Spinozzi D, Miron A, Bruinsma M, et al. (2018). Improving the success rate of human corneal endothelial cell cultures from single donor corneas with stabilization medium. Cell Tissue Bank, 19(1), 9-17.

Srinivas SP (2010). Dynamic regulation of barrier integrity of the corneal endothelium. Optom Vis Sci, 87(4): E239-254.

Stramer BM, Kwok MG, Farthing-Nayak PJ, et al. (2004). Monoclonal antibody (3G5)-defined ganglioside: cell surface marker of corneal keratocytes. Invest Ophthalmol Vis Sci, 45:807–12.

Tallentire A (1980). The spectrum of microbial radiation sensitivity. Radiat Phys Chem 15:83–89.

Talmi Y, Finkelstein Y, Zohar Y (1990). Use of human amniotic membrane as a biologic dressing. Eur J Plast Surg 13:160–162.

Tang K, Wu J, Xiong Z, et al. (2018). Human Acellular Amniotic Membrane: A Potential Osteoinductive Biomaterial for Bone Regeneration. J Biomater Appl, 32 (6), 754−764.
Tehrani FA, Ahmadiani A, Niknejad H (2013). The effects of preservation procedures on antibacterial property of amniotic membrane. Cryobiology, 67(3), 293-298.
Teichmann J, Valtink M, Nitschke M, et al. (2013). Tissue engineering of the corneal endothelium: A review of carrier materials." J Funct Biomater, 4(4): 178-208.
Thi BMH, Campolmi N, He Z, et al. (2014). Microarray analysis of cell cycle gene expression in adult human corneal endothelial cells. PLoS One, 9(4).
Thomasen H, Pauklin M, Steuhl K-P, Meller D (2009). Comparison of cryopreserved and airdried human amniotic membrane for ophthalmologic pplications. Graefes Arch Clin Exp Ophthalmol 247:1691–1700.
Toda A, Okabe M, Yoshida T, et al. (2007). The potential of amniotic membrane/amnion-derived cells for regeneration of various tissues. J Pharmacol Sci 105:215–228.
Tong CM, van Dijk K, Melles GR (2019). Update on Bowman layer transplantation. Curr Opin Ophthalmol, 30(4), 249-255.
Torricelli AA, Santhanam A, Wu J, Singh V, Wilson SE (2016). The corneal fibrosis response to epithelial–stromal injury. Exp Eye Res, 142, 110-118.
Torricelli AA, Singh V, Santhiago MR, Wilson SE (2013). The corneal epithelial basement membrane: structure, function, and disease. Invest Ophthalmol Vis Sci, 54(9), 6390-6400.
Trosan P, Smeringaiova I, Brejchova K, et al. (2018). The enzymatic de-epithelialization technique determines denuded amniotic membrane integrity and viability of harvested epithelial cells. PLoS One 13, e0194820.
Tseng S, Prabhasawat P, Lee S (1997). Amniotic membrane transplantation for conjunctival surface reconstruction. Am J Ophthalmol 124:765–774.
Tseng SC (1989). Concept and application of limbal stem cells. Eye (Lond) 3 (Pt 2), 141-157.
Ueno M, Asada K, Toda M, et al. (2016). MicroRNA profiles qualify phenotypic features of cultured human corneal endothelial cells. Invest Ophthalmol Vis Sci, 57(13), 5509-5517.
Uchida T, Sakai O, Imai H, Ueta T (2017). Role of Glutathione peroxidase 4 in corneal endothelial cells. Curr Eye Res, 42(3): 380-385.
Utheim TP, Aass Utheim Ø, Salvanos P, et al. (2018). Concise review: altered versus unaltered amniotic membrane as a substrate for limbal epithelial cells. Stem Cells Transl Med, 7(5), 415-427.
Van den Bogerd B (2020). Chapter 7: Designer Descemet membranes constituted of pdlla and functionalized gelatins as corneal endothelial scaffold. Pp. 133-171. In: Corneal endothelial tissue engineering: from biological to synthetic scaffolds (Doctoral dissertation, University of Antwerp).
Van den Bogerd B, Ní Dhubhghaill S, Zakaria N (2018a). Characterizing human decellularized crystalline lens capsules as a scaffold for corneal endothelial tissue engineering. J Tissue Eng Regen Med, 12(4): e2020-e2028.
Van den Bogerd B, Dhubhghaill SN, Koppen C, et al. (2018b). A review of the evidence for in vivo corneal endothelial regeneration. Surv Ophthalmol, 63(2), 149-165.
Van den Bogerd B, Zakaria N, Adam B, et al. (2019). Corneal Endothelial Cells Over the Past Decade: Are We Missing the Mark(er)?. Transl Vis Sci Technol, 8(6), 13-13.
Ventura ACS, Rodokanaki-von Schrenk A, Hollstein K, et al. (1997). Endothelial cell death in organ-cultured donor corneae: the influence of traumatic versus nontraumatic cause of death. Graefes Arch Clin Exp Ophthalmol, 235(4), 230-233.
Wagner M, Walter P, Salla S, et al. (2018). Cryopreservation of amniotic membrane with and without glycerol additive. Graefes Arch Clin Exp Ophthalmol, 256(6), 1117-1126.
Wagoner MD, Bohrer LR, Aldrich BT, et al. (2018). Feeder-free differentiation of cells exhibiting characteristics of corneal endothelium from human induced pluripotent stem cells. Biol Open 7(5).
Wagoner MD, Gonnah ES (2005). Corneal graft survival after prolonged storage in Optisol-GS. Cornea 24(8): 976-979.
Walshe J, Harkin DG (2014). Serial explant culture provides novel insights into the potential location and phenotype of corneal endothelial progenitor cells. Exp Eye Res, 127:9-13.

Waring III GO, Bourne WM, Edelhauser HF, Kenyon KR (1982). The corneal endothelium: normal and pathologic structure and function. Ophthalmology, 89(6), 531-590.

Wheelock MJ, Shintani Y, Maeda M, et al. (2008). Cadherin switching. J Cell Sci 121(Pt 6): 727-735.

Whittle WL, Gibb W, Challis JR (2000). The characterization of human amnion epithelial and mesenchymal cells: the cellular expression, activity and glucocorticoid regulation of prostaglandin Output. Placenta, 21:394–401.

Wilson SE, Hong JW (2000). Bowman's layer structure and function: critical or dispensable to corneal function? A hypothesis. Cornea, 19:417–20.

Wilson SL, Yang Y, El Haj AJ (2014). Corneal stromal cell plasticity: in vitro regulation of cell phenotype through cell-cell interactions in a three-dimensional model. Tissue Eng Part A, 20(1-2), 225-238.

Wu Q, Ouyang C, Xie L, Ling Y, Huang T (2017). The ROCK inhibitor, thiazovivin, inhibits human corneal endothelial-to-mesenchymal transition/epithelial-to-mesenchymal transition and increases ionic transporter expression. Int J Mol Med, 40(4): 1009-1018.

Yam GHF, Seah X, Yusoff NZBM, et al. (2019). Characterization of human transition zone reveals a putative progenitor-enriched niche of corneal endothelium. Cells, 8(10), 1244.

Yamaguchi M, Ebihara N, Shima N, et al. (2011). Adhesion, migration, and proliferation of cultured human corneal endothelial cells by laminin-5. Invest Ophthalmol Vis. Sci, 52,679–684.

Yoshihara M, Ohmiya H, Hara S, et al. (2015). Discovery of molecular markers to discriminate corneal endothelial cells in the human body. PLoS One, 10(3), e0117581.

Zhang Z-H, Miao Y-Y, Ke B-L, Liu K, Xu X (2018a). LY2109761, Transforming Growth Factor β receptor type I and type II dual inhibitor, is a novel approach to suppress endothelial mesenchymal transformation in human corneal endothelial cells." Cell Physiol Biochem, 50(3): 963-972.

Zhang Y, Cai S, Tseng SCG, Zhu YT (2018b). Isolation and expansion of multipotent progenitors from human trabecular meshwork. Sci Rep, 8(1): 2814.

Zhu C, Joyce, NC (2004). Proliferative response of corneal endothelial cells from young and older donors. Invest Ophthalmol Vis Sci, 45(6), 1743-1751.

Zhu SN, Nölle B, Duncker G (1997). Expression of adhesion molecule CD44 on human corneas. B J Ophthalmol, 81(1), 80-84.

Zhu YT, Hayashida Y, Kheirkhah A, et al. (2008). Characterization and comparison of intercellular adherent junctions expressed by human corneal endothelial cells in vivo and in vitro. Invest Ophthalmol Vis Sci, 49(9): 3879-3886.

Zhu YT, Chen HC, Chen SY, Tseng SC (2012). Nuclear p120 catenin unlocks mitotic block of contact-inhibited human corneal endothelial monolayers without disrupting adherent junctions. J Cell Sci 125(Pt 15): 3636-3648.

## A list of publications related to the Thesis

1. **Smeringaiova I**, Reinstein Merjava S, Stranak, Z, Studeny P, Bednar J, Jirsova K (2018). Endothelial wound repair of the organ-cultured porcine corneas. Curr Eye Research, 43(7), 856-865.
2. **Smeringaiova I**, Trosan P, Mrstinova MB, Matecha J, Burkert J, Bednar J, Jirsova, K (2017). Comparison of impact of two decontamination solutions on the viability of the cells in human amnion. Cell Tissue Bank, 18(3), 413-423.
3. **Smeringaiova I**, Nyc O, Trosan P, Spatenka J, Burkert J, Bednar J, Jirsova K (2018). Antimicrobial efficiency and stability of two decontamination solutions. Cell Tissue Bank, 19(4), 581-589.
4. Trosan P, **Smeringaiova I**, Brejchova K, Bednar J, Benada O, Kofronova O, Jirsova K (2018). The enzymatic de-epithelialization technique determines denuded amniotic membrane integrity and viability of harvested epithelial cells. PloS one, 13(3), e0194820.

## Publication not directly related to this Thesis

Azqueta A, Rundén-Pran E, Elje E, Nicolaissen B, Berg KH, **Smeringaiova I**, Jirsova K, Collins AR (2018). The comet assay applied to cells of the eye. Mutagenesis, 33(1), 21-24.